Administrative unit: **Università degli Studi di Padova**

Department: **Territorio e Sistemi Agro-Forestali (TESAF)**

PhD Program: **Land, Environment, Resources and Health (LERH)**

Batch: XXIX

Environmental effects and biophysical constraints on xylem physiology and tree growth in conifers in the Alps

PhD Program Coordinator: Prof. Davide Matteo Pettenella

Supervisor: Dr. Giai Petit

Co-Supervisor: Dr. Georg von Arx, WSL, Birmensdorf, Switzerland

External evaluators:

Prof. Sabine Rosner, BOKU University, Vienna, Austria

Prof. Jordi Martinez Vitalta, Universitat Autonoma de Barcelona, CREAF, Barcelona, Spain

PhD candidate: Angela Luisa Prendin

Sede amministrativa: **Università degli Studi di Padova**

Dipartimento di **Territorio e Sistemi Agro-Forestali (TESAF)**

Corso di dottorato di ricerca in: **Territorio, Ambiente, Risorse e Salute (TARS)**

Ciclo: XXIX

Effetti ambientali e limitazioni biofisiche sulla fisiologia dello xilema e l'accrescimento in conifere nelle Alpi

Coordinatore: Prof. Davide Matteo Pettenella

Supervisore: Dr. Giai Petit

Co-Supervisor: Dr. Georg von Arx, WSL, Birmensdorf, Switzerland

External evaluators:

Prof. Sabine Rosner, BOKU University, Vienna, Austria

Prof. Jordi Martinez Vitalta, Universitat Autonoma de Barcelona, CREAF, Barcelona, Spain

Dottoranda: Angela Luisa Prendin

Look deep into nature,

and then you will understand everything better.

Albert Einstein

Table of contents

Summary

Trees are impressive long-living organisms that continuously increase in size by many orders of magnitude during ontogeny by accumulating xylem biomass in stem, branches and roots. While growing taller, trees continuously adjust the xylem structure to achieve an optimal balance of carbon costs for the competing biomechanical and hydraulic requirements.

One of the main function of the xylem structure is the delivery of the water from the roots up to the leaves. This must be maintained during the ontogeny, when the hydrodynamic resistance increase due to the increase in the xylem path length. However, by widening the diameter of xylem conduit (from the stem apex downwards), trees are able to minimize the negative effect of height growth. Additionally, this widening is stable during ontogeny, thus determining the radial change in conduit dimension with cambial age (from the pith outwards), implying a dependency between the variation of conduit-lumen diameter with cambial age and the rates of stem elongation.

These adjustments in the xylem structure remain permanently fixed and chronologically archived in the secondary xylem, and, given the tight link between structures and functions, these provide a 'time component' to functional responses induced by xylem plasticity, thus allowing to reconstruct growth dynamics under different environmental conditions.

However, there is a lack of detailed information and standardized procedures to explore, at the intra-specific level, the long-term modifications of xylem traits over the full life-span of trees, together with their variability along axial and radial profiles. Additionally, little is known about the relationships between the structures and functions in a view of exploring the future challenges in how a plant's hydraulic architecture may respond to the ongoing climate change.

This thesis, represent a set of studies based on dendro-anatomical and physiological approaches aimed to:

- identify priorities and trade-offs among xylem functions;
- determine the anatomical traits responsible for them;
- retrospectively analyze how these relationships vary during ontogeny under different environmental condition;
- analyze the functional response to xylem modifications occurring during ontogeny;

- investigate the possibility of retrospectively analyzed height growth based on hydraulic radial profiles.

Furthermore, a guidance from sample collection to xylem anatomical data and a new approach to customize cell wall thickness measurements according to the specific aims of the study, were developed.

This thesis has highlighted that the xylem anatomical structure of conifer trees (*Larix decidua, Picea abies, Pinus cembra*) showed a high priority and biophysical determination of traits linked to hydraulic efficiency, such as conduit size, to efficiently support assimilation necessary for tree growth. Besides, other functional traits linked to mechanical support and metabolic xylem functions showed more plastic responses to intrinsic and extrinsic factors. Due to the ontogenetic stability of axial patterns of conduit size, it was possible, based on radial profiles of xylem conduit diameter of tree rings, to estimate tree growth rate, even if species-site specific, and make comparison between trees living in different epochs. In addition, despite the risk of becoming more vulnerable to air seeding cavitation, trees showed to prioritize of hydraulic efficiency vs. safety during the ontogenetic development, as the increase in xylem conductance with tree height determined a contextual decrease in the hydraulic safety margin.

This study showed the importance of taking into account the three dimensional anatomical trends to better understand of the trade-offs of hydraulic safety vs. efficiency shape up the tree architecture and affect its adjustments occurring during ontogeny to cope with the arising intrinsic (i.e., size-related) and extrinsic (i.e., environmental) constraints to growth.

Sommario

Gli alberi sono organismi viventi che aumentano continuamente di dimensione (anche diversi ordini di grandezza) durante l'ontogenesi, accumulando biomassa nel fusto, nei rami e nelle radici. Durante la crescita, la struttura xilematica degli alberi continua ad adattarsi mantenendo un equilibrio nell'ottimizzazione del carbonio, garantendo contemporaneamente un'adeguata stabilità meccanica ed efficienza idrica della pianta.

Il trasporto dell'acqua dalle radici fino alle foglie è una funzione fondamentale dello xilema e deve essere mantenuto efficiente durante tutte le fasi ontogenetiche. La resistenza idraulica del sistema infatti è fortemente influenzata dall'incremento della lunghezza del percorso idrico. Tuttavia, allargando la dimensione degli elementi di conduzione dello xilema (dall'apice alla la base del fusto), le piante sono in grado di minimizzare l'effetto negativo della crescita in altezza. Inoltre, data la stabilità di questo trend assiale durante l'ontogenesi, le dimensioni dei condotti xilematici aumentano anche in direzione radiale con l'età cambiale (dal midollo verso l'esterno), determinando una forte relazione tra la variazione del diametro dell'elemento conduttivo con l'età cambiale ed il tasso di allungamento del fusto.

Le modifiche nella struttura xilematica, rimanendo impresse e cronologicamente archiviate nel legno, rappresentano un'importante fonte di informazioni che permette di aggiungere una componente temporale legata a meccanismi funzionali e di plasticità xilematica e, quindi, permetterebbe di ricostruire le dinamiche di crescita in diverse condizioni ambientali.

Esiste tuttavia, una carenza di conoscenza e di procedure standard atte ad esplorare, a livello intra-specifico, le modificazioni a lungo termine dello xilema e la variabilità della sua struttura lungo profili assiali e radiali. Rimangono inoltre poco chiari i rapporti tra la struttura e la funzionalità, utili a prevedere in futuro eventuali adattamenti del sistema idraulico e metabolico al cambiamento climatico.

Questa tesi riporta una serie di studi che si basano su un approccio dendro-anatomico e fisiologico, allo scopo di:

- individuare priorità e compromessi tra le varie funzioni xilematiche;
- determinarne i tratti anatomici responsabili;
- analizzare in maniera retroattiva la loro variazione durante l'ontogenesi e in diverse condizioni ambientali;
- analizzare risposte funzionali alle modifiche anatomiche che occorrono durante l'ontogenesi;

- esaminare la possibilità di ricostruire i trend di accrescimento in altezza basandosi su profili idraulici radiali.

E' stata definita una guida alla standardizzazione della procedura, dalla raccolta del campione al dato anatomico dei tratti xilematici. Inoltre è stato sviluppato un nuovo approccio di quantificazione dello spessore della parete cellulare al fine di soddisfare gli obiettivi specifici dello studio.

La struttura xilematica delle conifere (*Larix decidua, Picea abies, Pinus cembra*) evidenzia priorità e determinazione biofisica di tratti legati all'efficienza idraulica, come le dimensioni delle tracheidi, al fine di sostenere l'assimilazione necessaria per la crescita degli alberi. Altri caratteri funzionali invece, legati al supporto meccanico ed all'attività metabolica, mostrano più plasticità a fattori intrinseci ed estrinseci.

Grazie alla stabilità del trend assiale dei condotti idraulici durante l'ontogenesi è stato possibile, basandosi sul conseguente pattern radiale, stimare il tasso di accrescimento delle piante, anche se specie-sito specifico, e confrontare quindi i trend con le piante che sono vissute in epoche diverse.

Nonostante il rischio di aumentare la vulnerabilità alla cavitazione, gli alberi tendono a priorizzare l'efficienza a discapito della sicurezza idraulica durante lo sviluppo ontogenetico, a causa dell'aumento della conduttanza e conseguente riduzione del margine di sicurezza idraulica.

Questo studio dimostra l'importanza di considerare la tridimensionalità dei trend anatomici al fine di comprendere meglio i rapporti tra la sicurezza idraulica e l'efficienza che modella l'architettura della pianta, influenzandone le modifiche ontogenetiche e compensandone i vincoli di crescita intrinsechi (dimensione-dipendenti) ed estrinseci (ambiente-dipendenti).

1. General introduction

1.1 State of the Art

Trees are long-living organism that continuously increase in size during ontogeny by accumulating xylem biomass in stem, branches and roots, adjusting the xylem structure to achieve an optimal balance among the competing needs of support, storage and transport.

At low temperatures, tree growth is particularly constrained. Two major mechanisms can explain the abrupt reduction in growth in cold environments (Rossi et al., 2008) and consequently the formation of an altitudinal/latitudinal treeline. According to the carbon source limitation hypothesis, low temperatures and short vegetation periods prevent a positive carbon balance of the tree burdened with a large proportion of non productive tissues with increasing altitude or latitude (Hattenschwiler 2002). In addition, at high altitude the CO_2 uptake by plants could be limited by the lower CO_2 partial pressure (Tranquillini, 1979) due to the decreasing air density with altitude (La Marche, 1984)

On the contrary, the carbon sink limitation hypothesis (Körner, 1998) proposed that a sink rather than a source limitation is affecting tree growth at low temperatures, asserting that the metabolic activity of fixing assimilated carbon into biomass is temperature limited, thus limiting the growth of both cambial and apical meristems, above and below the ground, and a global isotherm of 6-7°C set the limit to the tree growth form (Rossi et al., 2008, Korner, 2012). At the treeline, cambial growth is less constrained by the prevailing temperatures than apical growth. In fact, the diameter growth declines much slower than height growth towards the tree limit (Korner, 2012), and mean tree height decreases with increasing altitude or latitude (Hoch & Korner, 2005; Miyajima & Takahashi, 2007). In fact the stem apex is occupying a "colder"position (Korner, 2012), i.e., more coupled with the atmosphere and less protected during the winter when the crown protrudes from the snow becoming more vulnerable to ice blasting, wind desiccation (Baig & Tranquillini, 1980; Smith et al., 2003) and frost drought (Mayr et al., 2006, 2007). However, trees at the treeline evolved morphological and functional modification to cope with such severe climatic condition and environmental constraints (Petit et al., 2011).

Hydraulic constraints have been demonstrated to be among the major determinants of the maximum height of the trees (Koch et al. 2004). According to optimal allometric models (West

et al. 1999) that predicts a quantitative relationship between plant growth and carbon allocation, the hydraulic diameter of xylem conduits (Dh) should vary in relation to the distance from the stem apex (L) to guarantee a constant leaf-specific conductivity that is independent from the tree height. This relationship follows a power (scaling) function ($Dh \propto Lb$), with the exponent *b* often converging to the value of 0.2 (Anfodillo et al. 2006; Petit et al. 2007, Petit et al., 2009, Olson et al., 2014). This axial pattern (conduit widening) allows the maintenance of a functional hydraulic transport by minimizing the negative effect of path length on the total hydraulic resistance, while maintaining the safety against embolism formation at the apical level, where xylem smaller conduits are more resistant under higher xylem tensions (Hacke et al. 2016). A consequence of this strong mechanistic link between conduit lumen size, tree hydraulic architecture and height growth, is that the conduit-lumen diameter in a tree increases with cambial age at rates dependent on the rates of stem elongation during ontogeny (Carrer et al., 2015). A power-like trajectory can well describe the trend of time series of conduit size during ontogeny until tree maturity, where the leveling off of conduit time series should reflect the approaching to the maximum tree height, and any deviation from the curve may reflect a positive or negative pulse of height growth.

Cavitation, i.e. the formation of air bubble inside the xylem conducts when exposed to highly negative water potential, can also occur in conduits following freeze-thaw events, where crystallization of liquid water forces dissolved gas out of solution (Brodersen and McElrone 2013). This hydraulic dysfunction caused such a strong selective pressure that plants have evolved xylem anatomical properties to prevent cavitation (Brodribb and Holbrook 2005) and to restore the water transport capacity once embolisms have occurred (Brodersen and McElrone 2013). Recent studies suggested a potential role of xylem parenchyma in refilling conductive elements after embolism occurs (Salleo et al., 2009; Nardini et al., 2011).

In vascular plants, hydraulic safety against cavitation and efficiency of water transport commonly trade off (Meinzer 2010). Many traits may contribute to the safety–efficiency trade-off, but the interaction among these functional and anatomical traits has still to be fully understood (Gleason et al., 2015), maybe because the three dimensional patterns of xylem traits in a tree and their size-related modifications occurring during ontogeny are not always acknowledged.

The continuing rise in temperature and CO_2 concentration measured in the last decades has been hypothesized to stimulate the growth and this is probably the reason of the observed altitudinal and latitudinal treeline shift (La Marche 1984, Korner et al., 2012).

It has been argued that treeline trees may be particularly sensitive to CO_2 enrichment and increasing temperature (Smith et al., 2009; Korner, 2012), as they are exposed to lower partial pressure of atmospheric CO_2 (La Marche et al., 1984, Korner, 2003) and they grow close to their low temperature limit (Walther 2003, Dorrepaal et al., 2009).

The use of manipulative experiment is crucial to understand the carbon source-sink balance under different conditions (Fatichi et al., 2013). Only few elevated CO_2 experiments were applied to high latitude and high elevation vegetation in a relatively natural growth condition (Dawes et al., 2011). These studies broadly revealed that other variables, such as temperature and availability of nutrients or water, can influence CO_2 effects (Niklaus et Korner, 2004; Dawes et al., 2011) and that initial growth stimulation often declines after a few years (Korner, 2006). In general, an increase in growth and biomass production was observed in several experiments, although responses were often small or transient and varied across species and study sites (Rustad et al., 2001; Walker et al., 2006).

Only one long term study of simultaneously manipulating CO_2 concentration and soil temperature was completed at an alpine treeline ecosystem. This experiment was performed at Stillberg (Davos, CH) from 2001 to 2012 (Hattenschwiler et al., 2002-Dawes et al, 2015).

Little is known about how the xylem anatomical traits are adjusted to guarantee tree growth during the different phases of ontogeny, by providing the new requirements in terms of efficient and safe water transport, and biomechanical support under different environmental conditions. Specifically, there is a lack of studies at the intra-specific level, long-term modifications of xylem traits over the full life-span of trees, and variability along axial and radial profiles (Streit et al., 2014). Additionally, analysis of inter-annual variability in xylem parenchyma traits and their relationships with environmental variation has remained largely unexplored (Olano et al 2013).

In order to better understand how “plastically” the trees respond to environmental changes, there is the need to revisit and further explore the structure-function relationships at different levels of investigation, from the individual cell to whole plant level, and from individual plants to populations. It is important to better understand how plants balance their hydraulic architecture to optimize growth performance while guaranteeing the safety and efficiency of the entire xylem transport system.

The study of tree ring anatomy, that adds a ‘time component’ to the functional mechanisms of xylem plasticity, is emerging as a promising approach in tree biology and climate change research, particularly if complemented by physiological and ecological studies (Fonti et al.,

2010). I used both an anatomical and physiological approach to study the dynamics of growth, by analyzing how the structure-function relationships may change during ontogeny and under different environmental conditions in different conifer species in the Alps.

1.2 Aims of the study

This thesis deals with the effect of ontogeny and increased temperature and CO_2 concentration in the atmosphere on the dynamics of growth, through modifications of structural and functional scaling relationships in common conifer species in the Alps. The whole study is mainly based on a wood anatomical approach.

The overall research focuses on: i) wood anatomical responses to ontogeny and environment in *Larix decidua* at the Alpine treeline, ii) conduit-size based comparison of present and past height growth rates at three treeline sites in the Alps, iii) size-related changes in structural xylem features affecting the vulnerability to cavitation of leader shoots.

In addition I described the recent improvements in quantitative wood anatomy, to overcome the methodological limitations and time-consuming procedures of data collection and analysis.

In particular, the specific aims of the different studies presented are:

- To provide a guideline for quantitative wood anatomy (Article 1);
- To explore new perspectives for investigating structure-function relationships, tree stress responses, carbon allocation patterns and climate effects on tree structures based on cell wall thickness measurements (Article 2);
- To identify priorities and trade-offs among xylem functions and to retrospectively determine how these relationships varied during ontogeny and under different soil temperatures and atmospheric [CO_2] (Article 3);
- To evaluate a novel research perspectives on the use of quantitative wood anatomy to assess height growth patterns in conifer trees grown in different epochs at the treeline (Article 4);
- To evaluate the variation of vulnerability to embolism with tree size and to identify the tree structure adjustments that can explain it (Article 5).

1.3 Structure of the thesis

This thesis consists of 5 articles coming out from my PhD activity (chapters 2 and 6).

The first paper (Chapter 2) has been published in *Frontiers in Plant Science* in 2016 and it is a Method paper that describes the different steps from wood sample collection to xylem anatomical data, provides guidance and identifies pitfalls, and presents different image-analysis tools for the quantification of anatomical features, in particular of conducting cells. Following a rigid protocol and quality control as suggested in this paper, it is thus possible to obtain a large amount of quantitative data of xylem anatomical features that can be used as a powerful source of information for many research topics.

The second Method paper (Chapter 3) has received a major revision in *Tree Physiology*. It describes new research perspective from a novel approach to quantify tracheid wall thickness (CTW).

The approach to customize the CWT measurements according to the specific aims of the study, together with the high data production capacity, opens new perspectives for investigating structure-function relationships, tree stress responses, carbon allocation patterns of trees, and climate reconstruction based on intra-annual variability of wood density.

The following three chapters are the research papers related to the three main projects carried out during this PhD.

The third paper (Chapter 4) has been submitted to *New Phytologist*. It describes the axial allometry of different xylem anatomical structures in *Larix decidua*, and revealed a hierarchy in functional traits, showing a differential prioritization of hydraulic efficiency and safety to support the necessary carbon assimilation for tree growth. This work improved our mechanistic understanding on the interactions between tree growth and environmental conditions and thus on the responses of forests in cold environment to global change.

The forth paper (Chapter 5) is a manuscript to be submitted soon to a peer-reviewed journal. This work described how the ontogenetically stable axial conduit widening (i.e., the increase in conduit diameter from the stem apex to base) can be used to obtain information on the height growth pattern occurring during ontogeny through the analysis of the radial pattern of xylem conduit size. In addition, it describes a conduit based comparison of height growth patterns of conifer trees (*Larix decidua, Picea abies, Pinus cembra*) differing in age from three Alpine treeline sites.

The fifth paper (Chapter 6) is a manuscript to be submitted soon to a peer-reviewed journal. It describes the size-related trends in xylem anatomical features triggering the decrease in cavitation resistance of the leader shoots in taller *Picea abies* trees.

The thesis ends with a chapter (Chapter 7) with general conclusions.

2. Quantitative wood anatomy – practical guidelines

Georg von Arx[1*], Alan Crivellaro[2], Angela Luisa Prendin[2], Katarina Čufar[3], Marco Carrer[2]

[1] Swiss Federal Institute for Forest, Snow and Landscape Research WSL, Birmensdorf, Switzerland

[2] Università degli Studi di Padova, Dept. TeSAF, Legnaro, Italy

3 University of Ljubljana, Biotechnical Faculty, Department of Wood Science and Technology, Ljubljana, Slovenia

*** Corresponding author**

Keywords: anatomical sample preparation, dendro-anatomy, microscopic imaging, microtome sectioning, quantitative image analysis, QWA, tree-ring anatomy, wood sample collection.

This chapter is an edited version of: **von Arx G, Crivellaro A, Prendin AL, Čufar K, Carrer M**. **2016**. Quantitative wood anatomy—practical guidelines. *Frontiers in Plant Science* **7**: 781. Published online 2016 Jun 3. doi: 10.3389/fpls.2016.00781

2.1 Abstract

Quantitative wood anatomy analyzes the variability of xylem anatomical features in trees, shrubs and herbaceous species to address research questions related to plant functioning, growth and environment. Among the more frequently considered anatomical features are lumen dimensions and wall thickness of conducting cells, fibers and several ray properties. The structural properties of each xylem anatomical feature are mostly fixed once they are formed, and define to a large extent its functionality, including transport and storage of water, nutrients, sugars and hormones, and providing mechanical support. The anatomical features can often be localized within an annual growth ring, which allows to establish intra-annual past and present structure-function relationships and its sensitivity to environmental variability. However, there are many methodological obstacles to overcome when aiming at producing (large) data sets of xylem anatomical data.

Here we describe the different steps from wood sample collection to xylem anatomical data, provide guidance and identify pitfalls, and present different image-analysis tools for the quantification of anatomical features, in particular conducting cells. We show that each data production step from sample collection in the field, microslide preparation in the lab, image capturing through an optical microscope and image analysis with specific tools can readily introduce measurement errors between 5 to 30% and more, whereby the magnitude usually increases the smaller the anatomical features. Such measurement errors – if not avoided or corrected – may make it impossible to extract meaningful xylem anatomical data in light of the rather small range of variability in many anatomical features as observed, for example, within time series of individual plants. Following a rigid protocol and quality control as proposed in this paper is thus mandatory to use quantitative data of xylem anatomical features as a powerful source for many research topics.

2.2 Introduction

Quantitative wood anatomy as meant here investigates quantitatively how the variability in xylem anatomical features of trees, shrubs and herbaceous species is related to plant functioning, growth and environment, and often explores how these relationships change over time. Xylem performs a wide range of functions that are essential for plants to grow and survive. The xylem transports water, nutrients, sugars, and hormones; buffers water uptake and loss; supports the mass of the canopy plus loads from wind, snow, ice, fruits, and epiphytes; displays foliage and flowers to resources like light and pollinators. Many different ways have evolved to perform these functions, and in consequence, there is an enormous diversity of xylem anatomies that can be spotted through a microscope. Moreover, wood anatomical features represent a natural archive for growth-environment relationships and plant functioning with intra-annual resolution (Fonti et al., 2010). In fact, xylem cells can be localized at a certain position within a specific annual growth ring (e.g. earlywood or latewood), which is linked to the time of their formation. The xylem anatomical structure is influenced during its development by internal and external factors (e.g., Fonti et al., 2010; von Arx et al., 2012; Aloni, 2013; Fonti et al., 2013; Carrer et al., 2015), and mal-adjusted xylem structure may even be responsible for tree mortality (e.g., Hereş et al., 2014; Pellizzari et al., 2016). Quantitative wood anatomy capitalizes on the xylem anatomical structures mostly fixed in the stems once the cells are mature, and often focuses on a small number of cell types such as conduits (vessels or tracheids), parenchyma (axial and radial), and fibers.

Xylem anatomical features in plants are numerous, and sometime concern very small and delicate details (IAWA Committee, 1989; 2004; Crivellaro and Schweingruber, 2015). This necessitates careful processing and high accuracy during quantification, but also analyzing a sufficiently large and representative subset of the wood sample (Arbellay et al., 2012; Scholz et al., 2013; Seo et al., 2014; von Arx et al., 2015a). In other words, quantitative wood anatomy requires high-quality, high-resolution, and often large images of properly collected and prepared anatomical samples. Improved sample preparation protocols for these needs have lately been developed (Gärtner and Schweingruber, 2013; Yeung et al., 2015). Furthermore, recent improvements in computer performance, automated image-analysis systems (von Arx and Dietz, 2005; Fonti et al., 2009; von Arx et al., 2013; von Arx and Carrer, 2014) and processing and interpretation of anatomical data (Carrer et al., 2015) nowadays allow to

significantly increase the number of measured anatomical features. Together, these advancements are providing the basis to create unprecedented datasets in terms of size and quality, thus also allowing to use quantitative wood anatomy for an increasing number of different research topics such as climate-growth interactions (Olano et al., 2013; Castagneri et al., 2015; Rita et al., 2015), stress responses (Fonti et al., 2013), tree functioning (Petit et al., 2011; Olson et al., 2014; Guet et al., 2015; Pfautsch et al., 2016), functional anatomical properties to identify tree provenances most resistant to climate change impacts (Eilmann et al., 2014), and wood formation (Cuny et al., 2014; Pacheco et al., 2015) and production (Cuny et al., 2015) processes. However, the production of data meeting high quality requirements necessitates following a strict multi-step procedure, to avoid artifacts and mistakes that can significantly influence the measurements. This is critical considering the relatively small range of variability of many anatomical features, in time series often between 5 and 20% from year to year (Fonti et al., 2007; Olano et al., 2013; Fonti et al., 2015; von Arx et al., 2015a) as compared to even several fold in ring width.

This paper shows all sequential steps from sample collection to anatomical sample preparation and high-quality data production, and presents guidance and pitfalls of quantifying anatomical features. As such, it is intended to reflect the current state of the art for quantitative wood anatomy, particularly for the quantification of the most commonly investigated water-conducting xylem cells (conduits), but we anticipate that many aspects will be similar in other anatomical features of the xylem and even the phloem.

2.3 From sample to anatomical data: guidance and pitfalls

Step 1: Collecting samples in the field

Quantitative wood anatomy aims to extract information from anatomical structures of stems, shoots, branches, roots, rhizomes and even needles and leaf petioles of monocots and dicots. In many cases samples used for quantitative wood anatomy are taken with an increment borer. This tool was originally developed to collect samples for forest mensuration and dendrochronological investigations. When collecting increment cores for anatomical analyses, it is even more crucial than for other purposes to check the sharpness of the cutting edge of the borer's tip to avoid macro- and micro-cracks in the samples. This can be tested by punching out paper circles from a newspaper. Furthermore, it is very important to core in an exact radial direction, from the bark towards the pith, perpendicular to the axial direction of xylem cells, and keeping the borer in a fixed position while drilling. The use of a pusher is recommended

when collecting cores for anatomical analyses. Cores of 10-12 mm in diameter are preferable compared to the standard 5 mm or smaller, to have more material to work with and to minimize the risk of fractures and twisting. Wood samples can also be extracted from stem discs obtained with a chainsaw, whereas in branches and smaller plant stems and/or root collars the entire samples can be processed. For the storage of wood samples we refer to literature such as Gärtner and Schweingruber (2013). Collection of herbs requires to excavate the root collar, e.g. with common garden tools. When cutting small branches, twigs, and small stems from a plant with pruners, the first (squeezed) part of the sample needs to be removed with a small-jagged saw (in hard samples) or a razor blade (in soft samples) before preparing microsections to avoid cracks and fragmentation.

Step 2: Preparing microsections

General procedure

Typically, sample preparation involves producing microsections of 10-20 µm thickness with a sledge or rotary microtome, staining of the pallid cell walls with an agent as safranin, astrablue, toluidine blue, cresyl *violet* acetate and their combinations to increase contrast in an anatomical slide (Gärtner and Schweingruber, 2013; Yeung et al., 2015). Boiling or just soaking the samples in water, embedding in paraffin, or using corn starch solution often helps to avoid damage to cell structures when cutting (Schneider and Gärtner, 2013; Yeung et al., 2015). For samples with very narrow cell lumina rice starch gives better results than corn starch because of the smaller grain size. When analyzing relatively large cells as the earlywood vessels in ring-porous species, it is usually sufficient and more efficient to smooth the wood surface by sanding or cutting (for instance with a core microtome, Gärtner and Nievergelt, 2010), removing sawdust and tyloses using high-pressure air or water blast, and increasing contrast of the wood surface with chalk powder and black marker (Fonti et al., 2009; Gärtner and Schweingruber, 2013).

Microtome blades

Microtome blades must be sharp and without defects to avoid disrupting the delicate anatomical structures. Damages due to dull blades are usually more pronounced in thinner sections (Figure 1). Frequent replacement or use of a previously unused part of the blade (often after cutting one sample, or after an even surface of the sample was prepared) can avoid this problem. Furthermore, using high-quality blades can significantly reduce cutting artifacts (Figure 2). For both conifer and angiosperm samples, good results were reported when using Leica DB80 LX and Leica 819 low-profile blades (Leica Biosystems, Wetzlar, Germany), and

Feather N35HR and N35 blades (Feather Safety Razor Co., Ltd., Osaka, Japan) (e.g., Prislan et al., 2013; Gričar et al., 2014; Pacheco et al., 2015; Pellizzari et al., 2016), however the optimal blade depends on the microtome model and the sample properties (e.g., density of the material, part(s) of the stem, moisture content) and therefore requires lab-specific testing. Generally, for cutting xylem, blade types designed for hard tissues should be used.

Sample orientation while cutting sections

When analyzing cross-sections, the wood samples should be cut perpendicular to the axially oriented xylem cells to avoid over- and underestimation of the measured anatomical features (Figure 3). When cutting longitudinal (i.e. radial and tangential) sections wood samples should be cut parallel to the axially oriented xylem cells. This is important when analyzing, for instance, rays in tangential sections. Measurement errors due to improper sample orientation increase with cutting thickness.

Section thickness

A cutting thickness between 10 and 20 µm is usually optimal. Analyzing thick sections usually results in over- and underestimation of anatomical features such as cell wall thickness and cell lumen area (Figure 4). Thick sections also often appear out of focus. On the other hand, sections should not be too thin, since the tissue staining might be too weak to obtain target structures of sufficient contrast. Weak staining can be improved to a certain extent by prolonging the duration of the staining process or slightly increasing the concentration of the stain. In addition, sections from different species and even individuals can differ in staining intensity. However, as the example in Figure 4 shows, even in the optimal range the measured values can be influenced by different cutting thicknesses. It is therefore important to standardize cutting thickness for all samples of the same project. A good practice is also to record the thickness of each section, if not fully constant for all samples, thus allowing during data analysis to relate any outliers to potential cutting-thickness effects. It is also important to bear in mind that comparing absolute values among different projects could be biased if different cutting thicknesses were used.

Making permanent slides

Permanent slide preparation is recommended to make specimens last over a long time. The procedure requires to dehydrate sections after staining, and a mounting medium (e.g., Canada balsam, Euparal, Eukitt) to permanently fix the sections between two glass slides (Gärtner and Schweingruber, 2013). To avoid buckling of the section, which impairs a uniform focus when capturing an image, the slide with the cover slip is sandwiched between PVC strips with a small

magnet placed on the top of the slide on a metal plate to keep the sections flat and air bubbles out during drying in the oven. The oven is set at 60 °C for 12 h. Permanent slides, once prepared, can be used over and over again and can be stored for longer time periods than non-permanent slides.

Step 3: Microslide digitizing

Cleaning slides and cover glasses

Pollution hampers automatic detection of anatomical features during image analysis and increases manual editing effort needed to obtain accurate data. Microslides should be cleaned carefully before capturing images to avoid obscured and low-contrast image parts (Figure 5). Frequent sources of pollution are, for instance excessive mounting medium (Gärtner and Schweingruber, 2013), fingerprints and dust particles. After drying, any hard mounting media on top of the cover slip can be scraped off with razor blades.

Magnification

High-resolution digital images of anatomical sections are most commonly captured with a camera mounted on a optical microscope. Cameras integrated in the microscope system or standard cameras mounted with an appropriate adapter can be used. To observe and analyze conifers 10× objectives are usually recommended, which, depending on the camera, can give a resolution of 1.7 to 2.5 pixels·µm^{-1}. In angiosperms the 4× objectives giving a resolution of 0.7 to 1.0 pixels·µm^{-1} are usually sufficient, especially for analyzing larger cells as vessels in trees, whereas smaller cells such as fibers also often require 10× objectives.

Contrast and illumination settings

Insufficient staining (due to too short staining time and/or old staining solutions) as well as wrong illumination, improper white balance and over-illumination lead to poor image contrast (Figure 6). Poor image contrast can significantly hamper the accurate automatic detection of anatomical structures during image analysis.

The quality and accuracy of the image critically depend on proper microscope settings. In this respect, the Köhler illumination method represents a major step to improve image quality (McCrone, 1980) and should be applied as a standard.

Focusing

Careful focusing avoids obtaining blurred structures that can lead to measurement errors (Figure 7). Some systems offer automatic or semi-automatic focusing which contributes to consistently high image sharpness. When focusing manually, one should be aware that the live

view on the computer screen is often of reduced size; therefore one should use a 100% zooming window for focusing, if available. When not all regions of a microslide can be in focus because of buckling, z or focus stacking techniques, i.e. the combination of the focused image information from multiple images taken at different focal planes is a solution provided by some systems. Otherwise, the best and first solution would be to retry preparing a better microslide. In some wood samples this problem cannot be resolved even with careful microslide preparation. Then, excluding poorly focused regions from analysis is the best way to avoid measurement errors. Since the impact of poor focus depends on the size of the anatomical features (Figure 7), focusing the smaller target features (e.g., latewood lumina) is better than focusing larger target features (e.g., earlywood lumina).

Scanning

For analyzing relatively large anatomical features such as the earlywood vessels in ring-porous species, it is possible to capture an image directly from the prepared wood surface with a flatbed scanner using an optical resolution of 1500 to 2500 dpi (Fonti et al., 2009). For permanent anatomical slides, slide scanners are an efficient alternative to optical microscopes, because they can produce high-resolution (e.g., 2.0 pixels·μm^{-1}) images of entire anatomical samples, which avoids time-consuming image capturing and stitching (see next paragraph).

There are also several modifications of the aforementioned basic image capturing approaches, e.g. capturing images directly from the prepared wood surface with a dissecting microscope, thus combining efficient wood preparation with a higher optical resolution compared to flatbed scanners.

Stitching composite images

Quantification of anatomical structures requires high-resolution images in order to obtain accurate data. However, higher magnification goes along with smaller field of view. This means that the anatomical sample often does not fit into a single image frame captured with an optical microscope, particularly when working with larger samples as the ones used, for example, to build time series of anatomical features (tree-ring anatomy or dendro-anatomy). If no slide scanner is available (see above), this dilemma can be resolved by capturing several overlapping images and stitch them together (Figure 8).

For image stitching, overlapping images are produced using a microscope stage and systematically moving through the sample while capturing images. Re-focusing should be performed after every single or every few images. The overlap between individual images in angiosperm samples should be about 20% (Figure 8a), while in conifers we recommend about

30-40% to facilitate the stitching process. Overlapping images of a sample are then merged to an overall composite or panorama image using stitching software (Figure 8b). We recommend using specialized tools such as PTGui (New House Internet Services B.V., Rotterdam, NL) and AutoPano Pro (Kolor SAS, Francin, F) since they offer full control and reproducibility while producing distortion-free composite images. In contrast, some of the widely used stitching systems can produce distortions and artifacts which would lead to inaccurate results. With sufficient overlap and focused images PTGui and AutoPano Pro are usually able to create the composite image automatically. If not, both software allow to manually add control points, i.e. identical structures in the overlapping image parts. If the software are configured correctly, they are even able to correct any image distortions introduced by the optical system (Figure 8c; see von Arx *et al.* (2015b)), e.g. when not using the recommended distortion-free 'plan' type lenses.

Step 4: Quantifying anatomical features in anatomical images

Image analysis tools

Once the image is produced, image-analysis tools are used to quantify the anatomical features. While target structures can be outlined and measured manually, automated image analysis allows to quantify a larger number of anatomical features in a much shorter time, and in an objective and reproducible way. Several image-analysis tools are used for quantitative wood anatomy. They differ considerably in functionality, ranging from rather general image analysis software such as ImageJ (Rasband, 1997-2016) to very specialized tools such as WinCELL (Regent Instruments Inc., Québec, Canada) and ROXAS (von Arx, www.wsl.ch/roxas; Table 1). The choice of the most appropriate tool depends on the specific needs. For a general characterization of xylem anatomical features in rather small samples a general tool is sufficient. However, if the sample depth in terms of number of trees, years and anatomical features measured, but also the requirements in terms of specific and comprehensive output is important for the subsequent inferences, we recommend using specialized tools.

Despite the diversity of tools offering different levels of automation, specialization and usability, using them for quantification of anatomical features follows the same basic steps that are explained in the following.

Determining the spatial image resolution

To obtain the measurements in metric units the pixel-to-micrometer resolution needs to be determined first. Some microscopic imaging systems provide this information directly, or add

a spatial scale bar to the image that can be used as a reference. Where such information is missing, the best way to obtain the spatial resolution is to take a microscopic image of a stage micrometer or graticule (slide with an engraved high-accuracy micrometer scale) in the target magnification and measure several times the distance between two tick marks in pixels using a line tool. The obtained line length in pixels is then divided by the known line length in micrometers to receive the pixel-to-micrometer resolution. Selecting remote and different tick marks in each line measurement increases the robustness. In images from a flatbed scanner, the same information can be derived from the known resolution in dpi:

$$\frac{x}{25{,}400} \qquad \text{eq. 1}$$

Where *x* is the resolution of the scanned image in dpi. A resolution of 1500 dpi, for instance, corresponds to 0.059055 pixels·µm^{-1}

Image processing

In images showing deficiencies, the next step is image processing, which helps to increase contrast and enhance edges of target anatomical structures. Some specialized image analysis tools do this automatically. The example in Figure 9 shows how an unremoved dust particle on a permanent slide (cf. Figure 5) is removed by contrast homogenization, thus resulting in a more complete recognition of tracheid lumina. In general, image processing should be used conservatively as it can change the dimensions of anatomical features in the image. Generally, the better the quality of the anatomical sample and image the less image processing is required to detect and quantify the targeted anatomical structures.

Image segmentation

The original or processed image usually needs to be converted into a black-and-white (binary) image that allows discrimination between target and non-target structures (Figure 10). In this step called 'segmentation' or 'thresholding' a color or intensity value that optimizes this separation is – depending on the image-analysis tool – manually or automatically defined. Inhomogeneous image brightness and contrast due to inappropriate light source, uneven sample flatness or thickness and sample pollutions (cf. Figure 9) make it difficult or impossible to find a segmentation threshold that accurately discriminates between target and non-target structures in the entire image; such artifacts should therefore be avoided or corrected. The incorrect selection of a segmentation threshold can easily influence the data by 5-10%, particularly when the anatomical features in the image are not well defined because of poor contrast and focus. The segmented image is the basis for quantifying the anatomical features.

Detecting and measuring anatomical features

The segmented (binary) image is the basis for detecting and measuring anatomical features. Most image analysis tools represent the anatomical features as vectors instead of pixels (Table 1), which is usually better because irregularities can be corrected more easily (Figure 11), and the results are given in sub-pixel resolution.

Improving score and accuracy of anatomical feature detection using filters

Most image-analysis tools include size filters to automatically exclude objects that are too small or too large. Moreover, specialized tools offer automatic filters based on color and shape (Table 1). Some specialized tools such as ROXAS also include shape corrections, e.g. to correct for particles and ripped-off cell walls that protrude into the cell lumen (Figure 12), and context-based filters that allow, for example, to filter out cells that strongly deviate from the closest neighboring cells.

Manual editing

To obtain quality results and deal with image deficiencies, final manual editing is often necessary after automated detection and filtering of anatomical features. Specialized image-analysis tools offer efficient editing options for deleting, adjusting and adding anatomical features. However – and this cannot be stressed too much – it is generally several times more efficient to invest time into high-quality anatomical slides and images rather than to manually improve a suboptimal automated feature detection.

Xylem anatomical metrics and data storing

Specialized image-analysis tools automatically extract many metrics from the visual output and save them into data files, others offer manual export functions. Examples of primary, but also several derived anatomical metrics that are used to address many distinct research questions can be seen in the instruction film by von Arx *et al.* (2015b).

Among the primary measurements are: width and calendar year of annual rings, number, position and dimensions of conduits, resin ducts and rays (globally / within annual rings), cell wall thickness (conduits, fibers).

Among the many derived metrics calculated manually or automatically by some image analysis tools are: mean hydraulic diameter Dh (lumen diameter corresponding to the mean hydraulic conductivity of all conduits; Sperry et al., 1994), conduit and resin duct density (no./mm^2; Scholz et al., 2013), vessel grouping indices (connectivity among vessels; von Arx et al., 2013), Mork's index (an indicator for anatomical wood density in conifers; Denne, 1989), bending

resistance index $(t/b)^2$ (cell implosion safety; Hacke et al., 2001), theoretical hydraulic conductance based on Poiseuille's law (Tyree and Zimmermann, 2002).

Quality control

How much manual editing is needed? We recommend to define this by comparing the output of the target anatomical parameters after no, moderate and perfect manual editing for one to a few representative subset images (e.g. including 1000-2000 cells from both early- and latewood). If all previous steps were done properly the output with no or moderate editing will not deviate from the (near to perfect) output obtained after heavy-editing by more than 1-2%; this is an accuracy we deem sufficient for most purposes.

2.4 Conclusions

In this paper we provided some practical guidance and identified several pitfalls to successfully use quantitative wood anatomy in research. Producing xylem anatomical data is a challenging multi-step approach from sample collection to image analysis. As we showed with a few examples, potential measurement errors in many steps are between 5 to 20 or even 30%, which is in the same range as the variability of the anatomical metrics of interest, at least when excluding partly much stronger interspecific and ontogenetic variability. This is exacerbated by the fact that deficiencies in one step propagate to the next step, sometimes scaling up. The neglect of following a rigid and standardized procedure in terms of cutting thickness, staining, and illumination settings can therefore introduce considerable measurement errors and reduce the quality of the xylem anatomical dataset. While the specific measurement errors due to sample and image deficiencies can differ significantly within the smallest and the largest anatomical features, sometimes even changing from over- to underestimation, they are usually strongest in the smaller features such as latewood cell lumina and cell wall thickness. This is of particular relevance if the research goals are oriented towards, for example, intra-annual density profiles including maximum latewood density, or mechanical strength of cells. Although during image analysis the presented measurement errors can be reduced by defining specific settings for each image and manual editing, this is subjective, often very time-consuming, and generally still produces less accurate data than minimizing problems beforehand. The importance of producing high-quality anatomical slides and images can therefore not be stressed too much in terms of efficiency and accuracy. Then, quantitative wood anatomy is a very powerful tool that can give novel and mechanistic insights into the relationships between tree growth and environment over decades and even centuries.

Contributions

All authors planned and designed the research. GvA and MC prepared the anatomical images. GvA performed the quantitative analyses. GvA wrote the first draft of the manuscript, which was finalized with contributions from all authors.

Acknowledgments

We thank L. Schneider for sharing his experience in sample preparation, and L. Schneider and P. Züst for preparing some of anatomical microslides and images. GvA was supported by a grant from the Swiss State Secretariat for Education, Research and Innovation SERI (SBFI C14.0104). This work profited from discussions within the framework of the COST Action STReESS (COST-FP1106).

Tables

Table 1: Overview of some image-analysis tools used for quantifying anatomical features.

	Tool	Cell size	Cell wall thickness	Tree-ring analyses	Cell filtering	Object model	Interactive editing	Some Other features	License
Specialized tools	ROXAS	Yes	Automatic	Automatic	Size, color, shape, context	Vector	Yes	- Analyzing large images (up to 1,000,000 cells) - Large set of anatomical output parameters - Automatic image processing - Batch processing options - Online library & customization of tailored configurations	Free, but requires commercial Image-Pro Plus
	WinCELL	Yes	Automatic	Manual	Size, color, shape	Pixel	Yes	- Large set of anatomical output parameters - Batch processing options - Customizing tailored configurations - Microscope & scanner control	Commercial
General tools	ImageJ	Yes	Manual	No	Size, Shape	Vector	No	- Large collection of plugins by community - Macro development tools	Free
	CellProfiler	Yes	Manual	No	Size, color, shape	Vector	Yes	- Batch analyzing large sets (>1000) of images - Automating workflow using modules	Free
	Image-Pro Plus	Yes	Manual	No	Size, color, shape	Vector	Yes	- Powerful image processing and analysis functions - Macro development tools	Commercial
	NIS-Elements	Yes	Manual	No	Size, shape	Vector	Yes	- Macro development tools - Microscope control	Commercial
	AxioVision	Yes	Manual	No	Size, shape	Vector	Yes	- Automating workflow & macro development tools - Microscope control	Commercial

Figure captions

Figure 1: Damage to cell walls due to dull blades in *Pinus heldreichii* cross-sections of (a) 15 µm and (b) 30 µm thickness. In conifer samples, wall fragments rip off particularly easily at bordered pits. Such problems are aggravated in thinner sections as in panel (a). Scale bar = 100 µm.

Figure 2: *Pinus sylvestris* cross-sections of 15 µm thicknesses from the same wood piece cut with (a) cutter and (b) high-quality blades. Problems with disrupted cell structures can often be significantly reduced by using high-quality blades. Scale bar = 100 µm.

Figure 3: Cross-sections of *Pinus heldreichii* cut from a not properly oriented sample, i.e. cutting direction that is not perpendicular to the axial tracheid orientation. Non-orthogonal cross-sections result in underestimation of lumen area and overestimation of cell wall thickness. These measurement errors are weaker in (a) thinner than in (b) thicker sections as revealed after analyzing the entire images (c. 2500 cells; only subset images shown here) with the image-analysis tool ROXAS (cf. Table 1): mean cell lumen area in (b) was 43% smaller and mean tangential cell wall thickness 46% larger than in (a). Scale bar = 100 µm.

Figure 4: (a) Series of cross-sections of the same *Pinus heldreichii* wood piece using different cutting thicknesses from 10 to 40 µm (top row). The anatomical images are part of larger analyzed images containing each c. 4000 tracheids cells. The orientation of the samples is reasonably vertical, and images were produced keeping staining procedure and microscope settings standardized. Analyzing the images with the image-analysis tool ROXAS (cf. Table 1) using always the same settings reveals that the measured lumen area reduces markedly from the thinner to the thicker cross-sections (b). This effect is stronger for smaller cells with a 31% reduction in the lowest percentile of the cell lumen population (CA1) than for the largest cells with only 4-6% reduction (CA90, CA99). In contrast, the mean tangential cell wall thickness appears also for the thinnest walls (CWT1, belonging to the largest cells) up to 30% larger in thicker compared to thinner cross-sections. For the thickest cell walls (CWT99, belonging to the smallest cells) the

cutting-thickness error was up to 40%. Note that the quantification of the measurement errors is based on the shown example only. To a certain extent some of the cutting-thickness errors can be alleviated by adjusting the settings of the image analyses, particularly the segmentation threshold (see paragraph "4.4 Image segmentation" and Figure 10). Scale bar = 100 µm.

Figure 5: Image of a slide with some pollution as indicated by yellow arrows (a) before and (b) after cleaning (*Pinus sylvestris*). Scale bar = 100 µm.

Figure 6: Anatomical images of the same *Pinus sylvestris* microslide illustrating how imporper microscope settings such as (a) wrong white balance and (b) over-illumination reduce image contrast compared to (c) optimal settings. Suboptimal microscope settings may impede automatic detection of anatomical features and result in under- and overestimation of anatomical features. Scale bar = 100 µm.

Figure 7: The same anatomical microslide of *Pinus sylvestris* once captured (a) out of focus and (b) with optimal focus (only subset images shown). The entire images were analyzed with the image-analysis tool ROXAS (cf. Table 1) using always the same settings. In the out-of-focus image, 178 small tracheids out of totally 4240 (4.2%) were not detected, because lumina of very narrow tracheids were insufficiently defined. Accordingly, the lumen area corresponding to the smallest 1% of the measured values (CA1) were 69% larger in the poorly-focused than the well-focused image, while in the largest tracheids (CA99) the lumina appeared 1% smaller in the poorly -focused images. Similarly, the thickest tangential cell walls (CWT99, corresponding to the very small tracheids) were overestimated by 9% in the poorly-focused compared to the well-focused image, while they were underestimated by 4% towards the thinnest walls (CWT1). Scale bar = 100 µm.

Figure 8: (a) Overlapping high-resolution images stitched together using PTGui and (b) the obtained high-resolution image of an entire *Verbascum thapsus* root cross-section. The used overlap with neighboring images is visualized for one of the images with yellow dashed lines in (a). The input images contained distortions introduced by the used optical system, which were successfully removed by PTGui (verified by creating a composite

image of a stage micrometer and measuring the distances between tick marks, which yielded constant values throughout the image). Five randomly selected vessels along a transect (see labels in b) having an lumen area between 100 and 3500 μm^2 were subsequently measured using ROXAS using always the same settings in images stitched with the software PTGui, AutoStitch, Microsoft Image Composite Editor and Photoshop (Automatic and Reposition settings). Panel (c) shows the percentage deviation of the obtained values compared to the PTGui reference values. The values in all used stitching tools and settings deviate from the PTGui reference, thus indicating distortions. In addition, the magnitude of the deviations varied along the transect often changing from over- to underestimation. Note that Photoshop Reposition setting also produces distortion-free images if input images are already distortion-free, while AutoStitch still introduces distortions. Scale bar = 1 mm.

Figure 9: Top row shows how tracheid lumina obscured by a dust particle on the cover glass of a *Pinus leucodermis* sample remain undetected using ordinary image processing, bottom row shows how contrast homogenization technique (using the image analysis tool ROXAS in this case) allows to automatically detect all lumina. Scale bar = 100 μm.

Figure 10: (a) Anatomical image of a *Pinus sylvestris* sample with (b) visualization of the segmentation threshold by a green mask and (c) the resulting binary image after performing the segmentation, which is the basis for quantifying the anatomical features. Depending on the image-analysis software the segmentation is applied to the original or processed color image, or a gray-scale image resulting from one to several image-processing steps (cf. Figure 9). Scale bar = 100 μm.

Figure 11: Defining the anatomical features in a (a) sub-optimal image of *Quercus petrea* (surface scan, 2400 dpi) as (b) vector instead of (c) pixel objects allows to correct some sample artifacts, e.g. by applying a convex outline filter. Panel (d) compares the percent deviation of vessel lumen area when representing the identical vessels in the selected image as pixels vs. vectors after analyzing the entire sample (>2500 vessels) with the image-analysis tool ROXAS. 20.2% of the measured values deviate by ≥5% from the supposedly more accurate vector object value, and 4.3% by ≥10%. While underestimation

of lumen area in the pixel representation can be very strong due to artifacts as highlighted by the yellow arrows in (a-c), pixel representation also resulted in slight overestimation (<5%) of 21.6% of all vessels because of pixel rounding effects. Note that some of these deviations can be significantly reduced by manual editing. Scale bar = 1 mm.

Figure 12: (a) Cross-section of *Pinus sylvestris* showing ripped-off cell walls. (b) Same sample with overlay of detected lumen outlines (cyan) without any correction, resulting in measurement errors. (c) A convex outline filter can correct such artifacts, but may also cut off true concavities in the lumen outlines, e.g. due to pit inflections, while (d) a more powerful 'protrusion filter' (as implemented in the image-analysis tool ROXAS) better discriminates between artifacts and true concavities (*Pinus sylvestris*). Scale bar = 100 µm.

Figures

Figure 1:

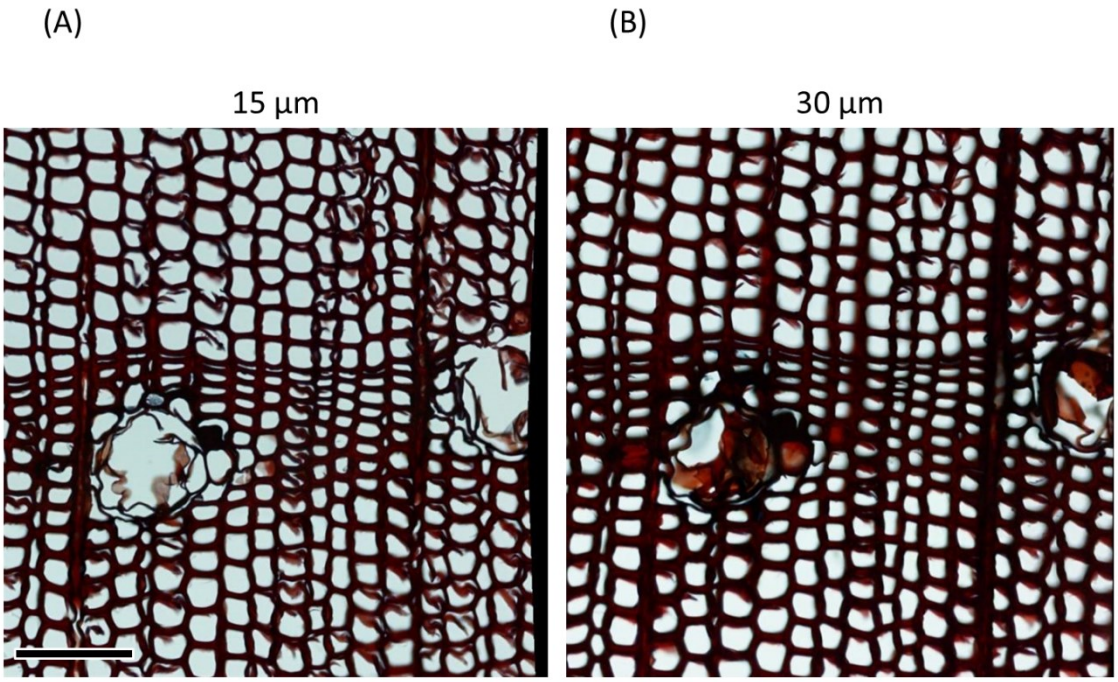

Figure 2:

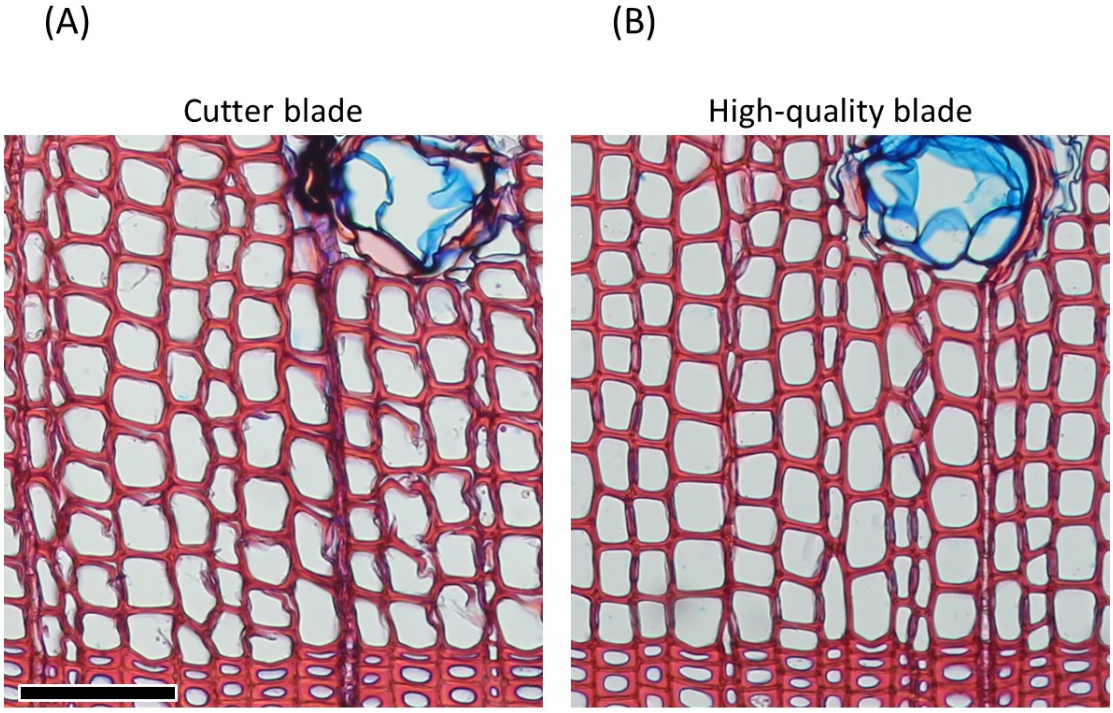

Figure 3:

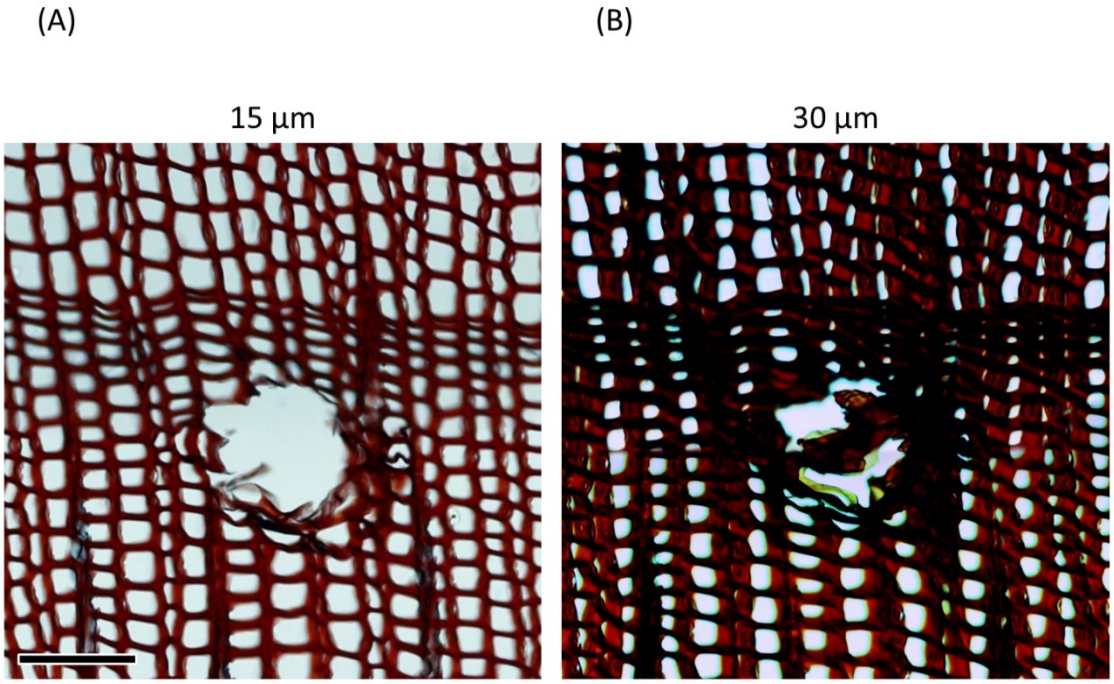

Figure 4:

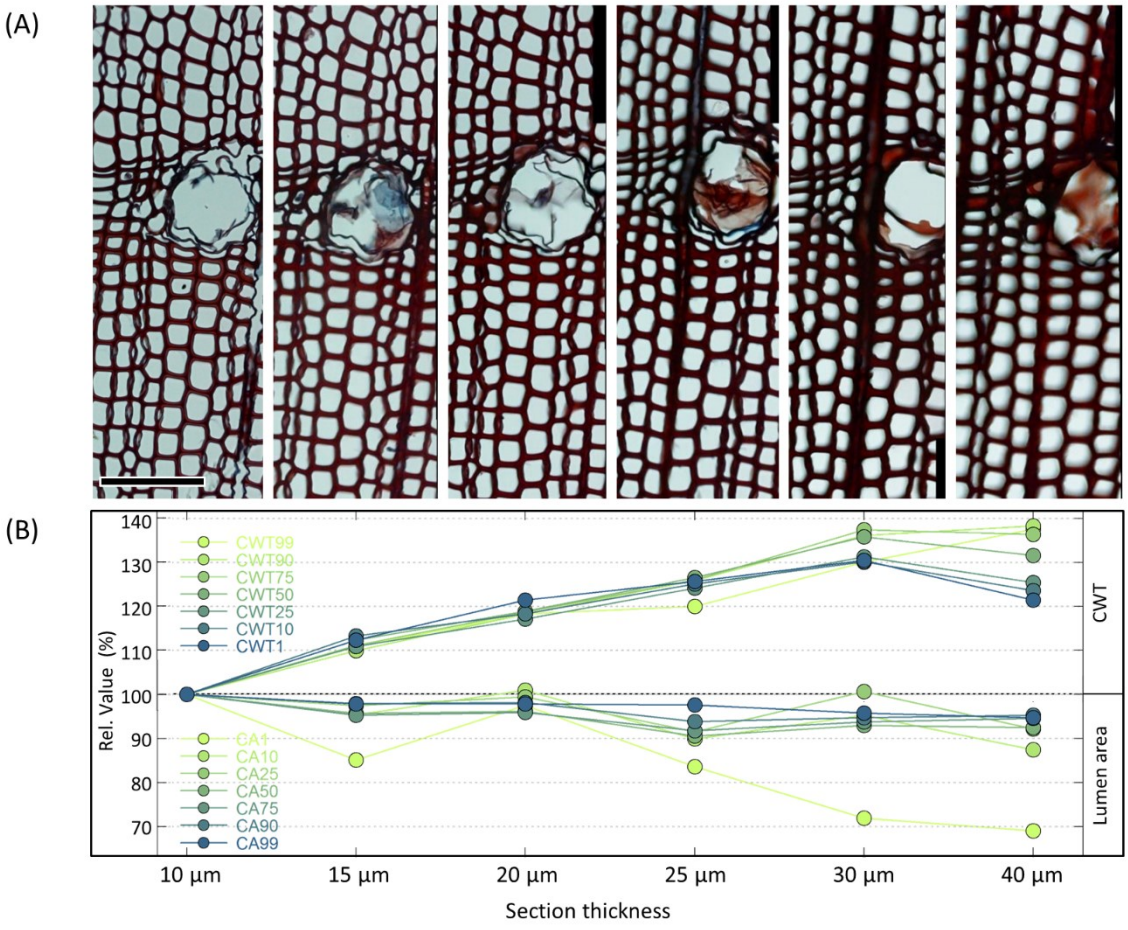

Figure 5:

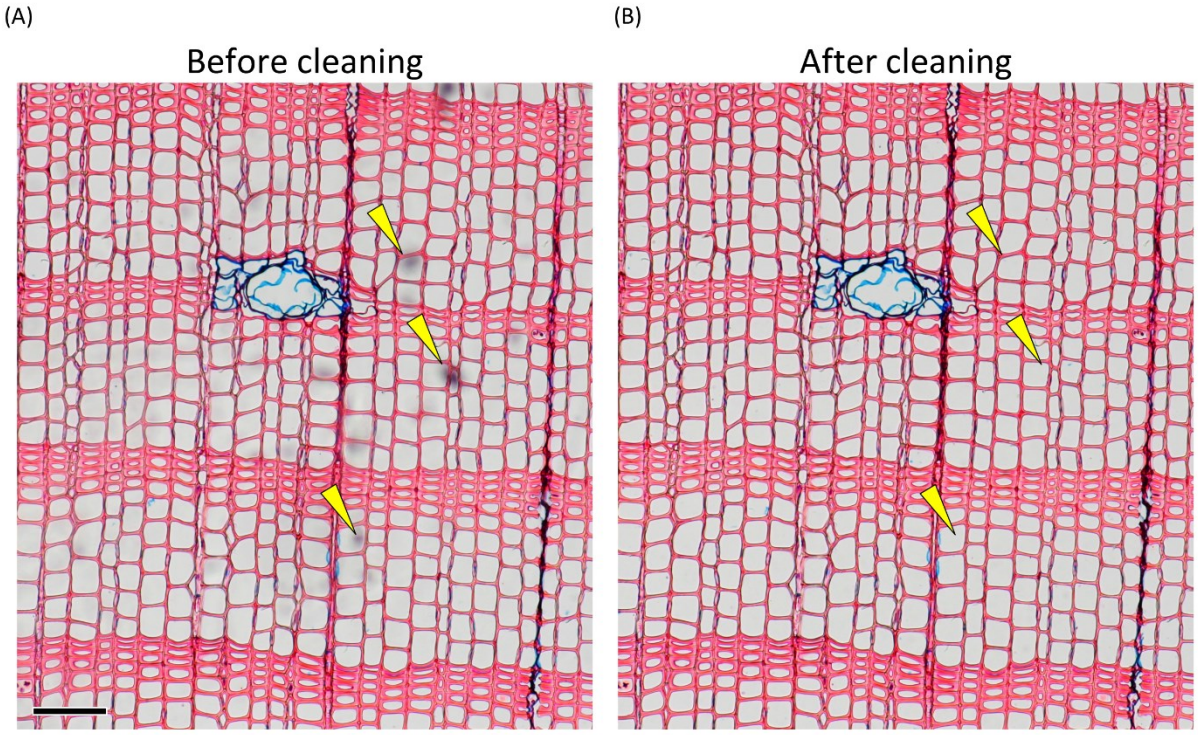

Figure 6:

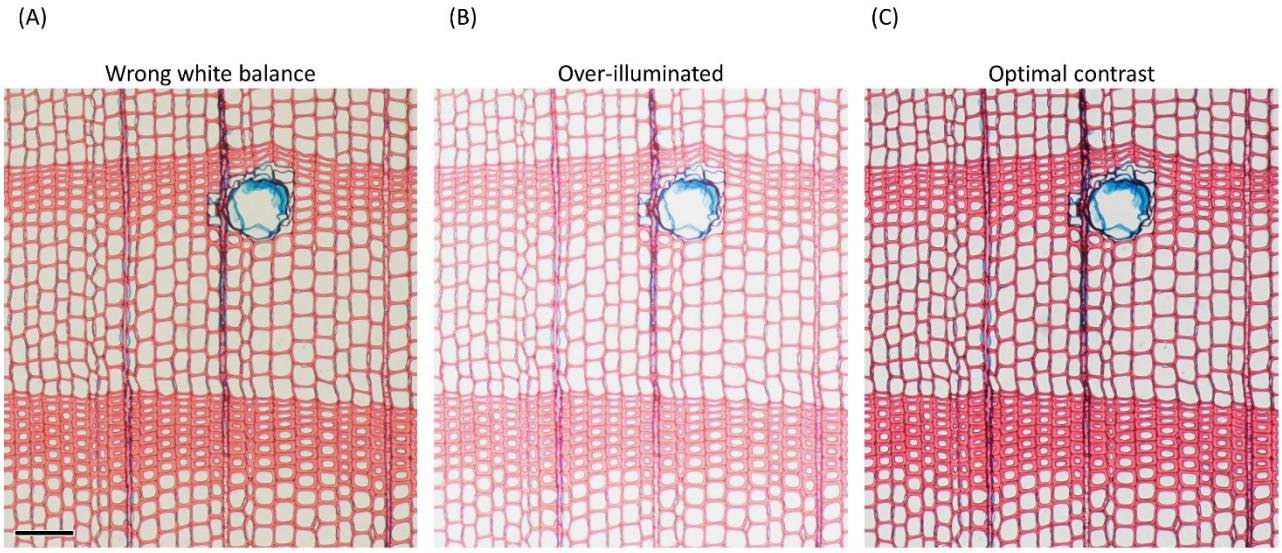

Figure 7:

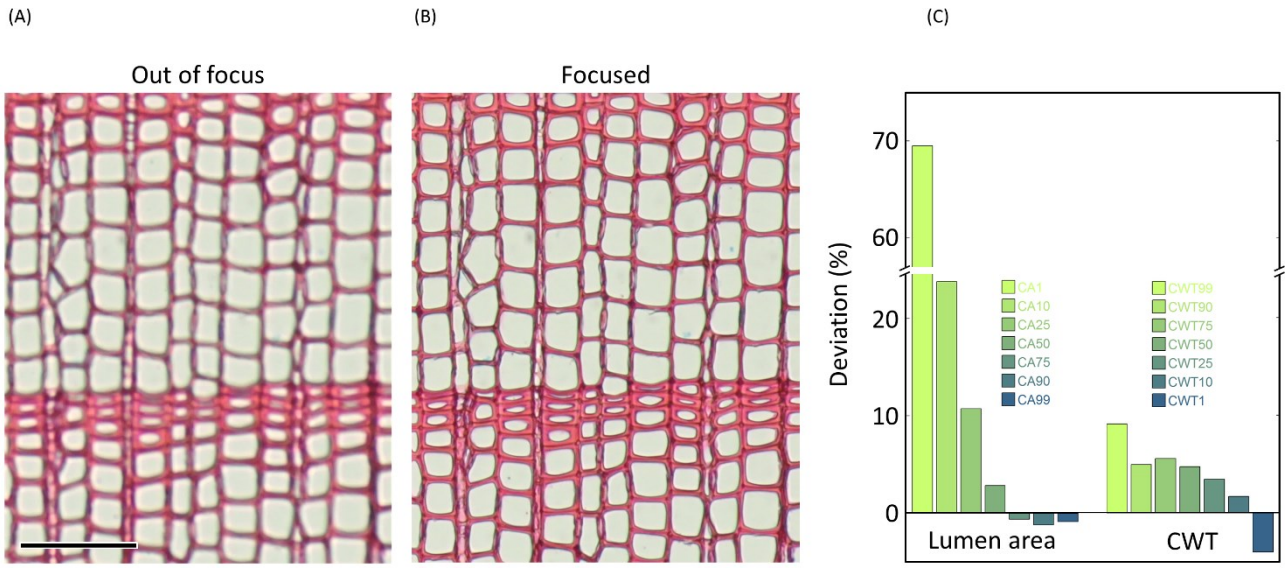

Figure 8:

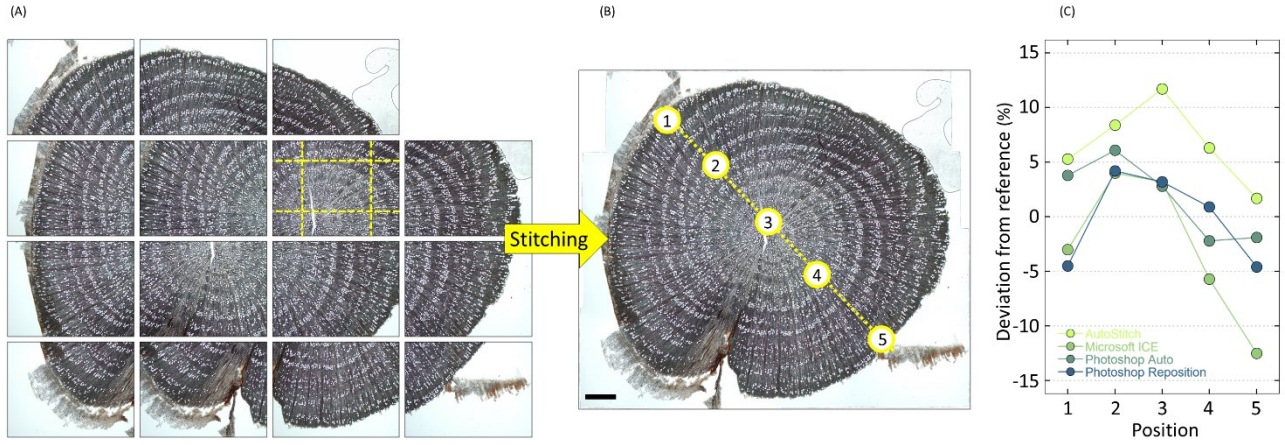

Figure 9:

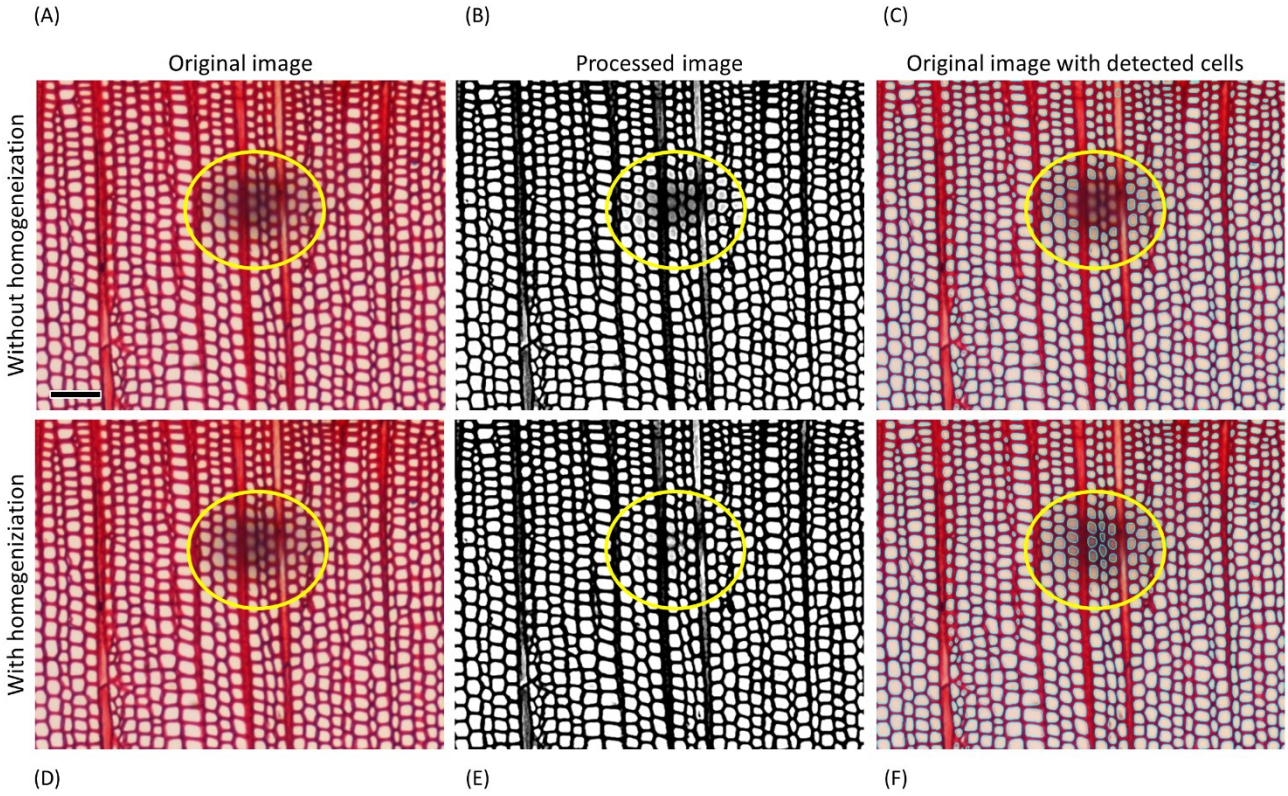

Figure 10:

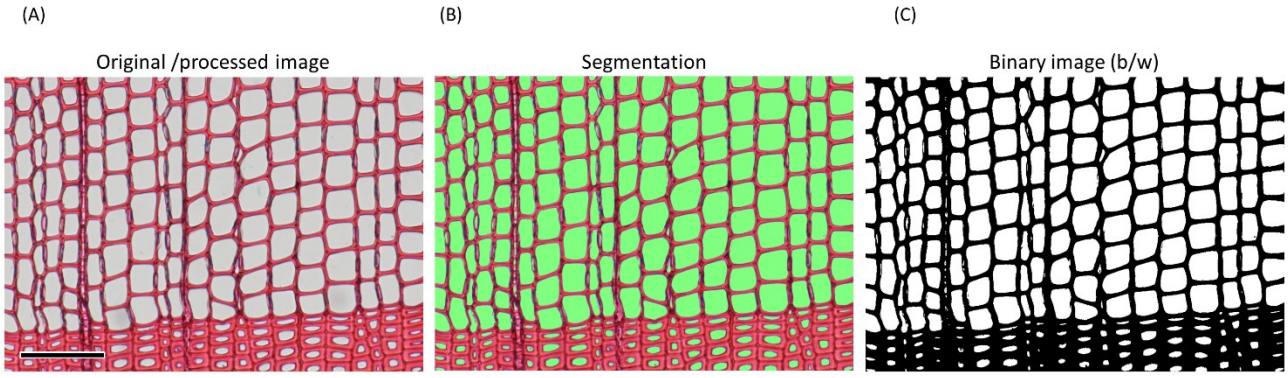

Figure 11:

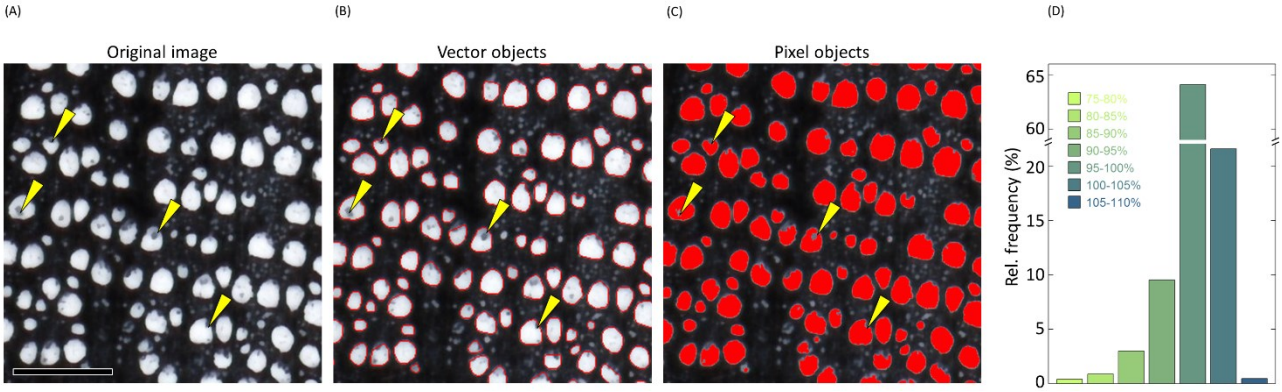

Figure 12:

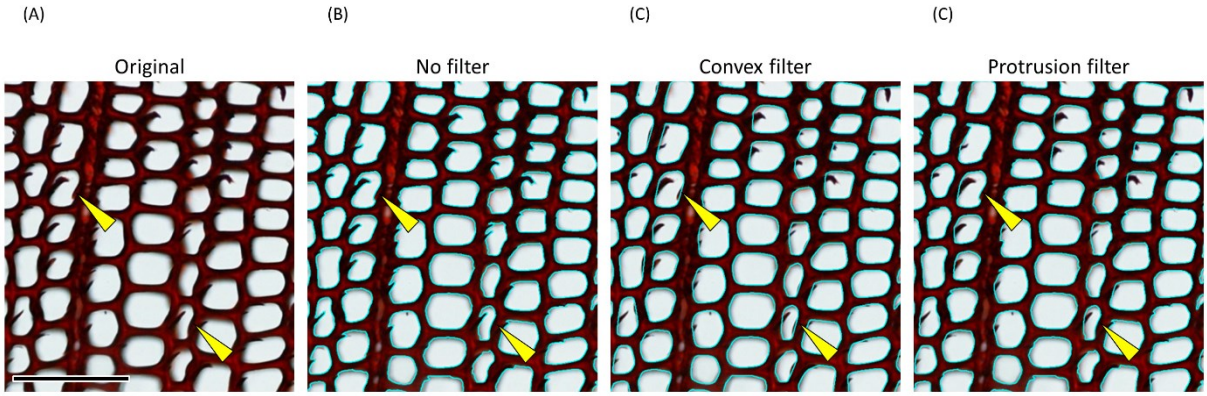

2.5 References

Aloni, R. (2013). Role of hormones in controlling vascular differentiation and the mechanism of lateral root initiation. *Planta* 238**,** 819-830.

Arbellay, E., Corona, C., Stoffel, M., Fonti, P., and Decaulne, A. (2012). Defining an Adequate Sample of Earlywood Vessels for Retrospective Injury Detection in Diffuse-Porous Species. *PLoS ONE* 7**,** e38824.

Carrer, M., von Arx, G., Castagnieri, D., and Petit, G. (2015). Distilling environmental information from time series of conduit size: the standardization issue and its relation to allometric and hydraulic constraints. *Tree Physiology* 35**,** 27-33.

Castagneri, D., Petit, G., and Carrer, M. (2015). Divergent climate response on hydraulic-related xylem anatomical traits of Picea abies along a 900-m altitudinal gradient. *Tree Physiology* 35**,** 1378-1387.

Crivellaro, A., and Schweingruber, F.H. (2015). *Stem Anatomical Features of Dicotyledons. Xylem, Phloem, Cortex and Periderm Characteristics for Ecological and Taxonomical Analyses.* Remagen-Oberwinter: Kessel Publishing House.

Cuny, H.E., Rathgeber, C.B., Frank, D., Fonti, P., Mäkinen, H., Prislan, P.*, et al.* (2015). Woody biomass production lags stem-girth increase by over one month in coniferous forests. *Nature Plants* 1**,** 15160.

Cuny, H.E., Rathgeber, C.B.K., Frank, D., Fonti, P., and Fournier, M. (2014). Kinetics of tracheid development explain conifer tree-ring structure. *New Phytologist* 203**,** 1231-1241.

Denne, M.P. (1989). Definition of latewood according to Mork (1928). *IAWA Bulletin* 10**,** 59-62.

Eilmann, B., Sterck, F., Wegner, L., De Vries, S.M.G., von Arx, G., Mohren, G.M.J.*, et al.* (2014). Wood structural differences between northern and southern beech provenances growing at a moderate site. *Tree Physiology* 34**,** 882-893.

Fonti, P., Bryukhanova, M.V., Myglan, V.S., Kirdyanov, A.V., Naumova, O.V., and Vaganov, E.A. (2013). Temperature-induced responses of xylem structure of Larix sibirica (Pinaceae) from Russian Altay. *American Journal of Botany* 100**,** 1332-1343.

Fonti, P., Eilmann, B., Garcia-Gonzalez, I., and von Arx, G. (2009). Expeditious building of ring-porous earlywood vessel chronologies without loosing signal information. *Trees-Structure And Function* 23**,** 665-671.

Fonti, P., Heller, O., Cherubini, P., Rigling, A., and Arend, M. (2013). Wood anatomical responses of oak saplings exposed to air warming and soil drought. *Plant Biology* 15**,** 210-219.

Fonti, P., Solomonoff, N., and García-González, I. (2007). Earlywood vessels of Castanea sativa record temperature before their formation. *New Phytologist* 173**,** 562-570.

Fonti, P., Tabakova, M., Kirdyanov, A., Bryukhanova, M., and von Arx, G. (2015). Variability of ray anatomy of Larix gmelinii along a forest productivity gradient in Siberia. *Trees - Structure and Function* 29**,** 1165-1175.

Fonti, P., von Arx, G., García-González, I., Eilmann, B., Sass-Klaassen, U., Gärtner, H.*, et al.* (2010). Studying global change through investigation of the plastic responses of xylem anatomy in tree rings. *New Phytologist* 185**,** 42-53.

Gärtner, H., and Nievergelt, D. (2010). The core-microtome: A new tool for surface preparation on cores and time series analysis of varying cell parameters. *Dendrochronologia* 28**,** 85-92.

Gärtner, H., and Schweingruber, F.H. (2013). *Microscopic preparation techniques for plant stem analysis.* Remagen: Kessel Publishing House.

Gričar, J., Prislan, P., Gryc, V., Vavrčík, H., De Luis, M., and Čufar, K. (2014). Plastic and locally adapted phenology in cambial seasonality and production of xylem and phloem cells in Picea abies from temperate environments. *Tree Physiology* 34**,** 869-881.

Guet, J., Fichot, R., Lédée, C., Laurans, F., Cochard, H., Delzon, S.*, et al.* (2015). Stem xylem resistance to cavitation is related to xylem structure but not to growth and water-use efficiency at the within-population level in Populus nigra L. *Journal of Experimental Botany* 66**,** 4643-4652.

Hacke, U.G., Sperry, J.S., Pockman, W.T., Davis, S.D., and Mcculloh, K.A. (2001). Trends in wood density and structure are linked to prevention of xylem implosion by negative pressure. *Oecologia* 126**,** 457-461.

Hereş, A.-M., Camarero, J., López, B., and Martínez-Vilalta, J. (2014). Declining hydraulic performances and low carbon investments in tree rings predate Scots pine drought-induced mortality. *Trees - Structure and Function* 28**,** 1737-1750.

Iawa Committee (1989). IAWA list of microscopic features for hardwood identification. *IAWA Bulletin* 10**,** 219-332.

Iawa Committee (2004). IAWA list of microscopic features for softwood identification. *IAWA Journal* 25**,** 1-70.

Mccrone, W.C. (1980). Checklist for true Kohler Illumination. *American Laboratory* 12**,** 96-98.

Olano, J.M., Arzac, A., García-Cervigón, A.I., von Arx, G., and Rozas, V. (2013). New star on the stage: amount of ray parenchyma in tree rings shows a link to climate. *New Phytologist* 198**,** 486-495.

Olson, M.E., Anfodillo, T., Rosell, J.A., Petit, G., Crivellaro, A., Isnard, S.*, et al.* (2014). Universal hydraulics of the flowering plants: vessel diameter scales with stem length across angiosperm lineages, habits and climates. *Ecology Letters* 17**,** 988–997.

Pacheco, A., Camarero, J.J., and Carrer, M. (2015). Linking wood anatomy and xylogenesis allows pinpointing of climate and drought influences on growth of coexisting conifers in continental Mediterranean climate. *Tree Physiology* 36**,** 502-512.

Pellizzari, E., Camarero, J.J., Gazol, A., Sangüesa-Barreda, G., and Carrer, M. (2016). Wood anatomy and carbon-isotope discrimination support long-term hydraulic deterioration as a major cause of drought-induced dieback. *Global Change Biology* 22**,** 2125-2137.

Petit, G., Anfodillo, T., Carraro, V., Grani, F., and Carrer, M. (2011). Hydraulic constraints limit height growth in trees at high altitude. *New Phytologist* 189**,** 241-252.

Pfautsch, S., Harbusch, M., Wesolowski, A., Smith, R., Macfarlane, C., Tjoelker, M.G.*, et al.* (2016). Climate determines vascular traits in the ecologically diverse genus Eucalyptus. *Ecology Letters* 19**,** 240-248.

Prislan, P., Gričar, J., De Luis, M., Smith, K.T., and Čufar, K. (2013). Phenological variation in xylem and phloem formation in Fagus sylvatica from two contrasting sites. *Agricultural and Forest Meteorology* 180**,** 142-151.

Rasband, W.S. (1997-2016). *ImageJ.* Bethesda, Maryland, USA: U. S. National Institutes of Health.

Rita, A., Cherubini, P., Leonardi, S., Todaro, L., and Borghetti, M. (2015). Functional adjustments of xylem anatomy to climatic variability: insights from long-term Ilex aquifolium tree-ring series. *Tree Physiology* 35**,** 817-828.

Schneider, L., and Gärtner, H. (2013). The advantage of using a starch based non-Newtonian fluid to prepare micro sections *Dendrochronologia* 31**,** 175-178.

Scholz, A., Klepsch, M., Karimi, Z., and Jansen, S. (2013). How to quantify conduits in wood? *Frontiers in Plant Science* 4.

Seo, J.-W., Smiljanic, M., and Wilmking, M. (2014). Optimizing cell-anatomical chronologies of Scots pine by stepwise increasing the number of radial tracheid rows included-Case study based on three Scandinavian sites. *Dendrochronologia* 32**,** 205-209.

Sperry, J.S., Nichols, K.L., June, E.M.S., and Eastlack, S.E. (1994). Xylem Embolism in Ring-Porous, Diffuse-Porous, and Coniferous Trees of Northern Utah and Interior Alaska. *Ecology* 75**,** 1736-1752.

Tyree, M.T., and Zimmermann, M.H. (2002). *Xylem structure and the ascent of sap.* Berlin, Heidelberg, New York, Tokyo: Springer.

von Arx, G., Archer, S.R., and Hughes, M.K. (2012). Long-term functional plasticity in plant hydraulic architecture in response to supplemental moisture. *Annals of Botany* 109**,** 1091-1100.

von Arx, G., Arzac, A., Olano, J.M., and Fonti, P. (2015a). Assessing conifer ray parenchyma for ecological studies: pitfalls and guidelines. *Frontiers in Plant Science* 6.

von Arx, G., and Carrer, M. (2014). ROXAS - a new tool to build centuries-long tracheid-lumen chronologies in conifers. *Dendrochronologia* 32**,** 290-293.

von Arx, G., and Dietz, H. (2005). Automated image analysis of annual rings in the roots of perennial forbs. *International Journal of Plant Sciences* 166**,** 723-732.

von Arx, G., Kueffer, C., and Fonti, P. (2013). Quantifying vessel grouping – added value from the image analysis tool ROXAS. *IAWA Journal* 34**,** 433-445.

von Arx, G., Stritih, A., Čufar, K., Crivellaro, A., and Carrer, M. (2015b). "Quantitative Wood Anatomy: From Sample to Data for Environmental Research". doi: 10.13140/RG.2.1.3323.0169

Yeung, E.C.T., Stasolla, C., Sumner, M.J., and Huang, B.Q. (2015). *Plant Microtechniques and Protocols.* Springer.

3. New research perspectives from a novel approach to quantify tracheid wall thickness

Angela Luisa Prendin[1*], Giai Petit[1], Marco Carrer[1], Patrick Fonti[2], Jesper Björklund[2], Georg von Arx[2]

[1] Department TeSAF, Dept. Territorio e Sistemi Agro-Forestali, Università degli Studi di Padova, Viale dell'Università 16, 35020 Legnaro (PD), Italy

[2] Swiss Federal Institute for Forest, Snow and Landscape Research WSL, Zürcherstrasse 111, 8903 Birmensdorf, Switzerland

*** Corresponding author**

Keywords: automated image analysis, carbon allocation, quantitative wood anatomy, radial cell wall thickness, ROXAS, tangential cell wall thickness

3.1 Abstract

The analysis of xylem cell anatomical features in dated tree-rings provides insight into xylem functional responses and past growth conditions at intra-annual resolution. So far, special focus has been given to the lumen of the water-conducting cells, whereas the equally relevant cell wall thickness (CWT) has been less investigated due to methodological limitations. Here we present a novel approach to measure tracheid CWT in high-resolution images of wood cross-sections based on recognized tracheid lumina that is implemented within the specialized image-analysis tool 'ROXAS'. Compared to the traditional manual line measurements along a selection of few radial files, this novel method: i) measures CWT of all tracheids in a tree ring, thus increasing the number of individual tracheid measurements by a factor of about ten to twenty; ii) measures separately the tangential and newly the radial walls; and iii) laterally expands the line measurements in a customizable way, thus integrating the wall thickening from the thinnest central part towards the corners of the tracheids. CWT measurements performed with this novel and the traditional manual approach showed comparable accuracy for several image resolutions, with an optimal accuracy-efficiency balance at 100× magnification. The configurable settings affected both the absolute and intra-annual patterns of CWT, in particular estimates of cell wall material resulted 10-13% larger with a higher level of wall integration. This versatility, together with the high data production capacity, thus allows to tailor the assessment of CWT to the goal of the study, which opens new research perspectives, e.g. for investigating structure-function relationships, tree stress responses and carbon allocation patterns, and for reconstructing climate based on intra- and interannual variability of wood density.

3.2 Introduction

Tracheids, appearing earlier in evolution than vessels, are the primary anatomical units of plant growth and carbon sequestration in conifers. Tracheary elements are connected through large, circular bordered pits that are concentrated at the tapered ends (in the radial walls) of the cells (Myburg and Sederoff 2001). These mature elements are terminally differentiated, empty dead cells for water conduction that may also function in mechanical support by means of their lignified, thickened and strong secondary cell walls (Myburg et al. 2013). Earlywood tracheids are characterized by wide lumina and mainly responsible for water transport from roots to leaves. Latewood tracheids, with the reduced lumen size and thicker cell walls, in contrast provide most of the mechanical support for the upright posture and general architecture of the plant (Denne, 1988; Koubaa *et al.*, 2002; Myburg et al. 2013). The structural properties of tracheids are strongly determined by genetic and hormonal control (Aloni, 2013) and functional needs (Carrer *et al.*, 2015), but also with significant imprints from environmental conditions (Park and Spiecker 2005, Handa et al. 2006, Cuny and Rathgeber 2016). Retrospectively relating the intra- and inter-ring variability of structural tracheid properties along series of dated tree rings ('quantitative wood anatomy'; see von Arx *et al.,* 2016) can therefore be used to infer past environmental conditions or tree functional responses (Fonti *et al.,* 2010). However, until now investigations have mainly focused on the variability of conductive ability through tracheid lumen dimensions, while only few studies investigated the wall thickness (CWT) (Spiecker et al. 2000, Park and Spiecker 2005) and SilviScan papers. Despite the important role of CWT for mechanical support, hydraulic safety and carbon allocation, as seen in investigations of structure-function relationships (Rosner *et al.,* 2016) and responses to extreme events inducing mortality (Heres *et al.*, 2014; Pellizzari *et al.*, 2016), but also when considering that CWT is a key feature determining the intra- and interannual variability of wood density, one of the most used proxy for climate reconstructions (e.g., Briffa *et al.,* 1998; Büntgen *et al.,* 2010) and global carbon budget (e.g., Cuny *et al.*, 2015).

Several measurements constraints still represent the main obstacle for a wider use of CWT in environmental research. Currently, one of the most applied approaches is to manually measure the thickness of the cell walls in images of anatomical cross-sections

by using a line-measuring tool available in many imaging software. Usually, a few radial files (from bark to pith) with large tracheids are selected, and measurements are performed through the centre of the tangential double-cell wall connecting two neighbouring tracheids. This approach is very time consuming and subjective in terms of positioning and length of the measurement lines. The consequence is that studies using this approach can be limited in representativeness and statistical robustness by the low number of samples (trees), annual rings and radial files (e.g., Seo *et al.*, 2014). In addition, the radial cell walls are usually not considered since earlywood tracheids frequently contain swollen walls around the pits, which in thinner sections appear with pit chamber, torus and margo (Baas *et al.*, 2004). However, ignoring the radial cell walls, which are usually thicker than the tangential cell walls (Cuny & Rathgeber, 2016), will bias results with systematic under-estimations of the total cell wall material.

Here we present how the latest version of the image analysis tool 'ROXAS' (von Arx & Dietz, 2005; von Arx & Carrer, 2014) helps to overcome methodological challenges of CWT measurements through a robust, comprehensive, and customizable approach. In particular, we i) explain how the novel measurements are automatically performed (thus increasing about ten to twenty fold the number of measured tracheids) and highlight the versatility of the measurements; ii) compare the proposed automatic approach for CWT measurement to the traditional manual line measurement and assess the influence of image resolution (e.g. magnifications), sample quality, and invested manual editing effort; and iii) evaluate the scientific relevance of our novel approach in terms of extracted information.

3.3 Materials and Methods

The image analysis tool ROXAS

ROXAS v3.0 is the most updated version of an image analysis tool specifically designed to identify cell lumina in cross-sections of angiosperms and conifers to quantify xylem cell structures. It is built around the image processing and analysis capabilities of Image-Pro Plus ≥v6.1 (Media Cybernetics, USA) and provides comprehensive output files (von Arx and Carrer 2014). ROXAS automatically derives several cell anatomical structures and annual ring borders, but also allows the user to manually edit mis-identified lumina (von

Arx and Carrer 2014). In addition to the previous version, automatic detection of other anatomical features such as conduit wall reinforcement $(t/b)^2$ and cell wall thickness (CWT) is now provided for each cell, as well as in summarized form for each annual ring. Numerous settings, saveable in configuration files, give the user the flexibility to optimize and customize the analysis and output for the characteristics of the species and/or image. The workflow does not differ from the previous version (von Arx and Carrer 2014). More specific information can be found in (von Arx & Dietz, 2005; Fonti *et al.*, 2009; von Arx *et al.*, 2013; Wegner et al. 2013; von Arx & Carrer, 2014), whereas for general information on output parameters, applications and availability we refer to www.wsl.ch/roxas.

Specification on the measurement of tracheid cell wall thickness

A new feature of ROXAS is that it measures CWT on each side of a tracheid (tangential walls: towards pith and bark, radial walls: left and right). The measurement assumes equal share of wall thickness between neighbouring tracheids, with a possible consequence of over-under estimation of radial cell wall thickness for early wood and late wood neighboring tracheids, overall when the transition is abrupt (Baas et al. 2004). Basically, watershed lines are added at equidistance between all neighbouring tracheid lumina that were previously identified, and the distance from each lumen to the centre of this watershed line is taken as the CWT value of a given tracheid (see Fig. 1 for further technical details). Since there is currently no option implemented to manually edit CWT in the image, the measurements depend on the accuracy of the identified tracheid lumina. Important to note is that suboptimal ROXAS configurations and/or too low image resolution can result in inaccurate quantifications of lumina and thus also inaccurate CWT output. Data produced with older versions of ROXAS (von Arx & Carrer, 2014) that only provided lumina-related output can easily be updated to include also CWT measurements. To improve the reliability of the measurements, the user can specify the maximum possible width of a CWT measurement depending on the lumen area of the tracheid, which is intended to reflect the fact that the large earlywood tracheids generally have thinner walls than the small latewood cells. In addition, to exclude wrong assessment for tracheids adjacent to xylem rays or resin ducts, an adjustable filter based on the ratio between the CWT on opposite sides of the tracheid (pith vs. bark and left vs. right side of the tracheid) automatically flags values that are larger than a specified ratio (e.g., 1.5).

Moreover, by adjusting the sensitivity of a shape correction filter ('protrusion filter') designed to remove concavities in the recognized lumen outlines, the user can customize the relevance of the wall rounding caused by the pit structure in the radial walls. Another important customizable feature specific to ROXAS is related to the settings specifying the proportion of the lumen diameter that has to be considered for the assessment of CWT (Fig. 1a,d). Indeed, the cell walls can be measured at the centre of the tracheids, which is equivalent to manual line measurements, or can integrate the measurement over a defined portion of the lumen diameter (see parameter *b* in Fig. 1a). It is also possible to automatically create several datasets of CWT measurements with different integration parameter *b* based on a single tracheid lumen analysis. In addition, while we focused here on conifer tracheids, ROXAS can also be used to measure CWT in fibers of angiosperms.

Evaluating the robustness of ROXAS CWT measurements

For the comparative analysis among different ways to assess CWT we made use of anatomical micro-sections of a 40-years old individual of *Larix decidua* Miller (see Fig. 4a for an example) and of a mature *Pinus sylvestris* L. (see Fig. 5). The cross-sections were prepared following the protocol for cutting micro-sections and for collecting high-resolution images proposed by (von Arx et al. 2016). In short, 10-12 µm thick sections were cut with a rotary microtome (Leica RM2245, Leica Biosystems, Nussloch, Germany), stained with safranin and astrablue, and permanently fixed with Eukitt (BiOptica, Milan, Italy). The images used for the analyses were captured using a light microscope connected to a digital camera (Nikon Eclipse 80i, Nikon, Tokyo, Japan) at different magnifications and then stitched using PTGui (version 8.3.3, New House Internet Services B.V., Rotterdam, NL).

In a first comparison, we tested the correspondence between tangential CWT values using the line-measuring tool in Image-Pro Plus v6.1 and automatic ROXAS measurements without integration (i.e. 0% integration). This comparison was performed with two cross-sections of *L. decidua*, from the stem base and apex, for which images were taken with three different magnifications (40×, 100× and 400×, corresponding to 0.833, 2.074 and 8.296 pixels/µm, respectively). In a second trial, we quantified the effort necessary to improve the accuracy of CWT measurements for anatomical samples of different quality. Therefore, we selected three cross-sections of *L. decidua* of high, intermediate and low

quality (Table 1) and performed three levels of editing effort following the automatic ROXAS analysis, I: no editing; II: removing mis-identified cells in resin ducts and rays, splitting merged cells; III: as II, but in addition removing lumina of pit pores, adding missing cells, correcting inaccurate tracheid outlines. Thirdly, we evaluated the CWT values measured by ROXAS with different cell wall integration levels (see Fig. 1) using an image of a cross-section of *L. decidua* (containing 226 cells), taken with 100× magnification (2.074 pixels/µm). Finally, to illustrate a time series of cell wall thickness (CWT) measured with ROXAS we used images taken with 100× magnification (2.074 pixels/µm) of cross-sections of a full core (from pith to bark) of a *P. sylvestis*. Statistical analyses were performed using R (version 3.1.1.; R Development Core Team, 2014).

3.4 Results and Discussion

The comparison between measurements performed manually and through automatic ROXAS analysis showed an almost perfect 1:1 correspondence between the 400× and 100× magnification (Fig. 2), as also evidenced by ≥95% explained variation. With 40× magnification there was still a high correspondence for both analysed images, even though the data was more scattered (r^2=0.78 and 0.86). CWT measured with 100× did also not deviate strongly from the one with 400× magnification independent from the different CWT dimensional classes – considered here as a proxy for the intra-annual variation from earlywood to latewood – whereas the values from the 40× magnification deviated markedly in both ROXAS and manual measurements (Fig. 3). However, an integration level *b* of 75% reduced the variability of CWT values considerably compared to manual line measurements, even at 40× (Fig. 3a, b vs. 3e, f). Overall, these results suggest that ROXAS and manual CWT measurements have a high correspondence, particularly for the 100× and 400× magnifications. The comparably weaker correspondence between the ROXAS and manual CWT values with 40× are due to 'pixel effects' (in our case, a wall of 3.6 µm was, for instance, represented by only 3 pixels) that led to more discrete and consequently over- or underestimated CWT values. However, such pixel effects due to relatively low image resolution on the level of individual cells likely average out by a larger number of cells and wood samples measured. On the other hand, the 100× magnification (corresponding to approx. 2 pixels/µm in most microscope systems) seems to generally best balance accuracy and efficiency.

The required editing effort to obtain accurate values were inversely linked with sample quality (Table 1). Moreover, independently from sample quality, the influence of editing effort varied among CWT values: the differences between no editing, intermediate editing and the near to perfect editing were larger for the smaller than the larger CWT percentiles. Overall, the deviation of no and intermediate editing from the near to perfect editing decreased from the poor to the good sample and image quality. These results highlight the importance of a careful sample preparation and image capturing (von Arx *et al.*, 2016). On one hand, with high quality images almost no manual editing is required to get accurate results, on the other hand, standardize the sample thickness resulted important (von Arx *et al.*, 2016).

The comparative analysis of the different integration levels for the CWT measurements (parameter *b* in Fig. 1a) showed that all levels of integration differed significantly from each other (Tukey's Honest Significant Difference test, $P<0.001$) except for the 0% and 25% levels ($P=0.864$; Fig. 4). This result demonstrates that the approach selected for assessing CWT affects the values by 5-10% and therefore we suggest selecting an integration level that fits the purpose of the study. For instance, for investigations of intra- and interannual wood density or estimations of biomass, where accurate absolute values of wall quantifications are important, a high level of integration (100%) should be preferred to avoid consistent underestimation as obtained with the line measurements (see Fig. 5b-e). In fact, underestimation of CWT by 10% would result in underestimation of cell wall material and therefore biomass by 13.1% in a tracheid of 10 μm^2 lumen area and 9.8% in a tracheid of 1000 μm^2 when assuming circular lumen shapes. In contrast, for investigations of mechanical cell strength $(t/b)^2$ (Hacke et al. 2001) a low level of integration (e.g., 0% or 25%) may better take into consideration the thinnest and thus weakest point within the cell walls.

As the example in Fig. 5 illustrates, different integration levels for the CWT measurements do not affect the intra-annual time series of CWT in a uniform way. Rather, the difference between the 0% and 100% integration level varies within and among tree rings. Similarly, averaging the tangential and radial CWT for latewood tracheids results in larger values than the ones obtained from tangential CWT only, but also here this difference varies considerably from year to year (Fig. 5b-d). This example thus demonstrates that different ways of measuring CWT might affect the information encoded in the cell wall properties.

The new versatility provides valuable access to a larger range of parameters to quantify the cell wall. Further study are certainly needed to better understand the radial or tangential CWT climate sensitivity. Maybe one could be associated with a superior summer temperature signal compared to the other. Hence by breaking down the, in this case, for dendroclimatologists very important "maximum latewood density" measurement (e.g., Briffa *et al.,* 1998) into primary components, it may be possible to understand the origin of its temperature signal, and perhaps also further refine performance of climate reconstructions. Note that we here only list a few examples that profit from this explosion in replication of measured cells, potential parameters and customizable settings.

Conclusions

Our evaluation demonstrates that the CWT values obtained with ROXAS are not only comparable to manual measurements and due to the automatic modus of ROXAS, are much more efficient and increase ten- to twentyfold the number of measured tracheids. Furthermore, profiting from the customizable settings to quantify different cell wall features, our approach will further expand the knowledge about tracheids. This is exemplified by the contrasting results obtained for radial and tangential CWT with regard to temperature sensitivity, and the more accurate account of the non-uniform CWT around the cell lumen, that may influence estimates of wall material by 10% and more. This increased power and versatility allows to efficiently create comprehensive datasets of cell anatomical features, including CWT, customized for a wide range of novel research applications.

Acknowledgements

We thank L. Schneider, D. Nievergelt and A. Verstege for their help preparing and analysing the anatomical samples used for Figs. 5 and 6. GvA was supported by a grant from the Swiss State Secretariat for Education, Research and Innovation SERI (C12.0100). This research profited from discussions in the COST Action F1106 "Studying Tree Responses to extreme Events".

Tables

Table 1. Effect of different editing effort (III – high, II – intermediate, I – none; see Material and Methods for further details) on cell wall thickness (CWT) measurements for anatomical samples and images of different quality captured with 100× magnification. Data for III refers to a given percentile from the measurement of a mean of n=1815 tracheids in a single annual ring, II and I express the relative change (in %) to III.

	Good *			Intermediate †			Poor ‡		
	III	II	I	III	II	I	III	II	I
CWT percentile	[µm]	(%)	(%)	[µm]	(%)	(%)	[µm]	(%)	(%)
1%	1.56	3.43	2.51	1.64	5.49	3.99	1.79	3.87	4.34
5%	1.75	1.00	1.00	1.88	6.38	7.82	2.00	3.71	4.00
10%	1.86	2.18	2.31	1.98	4.04	7.58	2.16	2.69	2.69
25%	2.07	2.70	3.28	2.19	5.02	6.85	2.59	2.66	3.38
50%	2.74	2.35	2.56	2.54	5.12	7.78	4.69	4.01	5.47
75%	3.78	0.58	0.58	3.68	6.25	10.46	5.60	1.32	1.06
90%	4.30	0.16	0.16	4.51	0.22	1.69	6.16	0.23	0.47
95%	4.50	0.38	0.54	4.87	0.69	0.13	6.51	0.91	1.96
99%	5.16	0.14	0.11	5.51	2.90	0.38	6.78	4.94	8.19

* optimal sample and image quality

† not perfectly orthogonal cross-section, not optimal illumination, wrong white balance

‡ damages of cell walls, light staining, slightly out of focus

Figure captions

Figure 1: Illustration of how ROXAS measures cell wall thickness (CWT). (a) On each side of a tracheid (towards pith, bark, left and right) a measuring window of width *b* expressed as a percentage of the lumen diameter *a* (e.g., 75%) is positioned to define the wall section used for CWT assessment. (b) After automatic and, if required, manually improved identification of tracheid lumina, ROXAS creates a distance map (i.e. each pixel outside of the lumina gets a grey-scale intensity corresponding to its Euclidean distance to the closest lumen). (c) The distance map is combined with a watershed image to obtain a 1-pixel thick line at equidistance to the closest tracheid lumina; each pixel of the lines in the resulting image contains its Euclidean distance to the closest tracheid lumen. The mean grey-scale intensity of the line segment within a given measuring window (here highlighted in red) is taken as the CWT value of the given side of the target tracheid. CWT is therefore integrated over a defined wall section, which is in contrast to the commonly used measurements through the centre of each tracheid side (see blue line in panel a). (d) Zoomed-in region of panel (c) illustrating how the different CWT values over different wall sections are integrated; the blue arrows and numbers above the watershed line indicate the CWT value at specific points of the cell wall, the red values below the watershed line indicate the integrated CWT values for different integration levels.

Figure 2: Comparison of cell wall thickness (CWT) measurements with ROXAS and manual line measurement at different magnifications for a wood sample from (a) the stem base and (b) apex of a 3-m tall *Larix decidua* tree. Lines and envelopes indicate linear regression lines and 95% confidence envelopes, statistics refer to the corresponding linear regression analyses (a: intercept, b: slope). All linear regressions are significant at $P<0.001$. For the ROXAS analyses the 0% cell wall integration setting was used, which corresponds to a line measurement (see Fig. 1). Image resolution: 40× – 0.833 pixel/ µm, 100× – 2.074 pixel/µm, 400× – 8.296 pixel/µm.

Figure 3: Variability of relative cell wall thickness (CWT) obtained with 100× and 40× compared to the 400× reference measurements for different CWT classes. (a,b) Manual line measurement, (c,d) ROXAS measurements using 0% cell wall integration setting

corresponding to line measurements (see Fig. 1), (e,f) ROXAS measurements using 75% cell wall integration. Identical tracheids were measured in all trials.

Figure 4: Variability of cell wall thickness (CWT) depending on the ROXAS integration setting *b*. (a) Analysed wood sample from the stem base of a 3-m tall *Larix decidua* tree captured at a magnification of 100× corresponding to a resolution of 2.074 pixel/µm. (b) Absolute and (c) relative CWT values with increasing integration level. Different subscript letters in (c) indicate significant differences of relative CWT based on Tukey's Honest Significant Difference test (using 0% integration level as the reference).

Figure 5: Illustrative time series of cell wall thickness (CWT) measured with ROXAS in an anatomical image taken with 100× magnification (2.361 pixel/µm) from a mature *Pinus sylvestris* L. tree. (a) Entire series, (b-d) cutout regions of panel (a) magnified threefold. Mean values at 10-µm steps were calculated (33.3 ± 0.5 (mean ± SE) cells per step) based on totally 30,359 measured cells and used for plotting. Black lines in all panels indicate values obtained with 100% cell wall integration setting based on tangential CWT (CWT_{TAN} 100%) , green lines in (b-d) show the tangential CWT values obtained with 0% cell wall integration (CWT_{TAN} 0%), which corresponds to line measurement (see Fig. 1). The cyan lines in (b-d) are also based on 100% integration, but taking the average of radial and tangential CWT for the latewood cells (CWT_{MOD} 100%). (e) Difference of CWT_{TAN} 100% and CWT_{TAN} 0% for earlywood (EW) and latewood (LW) for the data from (a); the difference depending on the cell wall integration level was significantly larger in the EW than the LW ($t=5.2$, $P<0.001$). Manual editing in ROXAS took 15 minutes in this high-quality sample. Scale bar in (a) corresponds to 500 µm.

Figures

Figure 1:

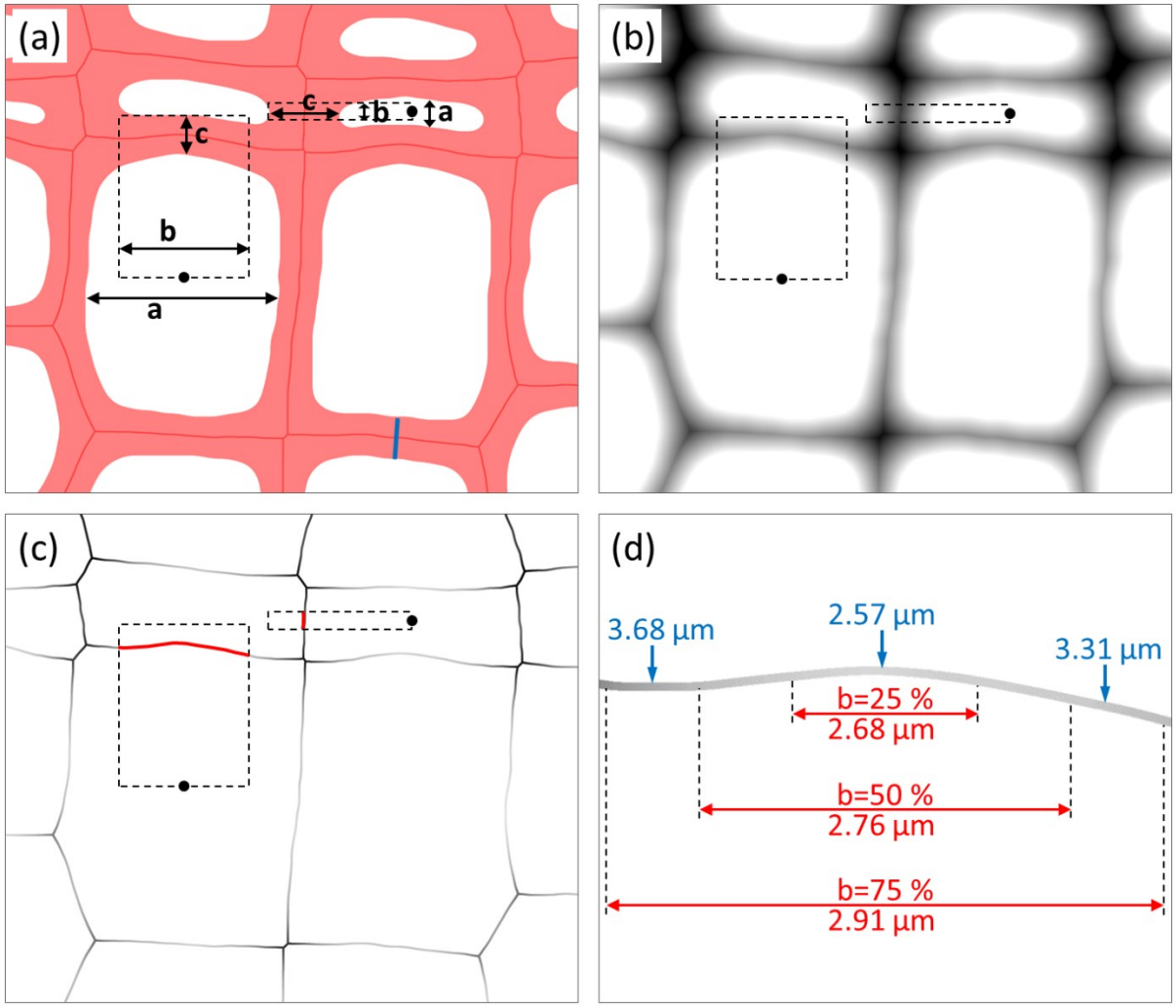

Figure 2:

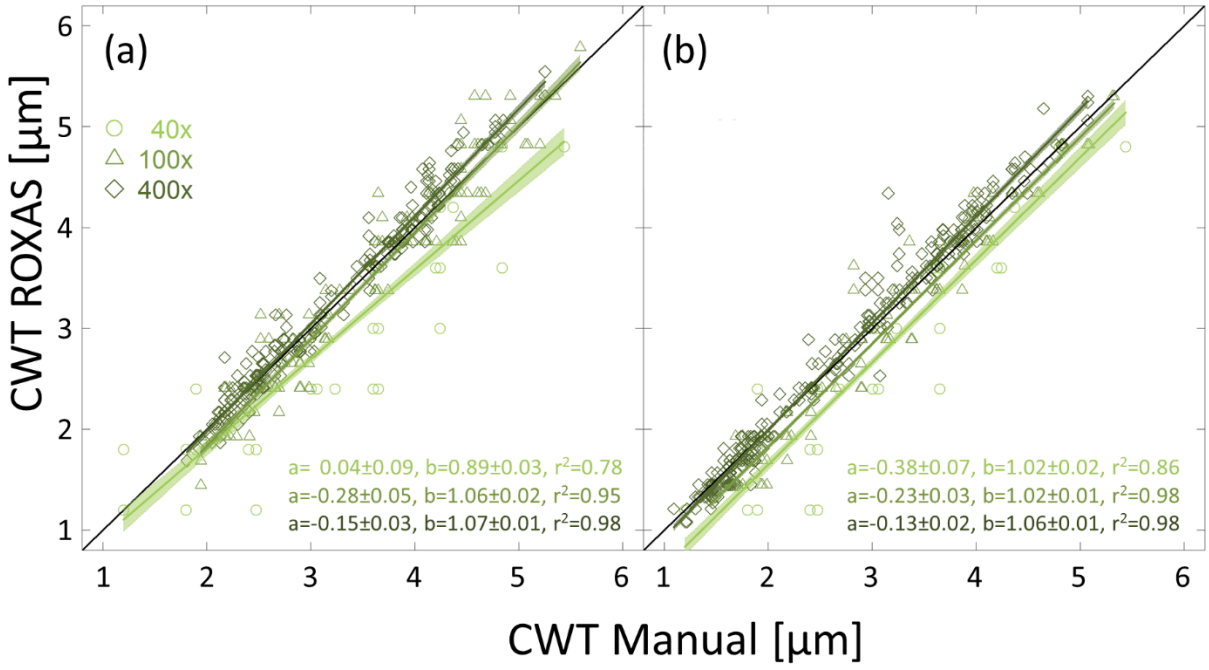

Figure 3:

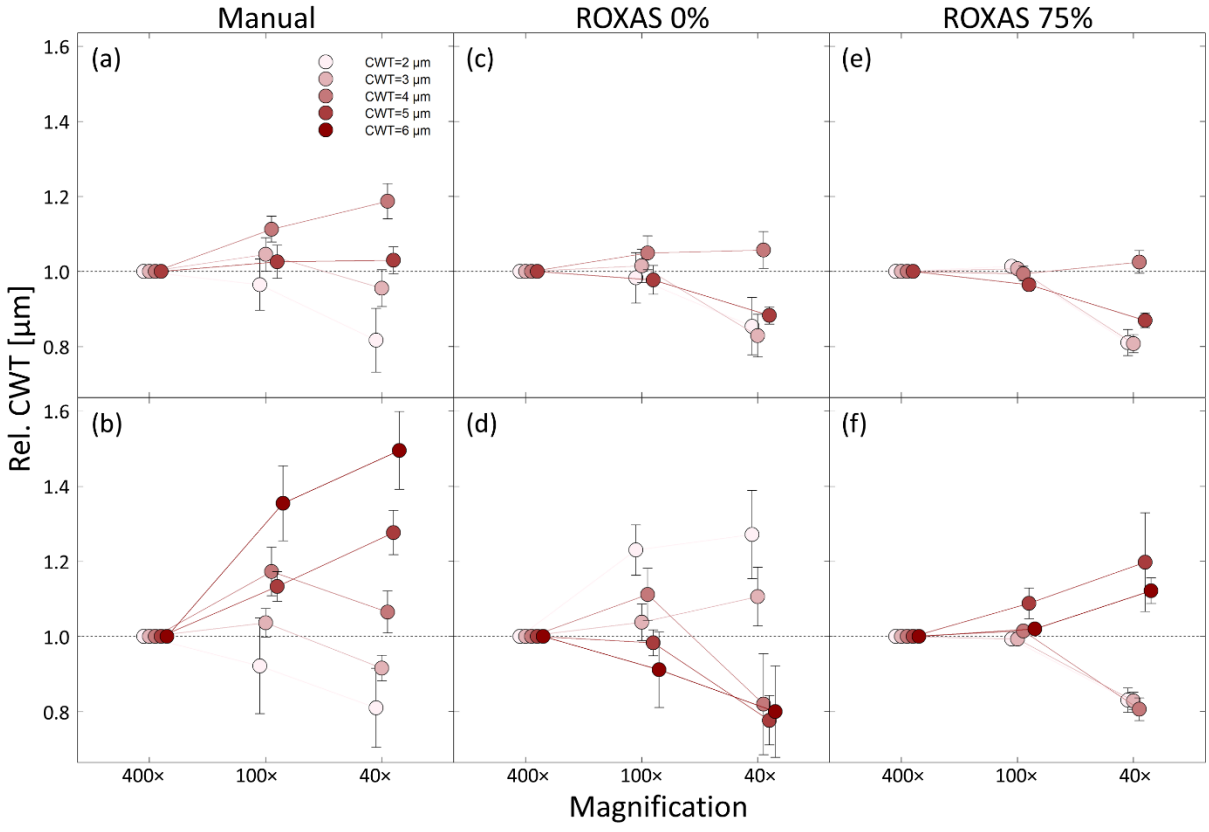

Figure 4:

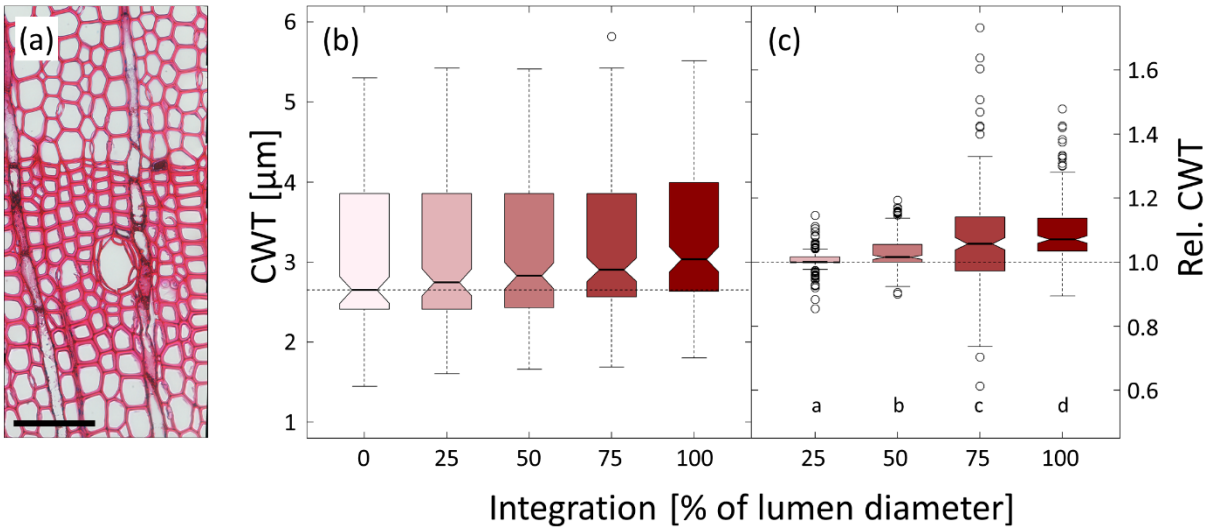

Figure 5:

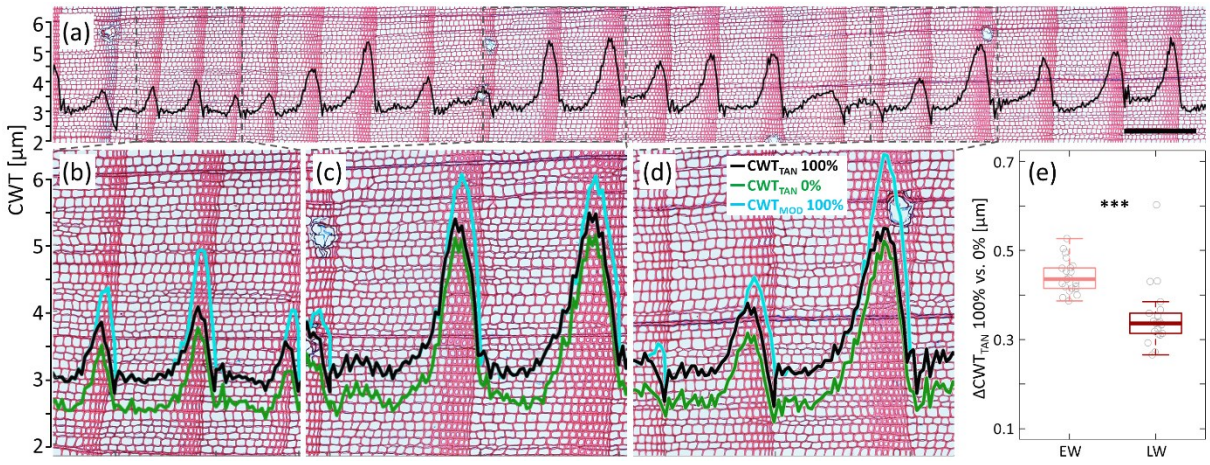

3.5 References

Aloni R (2013) Cellular Aspects of Wood Formation Fromm J (ed). Springer Berlin Heidelberg, Berlin, Heidelberg.

von Arx G, Archer SR, Hughes MK (2012) Long-term functional plasticity in plant hydraulic architecture in response to supplemental moisture. Ann Bot 109:1091–100.

von Arx G, Carrer M (2014) ROXAS – A new tool to build centuries-long tracheid-lumen chronologies in conifers. Dendrochronologia 32:290–293.

von Arx G, Crivellaro A, Prendin AL, Čufar K, Carrer M (2016) Quantitative Wood Anatomy—Practical Guidelines. Front Plant Sci 7:781.

von Arx G, Dietz H (2005) Automated Image Analysis of Annual Rings in the Roots of Perennial Forbs. Int J Plant Sci 166:723–732.

von Arx G, Kueffer C, Fonti P (2013) Quantifying plasticity in vessel grouping – added value from the image analysis tool ROXAS. IAWA J 34:433–445.

Baas P, Blokhina N, Fujii T, Gasson PE, Grosser D, Heinz I, Ilic J, Xiaomei J, Miller R, Newsom LA, Noshiro S, Richter HG, Suzuki M, Terrazas T, Wheeler E, Wiedenhoeft A (2004) IAWA List of microscopic features for softwood identification. IAWA J 25:1–70.

Briffa KR, Schweingruber FH, Jones PD, Osborn TJ, Shiyatov SG, Vaganov E a (1998) Reduced sensitivity of recent tree-growth to temperature at high northern latitudes. Nature 391:678–682.

Büntgen U, Frank D, Trouet V, Esper J (2010) Diverse climate sensitivity of Mediterranean tree-ring width and density. Trees 24:261–273.

Carrer M, von Arx G, Castagneri D, Petit G (2015) Distilling allometric and environmental information from time series of conduit size: the standardization issue and its relationship to tree hydraulic architecture. Tree Physiol 35:27–33.

Cuny HE, Rathgeber CBK (2016) Xylogenesis: Coniferous Trees of Temperate Forests Are Listening to the Climate Tale during the Growing Season But Only Remember the Last Words! Plant Physiol 171:306–317.

Denne MP (1988) Definition of Latewood According to Mork (1928). IAWA J 10:59–62.

Fonti P, Von Arx G, García-González I, Eilmann B, Sass-Klaassen U, Gärtner H, Eckstein D (2010) Studying global change through investigation of the plastic responses of xylem anatomy in tree rings. New Phytol 185:42–53.

Fonti P, Eilmann B, García-González I, von Arx G (2009) Expeditious building of ring-porous earlywood vessel chronologies without loosing signal information. Trees 23:665–671.

Fonti P, Heller O, Cherubini P, Rigling A, Arend M (2013) Wood anatomical responses of oak saplings exposed to air warming and soil drought. Plant Biol 15:210–219.

Hacke UG, Sperry JS, Pockman WT, Davis SD, McCulloh KA (2001) Trends in wood density and structure are linked to prevention of xylem implosion by negative pressure. Oecologia 126:457–461.

Handa IT, Körner C, Hättenschwiler S (2006) Conifer stem growth at the altitudinal treeline in response to four years of CO_2 enrichment. Glob Chang Biol 12:2417–2430.

Koubaa A, Zhang SYT, Makni S (2002) Defining the transition from earlywood to latewood in black spruce based on intra-ring wood density profiles from X-ray densitometry. Ann For Sci 59:511–518.

Morice CP, Kennedy JJ, Rayner NA, Jones PD (2012) Quantifying uncertainties in global and regional temperature change using an ensemble of observational estimates: The HadCRUT4 data set. J Geophys Res Atmos 117(D8).

Myburg AA, Lev-Yadun S, Sederoff RR (2013) Xylem Structure and Function. In: eLS. John Wiley & Sons, Ltd, Chichester, UK, pp 1–9.

Myburg AA, Sederoff RR (2001) Xylem Structure and Function. In: Encyclopedia of Life Sciences. John Wiley & Sons, Ltd, Chichester, UK, pp 1–9.

Park Y-I (David), Spiecker H (2005) Variations in the tree-ring structure of Norway spruce (*Picea abies*) under contrasting climates. Dendrochronologia 23:93–104.

Pellizzari E, Camarero JJ, Gazol A, Sangüesa-Barreda G, Carrer M (2016) Wood anatomy and carbon-isotope discrimination support long-term hydraulic deterioration as a major cause of drought-induced dieback. Glob Chang Biol:2125–2137.

R Development Core Team (2014) R: A language and environment for statistical computing.

Rosner S, Světlík J, Andreassen K, Børja I, Dalsgaard L, Evans R, Luss S, Tveito OE, Solberg S (2016) Novel Hydraulic Vulnerability Proxies for a Boreal Conifer Species Reveal That Opportunists May Have Lower Survival Prospects under Extreme Climatic Events. Front Plant Sci 7:831.

Seo J-W, Smiljanić M, Wilmking M (2014) Optimizing cell-anatomical chronologies of Scots pine by stepwise increasing the number of radial tracheid rows included—Case study based on three Scandinavian sites. Dendrochronologia 32:205–209.

Spiecker H, Schinker MG, Hansen J, Park Y-I, Ebding T, Döll W (2000) Cell structure in tree rings: Novel methods for preparation and image analysis of large cross sections. IAWA J 21:361–373.

Wegner L, Eilmann B, Sass-Klaassen U, von Arx G (2013) ROXAS – an efficient and accurate tool to detect vessels in diffuse-porous species. IAWA J 34:425–432.

4. Axial allometry of xylem anatomical structures reveals hierarchy in *Larix decidua* functional traits

A.L. Prendin[1*], G. Petit[1], P. Fonti[2], C. Rixen[3], M.A. Dawes[2,3], G. von Arx[2]

[1] Dept. Territorio e Sistemi Agro-Forestali, Università degli Studi di Padova, Legnaro (PD), Italy

[2] Swiss Federal Institute for Forest, Snow and Landscape Research WSL, Birmensdorf, Switzerland

[3] WSL Institute for Snow and Avalanche Research SLF, Davos, Switzerland

*** Corresponding author**

Keywords: axial allometry, cell wall thickness, elevated CO_2, ray parenchyma, soil warming, structure-function relationships, tracheid lumen size, tree-ring anatomy

4.1 Abstract

Trees continuously adjust their axial xylem structure to meet changing needs imposed by ontogenetic and environmental changes. These axial structure-function responses need to be coordinated among competing biophysical constraints to avoid failure of the xylem system. Here, we assessed axial variability of anatomical traits related to distinct xylem functions to identify priorities under different environmental conditions.

We performed detailed xylem cell anatomical quantification along the axis of 40-year-old *Larix decidua* trees planted at the Swiss treeline and exposed to a combination of CO_2 enrichment (+200 ppm) and soil warming (+4 °C) between 2001 and 2012.

The hydraulic efficiency, estimated by the mean hydraulic diameter (*Dh*), increased from the stem apex to base in a remarkably confined way, independent from experimental treatments and ontogeny. In contrast, axial trends of the other functional traits (hydraulic safety, mechanical support) showed greater flexibility in both respects or no axial trend (metabolic xylem function). Additionally, larger *Dh* at the stem apex promoted primary and secondary growth.

The xylem anatomical structure of *Larix* trees shows a high priority and biophysical determination of hydraulic efficiency to support assimilation necessary for tree growth, while the other traits respond more plastically to intrinsic and extrinsic factors.

4.2 Introduction

Plants have developed different mechanisms to continuously adjust to environmental variability and changing needs and priorities. Short-term responses of physiological processes at different organizational levels are common to all plant types (Larcher, 2003; Martorell *et al.*, 2015). However, especially for long-living trees that continuously increase in size and biomass (Chave *et al.*, 2009), adjustments involve profound structural changes in order to meet changing requirements for transport, support and storage. Indeed, many of these structural adjustments allow trees to acclimate to environmental changes and therefore to live for centuries or even millennia. On the other hand, the legacy of past structural adjustments can constrain future responses of physiological processes (Meinzer *et al.*, 2011; Anderegg *et al.*, 2013). Thus, investigating how tree structures and their associated functions change over time and in relation to environmental variability provides a deeper understanding of how tree growth interacts with the environment and helps to improve predictions of how forest ecosystems might be affected under different scenarios of climate change.

Dendro-anatomy is an emerging field that specifically focuses on the quantitative assessment of xylem tissues, cells and derived metrics or traits linked to specific functional roles. The approach is based on the fact that the xylem structural adjustments are permanently recorded and chronologically archived in the structure of the tree rings (Fonti *et al.*, 2010), thus allowing retrospective analysis of the structure-function responses of trees to climate variability (Fonti *&* Jansen, 2012). In conifers, the xylem is mainly composed of tracheids and parenchyma cells, both of which have multiple functional roles. Tracheids are axially-oriented, dead cells; in the earlywood they are characterized by wide lumina and thus represent 'highways' for axial water transport, while in the latewood their reduced lumen size and thicker cell walls provide mechanical support (Koubaa *et al.*, 2002; Baas *et al.*, 2004; Antony *et al.*, 2012). In contrast, parenchyma cells are living cells predominantly organized into rays running radially from the bark towards the pith, and thus they physiologically integrate the xylem with the phloem (Spicer, 2014; Pfautsch *et al.* 2015). Collectively, parenchyma cells act as a metabolically active tissue for transport and storage of carbon assimilates and water (Olano *et al.*, 2013; Fonti *et al.*, 2015; von Arx *et al.*, 2015) and contribute to regulate the

xylem hydraulics, e.g. through the osmo-regulation of axial and radial gradients of water potential (Brodersen & McElrone, 2013; Lintunen *et al.*, 2016) or by refilling embolized conductive elements (Salleo *et al.*, 2009; Nardini *et al.*, 2011). Studying how tracheids and parenchyma cells change within trees and in response to both increasing tree size and environmental variability might thus provide important insights into the plasticity of xylem functioning.

Currently, we only have a fragmentary understanding of the variability of relevant cell anatomical traits within the tree stem and roots. Theoretical models predict that the different anatomical traits should vary according to strict allometric axial scaling defined by biophysical constraints that are related to tree size (Savage *et al.*, 2010; West *et al.*, 1999). However, detailed empirical studies of within-plant patterns have mostly been limited to only the description of axial variability of the lumen size of xylem conduits (but see Lazzarin *et al.*, 2016). Both models and observations show that conduit lumen diameter increases from the stem apex to the base following a power-like trajectory ($y=a \cdot x^b$), with a scaling exponent generally converging towards a value of ~0.2 irrespective of species, environment or ontogenetic stage (Anfodillo *et al.*, 2013; Olson *et al.*, 2014). This pattern is explained by the biophysical law by Hagen and Poiseuille, according to which the hydraulic efficiency increases with conduit lumen diameter to the fourth power (Tyree & Zimmermann, 2002). Relatively small changes in conduit size therefore have a strong impact on hydraulic efficiency. Consequently, the progressively wider conduits from the apex to the stem base buffer the effect of increased path length on the accumulated axial hydraulic resistance, making it largely independent from tree height (West *et al.*, 1999; Petit & Anfodillo, 2009). In contrast, there is still little knowledge about the axial trend of other important xylem structure-function relationships, for example the hydraulic (cell implosion) safety, which can be estimated by the 'bending resistance index' ($[t/b]^2$, Hacke *et al.*, 2001), the mechanical support, or the abundance of metabolically active tissue. A few empirical studies have reported an increase in cell wall thickness – related to mechanical support for the tree body (e.g., Myburg *et al.*, 2013 – with increasing cambial age (Larson, 1963; Mitchell & Denne, 1997; Wimmer, 2002), while only limited information is available on within-tree variability in the abundance of ray parenchyma tissue (Bannan, 1937; Gartner *et al.*, 2000) and its sensitivity to environmental conditions (Eckstein, 2013; Olano *et al.*, 2013). Further, there is still a lack

of observations of how these and other functional traits co-vary both within the tree and over time, and thus we have only a limited understanding of how competing biophysical constraints, functional priorities, and trade-offs are modulated by ontogenetic development and environmental conditions (Gleason *et al.*, 2016; Bittencourt *et al.*, 2016). In this study, we used a dendro-anatomical approach to retrospectively analyze the plasticity of functionally relevant xylem anatomical traits along the tree axis. As a study framework, we selected a treeline experimental site. This temperature-limited ecotone is expected to be one of the terrestrial areas that is most sensitive to climate change, and it has therefore become a focus of recent research (Harsch *et al.*, 2009; Körner, 2012; Dawes *et al.*, 2015). Treelines are also particularly suitable for investigating the mechanisms of xylem growth responses to environmental changes (e.g., Petit *et al.*, 2011; Fatichi *et al.*, 2013; Fatichi *et al.*, 2014). The treeline trees selected for this study were exposed to a long-term experimental manipulation combining free air CO_2 enrichment (FACE) and soil warming (Hattenschwiler *et al.*, 2002; Dawes *et al.*, 2015). Prior assessments of *L. decidua* responses showed a stimulation of primary and secondary growth in stems and roots by the CO_2 enrichment (Hattenschwiler *et al.*, 2002; Handa *et al.*, 2005, 2006; Dawes *et al.*, 2011), which was partially explained by a larger leaf canopy resulting in increased photosynthetic carbon assimilation (Streit *et al.*, 2014), while the experimental soil warming did not stimulate above- or below-ground growth of *L. decidua* (Dawes *et al.*, 2015). Building upon this knowledge from previous studies at this site, we compared how the axial trends of four xylem functional traits in relation to hydraulic, biomechanical and metabolic requirements vary within dated annual rings from the stem apex to the roots. In doing so, we specifically aimed (1) to identify priorities and trade-offs among different xylem functions and (2) to determine if different environmental conditions and ontogeny influence these relationships.

4.3 Material and methods

4.3.1 Study site, experimental setup and tree selection

The study included trees from a long-term manipulation experiment performed within a 40-year-old afforestation of *Larix decidua* Miller and *Pinus mugo* subsp. *uncinata* (Ramond) located in the Swiss Alps at the Stillberg site near Davos (9°52'E, 46°46'N), just

above the current treeline at an altitude of 2180 m a.s.l. The manipulation experiment was performed between 2001 and 2012 and included different combinations of free air CO_2 enrichment (FACE) and soil warming (Table 1). CO_2 enrichment (+200 ppm higher than ambient CO_2 concentration) was performed from 2001 to 2009 and soil warming (+4 °C at 5 cm depth) was applied using heating cables on the soil surface (see Hattenschwiler *et al.*, 2002; Hagedorn *et al.* 2010; Dawes *et al.*, 2015 for details about the experimental setup).

We used eight *L. decidua* trees, with a minimum of two individuals per treatment combination: A_{2001}, A, EC, SW, ECSW, PECSW and PEC (Table 1). The study trees were selected based on the presence of a leader shoot, lack of mechanical and/or herbivore damage, lack of snow mold, and similar tree height at the beginning of the experiment.

4.3.2 Reconstruction of axial and radial growth

In order to capture the temporal variability of xylem anatomical traits along the stem axis, we reconstructed the apex-to-root axial trend within each tree ring layer to provide an annual resolution. Thus, for each selected tree, we extracted a total of 20 discs along the stem (14) and the main root (6) for the reconstruction of both the axial and radial growth. The average distance between neighboring discs was 11 cm. Tree-ring widths were measured along 8 equally spaced radii per disc and cross-dated to assign each ring to its year of formation. Annual stem and root elongation (ΔH) was obtained by linear interpolation of the inter-disc distance divided by the age difference between neighboring discs:

$$\Delta H = \frac{H_i - H_{i-1}}{RN_{i-1} - RN_i} \qquad \text{eq. 1}$$

where H_i and RN_i are the height from the ground and the ring number of the i^{th}-disc, respectively. The average age difference between neighboring discs varied from 1 to 14 years (with a median of 3 years) depending on the sample, thus giving reasonable confidence in the estimated annual stem elongation data. Finally, to reconstruct the axial position at the time of ring formation, for each annual ring within a given disc, we calculated the distance from the stem apex (L) as the difference between the

reconstructed tree height and the distance from the ground (for root discs *L* was calculated as the sum of tree height and axial distance from the ground).

4.3.4 Cell anatomical measurements

Xylem cell anatomical measurements were performed with image analysis for a subset of the stem discs. In total we selected ten axially well-distributed discs per tree, six from the stem and four from the roots. We followed the standard protocol for cutting micro-sections and collecting high-resolution images proposed by von Arx *et al.* (2016). From each disc, we extracted radial wood samples from opposite radii and produced 10-15 µm thick cross-sections using a rotary microtome (Leica RM2245, Leica Biosystems, Nussloch, Germany). In addition, for ray parenchyma quantification (see below), we cut three tangential sections from each wood sample within the annual rings formed in 2000, 2006 and 2011 to include years from all the different treatment combinations (Table 1). All sections were stained with safranin and astrablue and permanently fixed with Eukitt (BiOptica, Milan, Italy). Overlapping images of the cross-sections and tangential sections were captured at 100× magnification using a light microscope connected to a digital camera (Nikon Eclipse 80i,Nikon, Tokyo, Japan), and then stitched using PTGui (version 8.3.3, New House Internet Services B.V., Rotterdam, NL) to obtain high-resolution images (2.07 pixels/µm). Image analysis was performed with ROXAS version 2.1 (von Arx & Dietz, 2005; von Arx & Carrer, 2014), which provided measurements of cell anatomical features, such as tracheid lumen area and wall thickness from cross-sections and ray cell lumen area from tangential sections. In total, we analyzed the anatomical traits for ~4000 rings using measurements from >5 million tracheids.

4.3.5 Functional anatomical traits

For each annual ring on each disc, we derived xylem functional traits using the aforementioned basic anatomical measurements (Table 2). Since earlywood (EW) and latewood (LW) tracheids provide different functions, the tracheids were assigned to each tissue based on Mork's index (Denne, 1988). As a proxy for the hydraulic efficiency, we used the mean hydraulic diameter (*Dh*) (Kolb & Sperry, 1999), calculated as:

$$Dh = \frac{\sum d_n 5}{\sum d_n 4} \quad \text{eq. 2}$$

where d_n is the lumen diameter of the n^{th}-conduit, assumed to be circular. As an indicator of the hydraulic safety from cell implosion, we used the 'bending resistance index' of earlywood tracheids (BI_{EW}; Hacke *et al.*, 2001), calculated as:

$$BI_{EW} = \left(\frac{dCWT}{d}\right)^2 \quad \text{eq. 3}$$

where dCWT is the double cell wall thickness and d is the lumen diameter measured perpendicularly to CWT. This produced two values per tracheid, one with radial and one with tangential orientation of lumen diameter. For each tracheid, the smaller of the two values was used to better reflect the risk of cell implosion. The mechanical support function of the xylem was estimated as the mean cell wall thickness of latewood tracheids (CWT_{LW}), whereas the percent area of ray parenchyma (*RPD*) was used as a measure of the metabolically active tissue.

Additionally, we determined the 'hydraulic carbon use efficiency' index (*HCUE*) to express the hydraulic return for a given carbon investment. HCUE was calculated for each ring as the ratio of the accumulated conductance of all tracheids (*Kh* according to Poiseuille's law) to the accumulated wall area of all tracheids (CWA_{RING}). Finally, as a proxy for growth, the ring area (*RA*) of each ring in each disc was estimated assuming a circular stem cross-section.

4.3.6 Estimation of axial scaling and treatment effects

For each functional trait, we fitted linear, power and exponential functions to identify which function best described the axial scaling. Fitting was performed only for stem annual rings from control trees (treatments A_{2001} and A) to avoid potential confounding treatment effects. In addition, to check for ontogenetic trends, we computed the scaling exponents ('slope') and allometric constants ('intercept') throughout the life of each tree using a model type II regression analysis with the reduced major axis (RMA) protocol in the lmodel2 R package (Legendre, 2014). When necessary to obtain significant fits, we based this analysis on data from a moving window of three neighboring annual rings to

increase the number of axial points (BI_{EW} and CWT_{LW}). This analysis could only be performed with data from 2001 to 2012, thus not covering the first 30 years of tree growth. Similarly, we established the relationships among functional traits (*Dh*, BI_{EW}, CWT_{LW} and *RPD*) in terms of axial scaling and trade-offs by identifying the function (linear, power or exponential) that provided the highest R^2. In addition, we tested the relationship between each functional trait (*Dh*, BI_{EW}, CWT_{LW} and *RPD*) and each growth parameter (*ΔH and RAI*).

Treatment effects on the axial patterns were tested using linear mixed-effects models fitted with restricted maximum likelihood. We established a model for each explanatory variable (Dh_{ROOT}, BI_{EW}, CWT_{LW}, *RPD and HCUE),* where distance from the apex (*L*), treatment combinations (see Table 1) and their interactions were included as fixed effects, and tree identity and disc height along the tree axis were included as random factors in all initial models, reflecting the experimental design and the sample collection. Data were $\log_{10}$-transformed to comply with assumptions of normality and homoscedasticity (Zar, 1999). For the Dh_{STEM} model, we additionally included Dh_{APEX} as a fixed effect to account for its strong influence on Dh_{STEM}, as found in a previous study (Petit *et al.*, 2011). For this model, we only considered annual rings for which apical data (defined as ≤1 cm from tree top) were available. The best model was chosen based on AICc using the maximum likelihood method (Zuur *et al.*, 2009). When several models showed similar AICc values (ΔAICc < 2, Burnham & Anderson, 2002), they were refitted with the REML method to obtain estimates and significance values of effects, and the simplest model with significant fixed effects was chosen as the 'optimal' model. The significance of the fixed effects was tested with F tests (Pinheiro & Bates, 2000). When the target functional trait did not exhibit a significant axial trend, the difference between treatment combinations was tested with Tukey's Honest Significance test based on ANOVA. All analyses were performed using R (version 3.1.1.; R Development Core Team, 2014), and linear mixed-effects models were run using the lme4 (Bates *et al.*, 2015) and MUMIN packages (Barton & Barton, 2013).

4.4 Results

4.4.1 Axial allometry

The analysis of the functional trait variability along the whole tree axis using different parametric functions (Fig. 1a-d) revealed that the power function provided the best fit to the data, with R^2 values ranging from 0.81 (*Dh*) to 0.16 (CWT_{LW}) (Table 3). However, for CWT_{LW} the power fitting performed only slightly better than the linear and exponential ones. Tracheid hydraulic diameter (*Dh*) increased continuously down the stem and further along the roots (e.g., see the whole stem-root axial profile for the xylem produced in the year 2011 for the tree E3L1 shown in Fig. 1a). This widening pattern was narrowly confined for the stem, thus indicating only small differences among individuals and no significant changes throughout ontogeny (P=0.08). For each year of growth, *Dh* in the roots was larger than in the stem, generally increased with *L* at faster rates than in the stem, and showed more variation in the data (R^2=*0.10*) (Fig. 1a). The bending resistance index of earlywood tracheids (BI_{EW}) decreased continuously from the stem apex to the stem base and further below ground along the roots. In the stem, *L* explained 46% of the total variance in BI_{EW} (Table 3), while in the roots this relationship was not significant (P=0.31) (Fig. 1 b). Additionally, the scaling exponent (*b*) of the relationship of BI_{EW} vs. distance from the apex (*L*) progressively decreased with age (R^2=0.48, P<0.001). The cell wall thickness of the latewood tracheids (CWT_{LW}) increased continuously from the stem apex to the base and further along the roots. The inter-annual variability was substantial in this trait, as shown by the low R^2 of 0.16 for the stem (Table 3) and the non-significant relationship for the roots (P=0.90) (Fig. 1c). Furthermore, the scaling exponent (*b*) of the relationship of CWT_{LW} vs. *L* progressively increased with age (R^2=0.46, P=0.013). However, this ontogenetic trend was only significant when a power function was used but not when linear or exponential fitting was applied (P=0.71 and P=0.11, respectively). The percent area of ray parenchyma (*RPD*) did not change significantly along the stem (P=0.53) or root (P=0.83) (Fig. 1d).

4.4.2 Trait trade-offs, cost for hydraulic efficiency and effect on growth

Pairwise comparisons between functional traits revealed a significant trade-off between hydraulic efficiency and safety (*Dh* vs. BI_{EW}). This relationship applied to both tree organs

but was stronger in the stem (R^2=0.56) than in the roots (R^2=0.44). Furthermore, stem hydraulic efficiency was weakly but positively linked (R^2=0.17, Fig. 2, Table 3) to mechanical support (*Dh* vs. CWT_{LW}).

The analyses of *HCUE*, the ratio between hydraulic conductance and structural costs, indicated that, per unit of conductance, construction costs increase with height along the stem (Fig. 3, Table 3).

Of all the considered functional traits, only the hydraulic diameter at the stem apex (Dh_{APEX}) had a significant effect on growth (Fig. 4; other data not shown). Indeed, Dh_{APEX} explained 31% and 46% of the total variance in ΔH and *RAI*, respectively.

4.4.3 Treatment effects on axial allometry

The linear mixed-effect models used to test for the importance of treatments for the axial scaling of Dh_{STEM} did not reveal any significant effects (Table 4, Fig. 1e). Along the roots, *Dh* was in general wider before 2001, whereas all treatment combinations except EC (elevated CO_2) showed a significant overall reduction in Dh_{ROOT} (Table 4, Fig. 1f). Treatment effects on BI_{EW} were found for the combination of soil warming and elevated CO_2 (ECSW), also after CO_2 fumigation ceased in 2009 (PECSW), as shown by a steeper increase in BI_{EW} with increasing distance from the apex. The model results for CWT_{LW} were analogous to the ones for BI_{EW} (Table 4, Fig. 1g). Similarly, the axial scaling of *HCUE* was influenced by the same treatment combinations as BI_{EW} and CWT_{LW}, but with inversed relationships. In addition, *HCUE* for A_{2001} was smaller at the stem apex (i.e., smaller intercept *a*) but increased along the stem at a faster rate (larger *b*) than for the same trees after having grown taller, irrespective of treatments. *RPD* showed no significant axial variation, and the one-way ANOVA performed instead to test for treatment effects revealed that only soil warming (SW) had a significant negative effect on the production of ray parenchyma (*P*=0.035).

4.5 Discussion

4.5.1 Axial scaling of functional traits are linked to biophysical principles

Our description of xylem anatomical traits showed characteristic axial scaling that can be attributed to different biophysical principles. As expected, the hydraulic efficiency (D_h) scaled along the stem following a power function with a scaling exponent (b=0.17) very similar to values reported in other studies (Anfodillo *et al.*, 2013; Olson *et al.*, 2014), thus supporting the remarkable universality of the axial conduit widening in vascular plants (West *et al.*, 1999; Olson *et al.*, 2014). Furthermore, in all trees and under all treatment combinations, xylem tracheids in the roots were wider than along the stem, in agreement with previous studies (McElrone *et al.*, 2004; Petit *et al.*, 2009; Petit *et al.*, 2010). This strict axial configuration characterized by the downwards conduit widening represents a biophysical optimization to buffer the increasing hydraulic resistance due to a longer path length as trees grow taller (West *et al.*, 1999; Petit *et al.*, 2009). Instead, the earlywood hydraulic safety (BI_{EW}) increased towards the apex, i.e. in parallel with the decrease in the water potential towards the apex (Domec *et al.*, 2005). The observed axial pattern of latewood cell wall thickness (Fig. 1c) revealed an increasing allocation of cell wall material with increasing distance from the apex, thus indicating an increasing need for mechanical support. However, this increase was relatively small compared to, for example, the increase in accumulated biomass to the power of three to four when moving down the stem, as reconstructed for an individual of *Abies procera* (King, 2011), thus suggesting a complex relationship between cell wall thickness and the mechanical support provided.

In contrast to the other functional traits, we did not find a consistent or clearly defined axial trend for the percent area of ray parenchyma (*RPD*). The variability along the stem axis was very large both between and within trees (ranging from 0.12 to 2.55%). This finding confirms previous observations that the ray proportion of conifers varies widely, both among individuals (Fonti *et al.*, 2015) and within the stem (DeSmidt, 1922; Baker *et al.*, 2000; von Arx et al., 2015), with only a relatively weak influence of environmental conditions (Esteban *et al.*, 2012; Olano *et al.*, 2013) and/or functional needs such as storage space requirements (von Arx *et al.*, pers. comm.).

Generally, the trends observed in the roots were consistent with those observed in the stem but were much weaker. This increased variability might be because, compared to

stems, roots perform more tasks (e.g., flexibility, stiffness, anchorage) within a less homogeneous medium (different soil texture and depth) (Gärtner *et al.*, 2001).

4.5.2 Hydraulic efficiency shows no ontogenetic trend but trades off with hydraulic safety

During ontogeny, adjustments of the xylem structure are necessary to meet the changing functional needs as tree size increases. Despite these expected modifications, the power fitting observed for the hydraulic efficiency (*Dh*) appeared to be very stable and independent from the ontogenetic tree development, suggesting a very strong biophysical control over the axial design of hydraulic efficiency. In contrast, the hydraulic safety (BI_{EW}) showed a slight change in the axial scaling that suggests a decrease in safety with increasing age/size. A possible explanation for this ontogenetic trend is that larger trees have a deeper root system with better access to soil water. Similarly, at least when using power fitting, the axial scaling of the mechanical support (cell wall thickness) changed in a way that suggested an increase during the course of a tree's life for a given distance from the apex. This may reflect size-related changes in tree architecture, since many trees invest increasingly into lateral structures as they grow taller, which requires stronger wood to support it (King, 2011).

Limited resources to form wood and differing biophysical constraints inherently imply trade-offs between the xylem functional needs, as demonstrated by the observed competing axial structural adjustments observed in our study (Fig. 2). Specifically, we confirmed the presence of a trade-off between hydraulic efficiency and safety (Sperry *et al.*, 2008). In contrast, the positive relationship we observed between mechanical stability and hydraulic efficiency is an example of co-variation of different functional needs along the tree axis. The observed hydraulic efficiency vs. safety trade-off is related to the fact that tracheids with narrow lumina are less efficient in transporting water but more resistant to implosion and xylem cavitation (Gleason *et al.*, 2016). Our results suggest that this relationship changes along the stem axis in order to prioritize safety towards the stem apex and efficiency toward the stem base (Fig. 2). This result is supported by the fact that the construction costs for the hydraulic system (*HCUE* , i.e. the hydraulic conductance per unit of cell wall area) were higher towards the stem apex (Fig. 3, Table 3). This could be explained by the importance of an undamaged apex to sustain height growth and compete

with neighboring trees, particularly in a conifer with clear apical dominance such as *L. decidua*. In fact, especially in winter, the apex protrudes from the snow and may be particularly vulnerable to ice blasting, wind desiccation (Baig & Tranquillini, 1980; Smith *et al.*, 2003) and frost drought (Mayr *et al.*, 2006a; Mayr *et al.*, 2006b).

4.5.3 Environmental conditions have little influence on the axial scaling of functional traits

Our results suggest that altered environmental conditions, in this case warmer soil and CO_2 enrichment, do not strongly influence the scaling of the analyzed functional traits along the stem (Table 3). Effects of environmental conditions emerged only in the functional traits that did not show a very strong biophysical determination, for example the mean hydraulic diameter in the roots and the percent area of ray parenchyma. Specifically, the soil warming treatment had only a local effect restricted to root xylem anatomy. The significant decrease in lumen size of root tracheids (Dh_{ROOT}) under soil warming implies reduced overall root conductance because no significant compensating increase in root biomass was observed (Dawes *et al.*, 2015). However, due to the comparably minimal hydraulic resistance of the large root tracheids, this decrease in lumen size has almost no effect on overall pathway length resistance and therefore likely no functional relevance for whole plant conductance, transpiration and photosynthesis. Soil warming also reduced the percent area of ray parenchyma along the stem (RPD_{STEM}) but not in the roots (RPD_{ROOT}). However, treeline trees are usually relatively rich in NSCs and starch reserves (Hoch & Körner, 2012), and the different warming effects on *RPD* in the stem and roots may reflect an osmotic adjustment of the root-to-leaf gradient of water potential that effectively influences the translocation of sugars within the plant (Hölttä *et al.*, 2006; Dawes *et al.*, 2014).

Furthermore, our results showed a weak increase in BI_{EW} and CWT_{LW} with increasing distance from apex (L) under ECSW and PECSW, meaning that trees could profit from the larger amount of photosynthates available under elevated CO_2 by improving the mechanical stability (Fig. 1f, Fig. 1g). At the same time, the significantly lower values of BI_{EW} and CWT_{LW} close to the stem apex under CO_2 enrichment could explain the increase in freezing sensitivity of trees exposed to elevated CO_2, particularly in taller trees, as previously observed for the period 2005-2010 (Martin *et al.*, 2010; Rixen *et al.*, 2012).

4.5.4 Mean hydraulic diameter at the apex promotes growth

The observed within-tree variability of anatomical traits and its influence on tree functioning lead to the obvious question about the relevance for growth. Of all the functional traits analyzed in this respect, only the mean hydraulic diameter at the stem apex (Dh_{APEX}) was important, explaining 31% and 46% of the variability in stem elongation and ring area at the stem base, respectively (Fig. 4). Our result thus support the hypothesis that an increase in the conductivity of the stem apex (i.e., the plant's hydraulic bottleneck, where most of the path length resistance is located) releases the hydraulic constraints on water transport, thus favoring gas exchange and ultimately growth (Petit *et al.*, 2011).

4.5.5 Conclusions

With this study, we tested a novel approach to retrospectively analyze the axial variability of different xylem functional traits in response to ontogenetic development and environmental variability, represented here by experimental manipulation of CO_2 and temperature.

The observed low plasticity driven by a strong biophysical constraint on the axial pattern of *Dh* strongly suggests that trees generally prioritize hydraulic efficiency over other xylem functions. The higher axial variability of the other functional traits (hydraulic safety, mechanical support, metabolic functions) potentially indicates a greater ability or need of the trees to respond to the environment or to ontogenetic development, although these effects seem rather weak. The functional priority of hydraulic efficiency, as demonstrated by the very confined axial patterns, was also apparent at the tree apex, which represents the hydraulic bottleneck: there, a small increase in *Dh* significantly enhances water transport, thus fueling photosynthesis, which provides the necessary resources for growth. Moreover, our findings indicate that carbon allocation along the stem axis is adjusted in order to supply the locally and temporally most important functional need. In particular, higher priority to hydraulic safety is given towards the stem apex, while conductance and mechanical support gain relatively more importance towards the stem base. In conclusion, our study suggests that prioritized xylem functional

traits show a very strong biophysical determination, while subordinate traits respond more plastically to intrinsic and extrinsic factors.

Acknowledgments

We thank S. Hättenschwiler for initiating and F. Hagedorn for running the 12-year CO_2 enrichment and soil warming experiment, as well as many colleagues at the WSL and SLF for assistance with field work and technical support. We acknowledge S. Lechthaler in particular for helping with measurements on tangential sections. Major funding sources for this treeline experiment included the Swiss National Science Foundation from 2001-2005 (grant 31-061428.00 to S. Hättenschwiler) and from 2007-2010 (grant 315200-116861 to CR); the Velux Foundation from 2007 to 2012 (grant 371 to F. Hagedorn); and the WSL from 2012 to 2016 (grant to CR and MD). This particular study was supported by the COST Action F1106 "Studying Tree Responses to extreme Events". GvA was supported by grants from the Swiss State Secretariat for Education, Research and Innovation SERI (SBFI C14.0104 and C12.0100).

Tables

Table 1: Timeline of the treatments and treatment combinations during the FACE and soil warming experiment at Stillberg (Davos, Switzerland). A_{2001}: ambient conditions before the beginning of the experiment; A: ambient conditions (control); EC: elevated CO_2; SW: soil warming, ECSW: elevated CO_2 and soil warming, PECSW: post elevated CO_2 and soil warming; PEC: post elevated CO_2 at ambient conditions. Each row of the timeline corresponds to n=2 trees.

	n	1983-2000	2001	2002	2003	2004	2005	2006	2007	2008	2009	2010	2011	2012
Combined treatments	2	A_{2001}	EC						ECSW			PECSW		
	2	A_{2001}	EC									PEC		
	2	A_{2001}	A						SW					
	2	A_{2001}	A											

Table 2: Acronyms and descriptions of variables used in this study.

Variable		Description	Function	Reference
Descriptive	***L***	Distance from the apex	-	
	H	Tree height	-	
Functional traits	***Dh***	Tracheid hydraulic diameter	Hydraulic efficiency	Kolb & Sperry, 1999
	$\boldsymbol{BI_{EW}}$	Bending resistance index of earlywood tracheids	Hydraulic safety	Hacke *et al*., 2001
	$\boldsymbol{CWT_{LW}}$	Cell wall thickness of latewood tracheids (proxy for density)	Mechanical support	Myburg *et al.*, 2013
	CWA	Cell wall area	Mechanical support	
	RA	Ring area	Hydraulic efficiency & mechanical support	
	RPD	Percentage area of ray parenchyma cells on tangential section	Metabolic functions, e.g., capacity of carbon & water storage and radial transport	Spicer *et al*., 2014; von Arx *et al*., 2015
	Kh	Total conductivity	Hydraulic efficiency	Tyree & Zimmermann, 2002
Economics	***HCUE***	Hydraulic carbon use efficiency: Kh/CWA_{RING}	-	
Growth	***ΔH***	Annual stem elongation	-	
	RAI	Annual ring area index (*RA* standardized to remove the general axial pattern)		

Table 3: Linear, power and exponential fitting parameters (mean ± 1 Standard error) *a*: *y*-intercept, *b*: slope), coefficient of determination (R^2) and significance (*P*) of the relationships assessed for the different trait variables. Relationships were only assessed for control trees not undergoing any CO_2 enrichment or soil warming treatment (A_{2001} and A; n=8 trees until 2001, n=4 from 2001 to 2006, n=2 from 2007 to 2012). See Table 2 for explanations of acronyms.

		Linear (y = a + b×L				**Power ($Log_{10}(y) = a + b \times Log_{10}(L)$**				**Exponential ($y = a + L^b$)**			
		a	***b***	***R²***	***P***	***a***	***b***	***R²***	***P***	***a***	***b***	***R²***	***P***
Variation in functional trait	*Dh* vs *L*	14.90 ± 0.21	0.07 ± 2.25×10^{-3}	0.72	<0.001	1.00 ± 0.01	0.17 ± 0.01	0.81	<0.001	2.86 ± 0.02	2.18×10^{-3} ± 1.28×10^{-4}	0.66	<0.001
	BI_{EW} vs *L*	0.02 ± 4.17×10^{-4}	-5.63×10^{-5} ± 4.5×10^{-6}	0.31	<0.001	-1.50 ± 0.02	-0.15 ± 0.01	0.46	<0.001	-3.81 ± 0.04	-2.62×10^{-3} ± 3.35×10^{-4}	0.28	<0.001
	CWT_{LW} vs *L*	3.35 ± 0.05	4.09×10^{-3} ± 5.35×10^{-4}	0.15	<0.001	0.47 ± 0.01	0.05 ± 0.01	0.16	<0.001	1.22 ± 0.03	1.02×10^{-3} ± 1.38×10^{-4}	0.15	<0.001
Trade-off	Dh_{STEM} vs BI_{EW}	0.04 ± 9.13×10^{-4}	-0.001 ± 4.51×10^{-5}	0.55	<0.001	-0.64 ± 0.05	-0.86 ± 0.04	0.56	<0.001	-2.97 ± 0.04	-0.05 ± 2.12×10^{-3}	0.60	<0.001
	Dh_{ROOT} vs BI_{EW}	0.003 ± 9.44×10^{-4}	-4.73×10^{-4} ± 2.54×10^{-5}	0.40	<0.001	-0.01 ± 0.09	-1.19 ± 0.06	0.44	<0.001	-2.98 ± 0.06	-0.03 ± 1.19×10^{-3}	0.43	<0.001
Relationship	Dh_{STEM} vs CWT_{LW}	2.5 ± 0.13	0.06 ± 0.01	0.19	<0.001	0.19 ± 0.04	0.28 ± 0.03	0.17	<0.001	0.98 ± 0.04	0.02 ± 1.81×10^{-3}	0.14	<0.001
Economics	*HCUE* vs *L*	1.64×10^{-15} ± 2.24×10^{-16}	2.52×10^{-17} ± 2.42×10^{-18}	0.25	<0.001	-15.22 ± 0.04	0.46 ± 0.02	0.44	<0.001	-2.99 ± 0.06	-0.03 ± 1.78×10^{-3}	0.21	<0.001
Growth	ΔH vs Dh_{APEX}	-0.06 ± 0.25	0.09 ± 0.02	0.28	<0.001	-1.57 ± 0.56	2.44 ± 0.53	0.31	<0.001	-0.99 ± 0.28	0.08 ± 0.02	0.28	0.007
	RAI vs Dh_{APEX}	0.60 ± 0.06	0.03 ± 0.01	0.42	<0.001	0.10 ± 0.13	0.80 ± 0.12	0.46	<0.001	-0.41 ± 0.07	0.03 ± 5.41×10^{-3}	0.43	<0.001

Table 4: Results of the optimal linear mixed-effect models predicting the treatment effects on the different functional (A) and cost (B) traits and the interaction between treatment and $Log_{10}L$ (see methods for details). Numbers indicate the estimates ± 1 SE. See Table 1 and 2 for explanations of acronyms. * P< 0.05, ** P< 0.01 and *** P< 0.001.

	(A) FUNCTIONAL TRAITS				(B) CARBON COST
Fixed effects	**$Log_{10}Dh_{STEM}$**	**$Log_{10}Dh_{ROOT}$**	**$Log_{10}BI_{EW}$**	**$Log_{10}CWT_{LW}$**	**$Log_{10}HCUE$**
Intercept (A)	**0.82 ± 0.06*** **	**1.45 ± 0.05*** **	**-1.52 ± 0.04*** **	**0.49 ± 0.02*** **	**-18.34 ± 0.07*** **
$Log_{10}L$ (A)	**0.18 ± 0.01*** **	**0.04±0.02***	**-0.13 ± 0.01*** **	**0.04 ± 0.01*** **	**0.3 ± 0.02*** **
$Log_{10}Dh_{APEX}$ (A)	**0.15 ±0.06****	-	-	-	-
A_{2001}	-	**0.03 ± 0.01****	0.03 ± 0.03	-0.04 ± 0.02	**-0.09 ± 0.05***
EC	-	0.00 ± 0.01	0.05 ± 0.04	-0.04 ± 0.03	0.08 ± 0.06
ECSW	-	**-0.06 ± 0.02*** **	**-0.28 ± 0.06*** **	**-0.15 ± 0.05****	**0.52 ± 0.11****
SW	-	**-0.04 ± 0.01*** **	-0.05 ± 0.04	0.02 ± 0.03	-0.11 ± 0.07
PECSW	-	**-0.03 ± 0.02***	**-0.38 ± 0.09*** **	**-0.25 ± 0.07*** **	**0.75 ± 0.17*** **
PEC	-	**-0.04 ± 0.02***	0.07 ± 0.12	-0.16 ± 0.09	**0.06 ± 0.2**
$Log_{10}L \times A_{2001}$	-		-0.01 ± 0.02	0.02 ± 0.01	**0.06 ± 0.03***
$Log_{10}L \times$ EC	-		-0.03 ± 0.02	0.02 ± 0.01	-0.02 ± 0.03
$Log_{10}L \times$ ECSW	-		**0.13 ± 0.03*** **	**0.08 ± 0.02*** **	**-0.23 ± 0.05*** **
$Log_{10}L \times$ SW	-		0.01 ± 0.02	0.01 ± 0.02	0.04 ± 0.03
$Log_{10}L \times$ PECSW	-		**0.15 ± 0.04*** **	**0.10 ± 0.03*** **	**-0.26 ± 0.08****
$Log_{10}L \times$ PEC	-		-0.06 ± 0.05	0.05 ± 0.04	0.08± 0.09

Figures captions

Fig. 1: Axial variability of functional traits as a function of distance from the apex (*L*) along the stem and root of the investigated *Larix decidua* trees. Left panels show the axial trends of (a) hydraulic diameter (*Dh*), (b) bending resistance index of earlywood tracheids (BI_{EW}), (c) cell wall thickness of latewood tracheids (CWT_{LW}) and (d) density area of ray parenchyma (*RDP*). Filled and open grey circles represent the stem and root data, respectively. As an arbitrary example, red circles represent the axial variability (stem and root combined) in the year 2011 for a single tree (E3L1). Solid lines show the best fitting curves, whose details are reported in Table 3. In the right panels (e-g), the black lines denote the linear regression lines of the $\log_{10}$-$\log_{10}$ transformed variables for each selected functional trait ((e): *Dh*; (f): BI_{EW}; (g): CWT_{LW}) of control trees (A_{2001}, A). Colored lines indicate the significant treatment effects (see Table 4 for details). (h) Mean ± 1 SE of *RPD* grouped per treatment for stem (filled circles) and root (open squares). See Tables 1 and 2 for explanations of acronyms.

Fig. 2: Reciprocal relationships between functional traits (*Dh*, BI_{EW}, CTW_{LW} and *RPD*) in the stem (upper right plots) and root (lower left plots). Solid lines indicate the significant power curves that fit the data best (see Table 3).

Fig. 3: Variability of hydraulic carbon use efficiency (*HCUE*) with increasing distance from the apex (*L*), based on $\log_{10}$-transformed data. The black line refers to the HCUE trend of control trees only, whereas colored lines indicate the significant treatment effects (see Table 3 for details).

Fig. 4: Relationship between the mean hydraulic diameter of apical tracheids (Dh_{APEX}: *Dh* at $L \leq 1$ cm) and (a) ΔH (annual stem elongation rate) and (b) *RAI* (ring area index, i.e., the ring area (RA) at the stem base standardized to remove the general axial pattern of *RA* vs. *L*, see Table 2). Solid lines represent the fitted linear regressions.

Figures

Fig. 1:

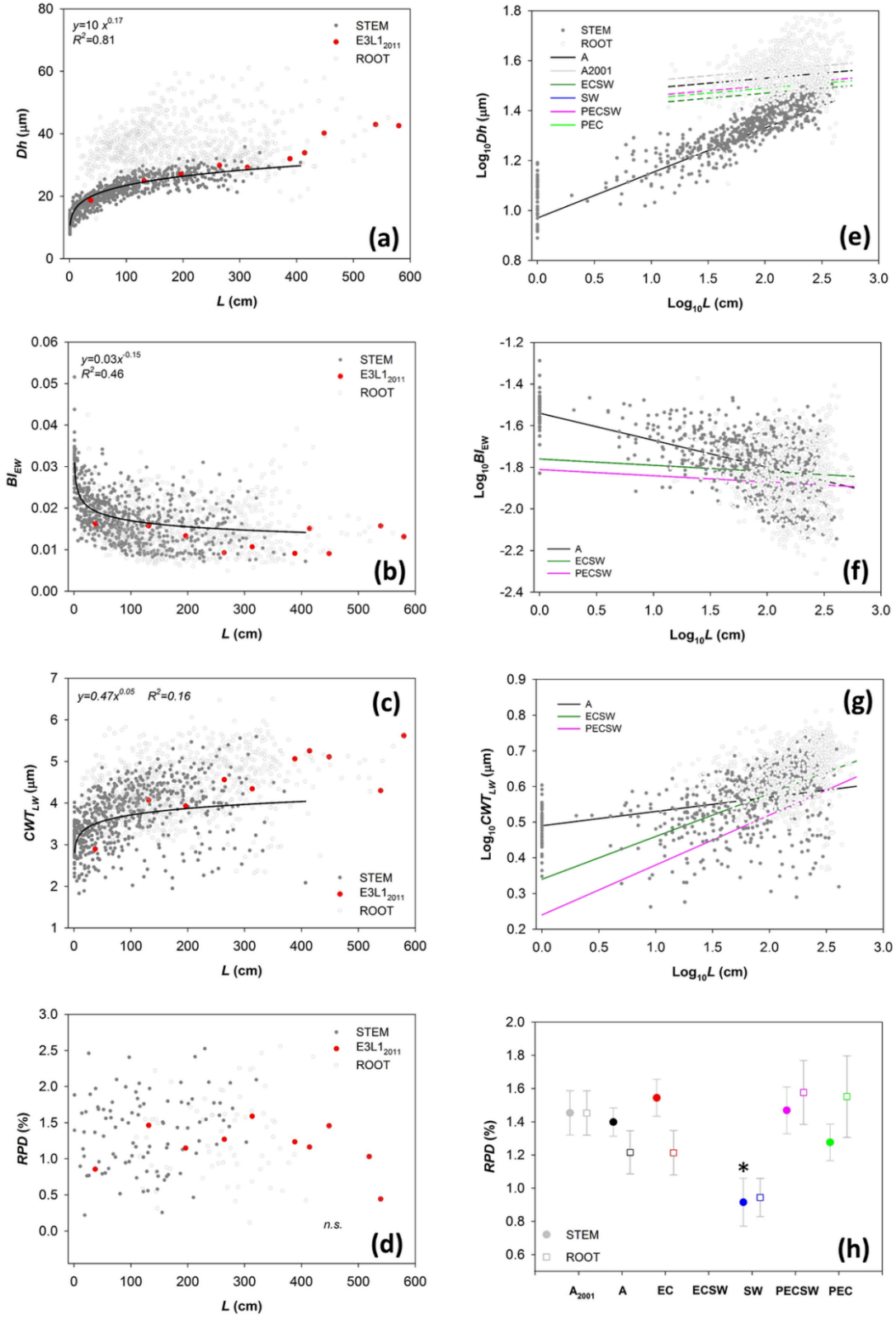

Fig. 2:

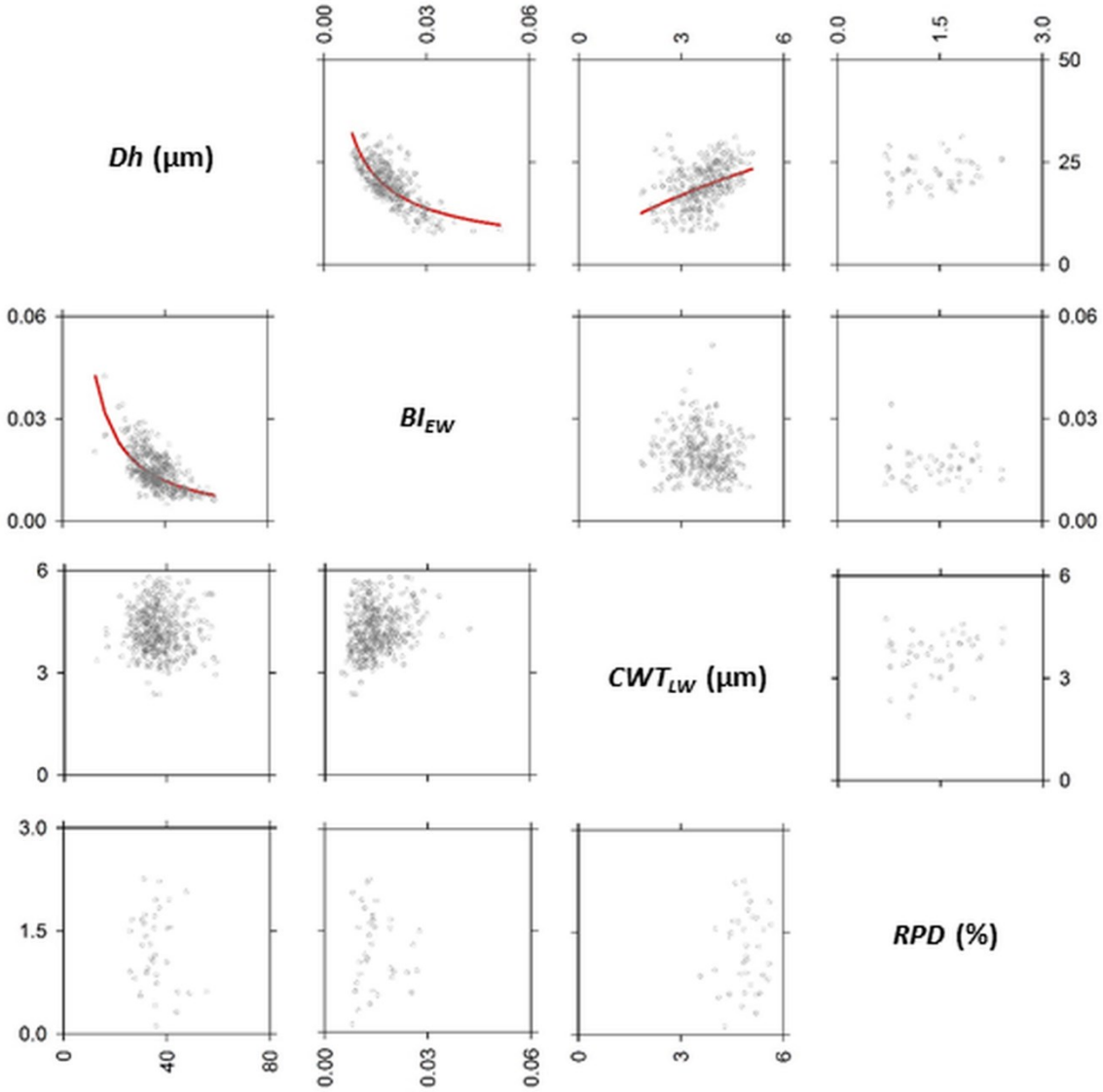
Dh (µm)
BI_EW
CWT_LW (µm)
RPD (%)
0.00
0.03
0.06
0
3
6
0.0
1.5
3.0
50
25
0
0.06
0.03
0.00
6
3
0
3.0
1.5
0.0
0
40
80

Fig. 3:

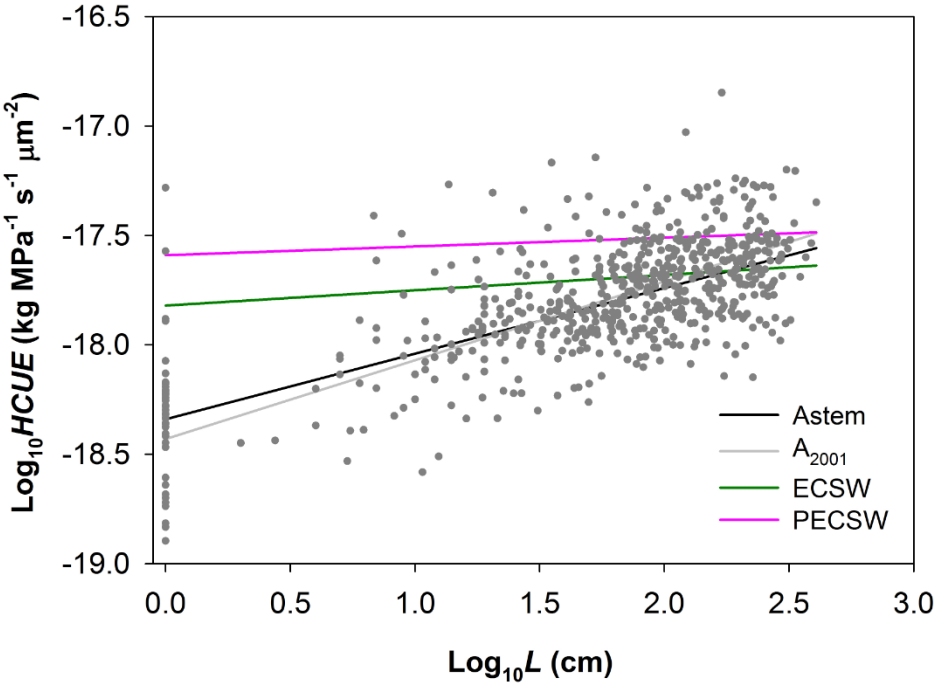
-16.5
-17.0
-17.5
-18.0
-18.5
-19.0
0.0
0.5
1.0
1.5
2.0
2.5
3.0
Log10HCUE (kg MPa-1 s-1 µm-2)
Log10L (cm)
Astem
A2001
ECSW
PECSW

Fig. 4:

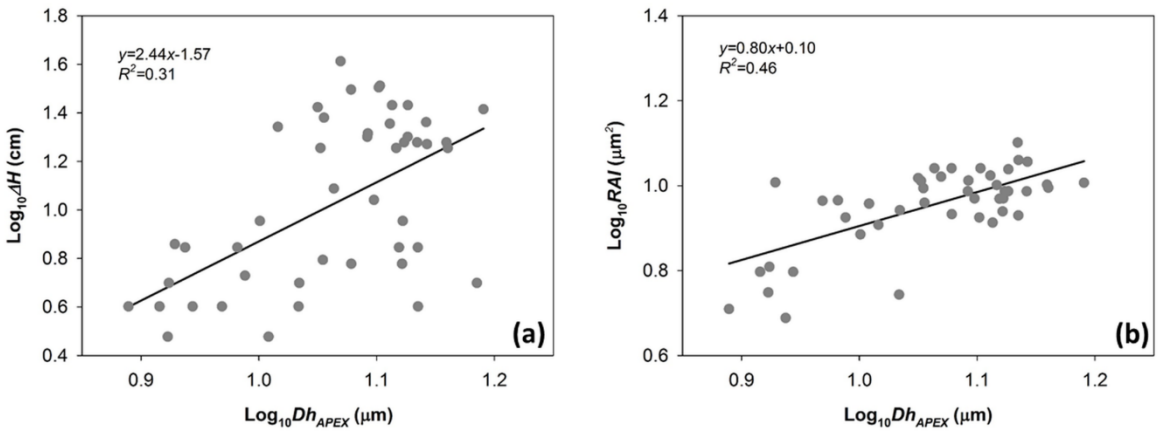
y=2.44x-1.57
R2=0.31
(a)
Log10ΔH (cm)
Log10DhAPEX (µm)
y=0.80x+0.10
R2=0.46
(b)
Log10RAI (µm2)
Log10DhAPEX (µm)

4.6 References

Anderegg WRL, Plavcová L, Anderegg LDL, Hacke UG, Berry JA, Field CB. 2013. Drought's legacy: multiyear hydraulic deterioration underlies widespread aspen forest die-off and portends increased future risk. *Global Change Biology* **19**: 1188–1196.

Anfodillo T, Petit G, Crivellaro A. 2013. Axial conduit widening in woody species: a still neglected anatomical pattern. *IAWA Journal* **34**: 352–364.

Antony F, Schimleck L, Daniels R. 2012. A comparison of earlywood-latewood demarcation methods – A case study in loblolly pine. *IAWA journal* **33**: 187–195.

von Arx G, Arzac A, Olano JM, Fonti P. 2015. Assessing conifer ray parenchyma for ecological studies: pitfalls and guidelines. *Frontiers in plant science* **6**: 1016.

von Arx G, Carrer M. 2014. ROXAS – A new tool to build centuries-long tracheid-lumen chronologies in conifers. *Dendrochronologia* **32**: 290–293.

von Arx G, Crivellaro A, Prendin AL, Čufar K, Carrer M. 2016. Quantitative wood anatomy—practical guidelines. *Frontiers in Plant Science* **7**: 781.

von Arx G, Dietz H. 2005. Automated image analysis of annual rings in the roots of perennial forbs. *International Journal of Plant Sciences* **166**: 723–732.

Baas P, Blokhina N, Fujii T, Gasson PE, Grosser D, Heinz I, Ilic J, Xiaomei J, Miller R, Newsom LA, *et al.* 2004. IAWA List of microscopic features for softwood identification. *IAWA Journal* **25**: 1–70.

Baig MN, Tranquillini W. 1980. The effects of wind and temperature on cuticular transpiration of *Picea abies* and *Pinus cembra* and their significance in dessication damage at the alpine treeline. *Oecologia* **47**: 252–256.

Baker DC, Spicer R, Gartner BL. 2000. Distribution and vitality of xylem rays in relation to tree leaf area in Douglas-fir. *IAWA Journal* **21**: 389–401.

Bannan MW. 1937. Observations on the distribution of xylem-ray tissue in conifers. *Annals of Botany* **1**: 717–726.

Barton K, Barton MK. 2013. MuMIn: multi-model interference. Rpackage version 1.9.5 (2013) Available at http://r-forge.r-project.org/projects/mumin/10/6/2013

Bates D, Mächler M, Bolker B, Walker S. 2015. Fitting linear mixed-effects models using lme4. *Journal of Statistical Software* **67**: arXiv:1406.5823.

Bittencourt PRL, Pereira L, Oliveira RS. 2016. On xylem hydraulic efficiencies, wood space-use and the safety-efficiency tradeoff. *New Phytologist* **211**: 1152–1155.

Brodersen CR, McElrone AJ. 2013. Maintenance of xylem network transport capacity: a review of embolism repair in vascular plants. *Frontiers in Plant Science* **4**: 1–11.

Burnham KP, Anderson DR. 2002. *Model selection and multimodel inference A practical information-theoretic approach (2nd edition)*. Ecological Modeling

Chave J, Coomes D, Jansen S, Lewis SL, Swenson NG, Zanne AE. 2009. Towards a worldwide wood economics spectrum. *Ecology Letters* **12**: 351–366.

Dawes MA, Hättenschwiler S, Bebi P, Hagedorn F, Handa IT, Körner C, Rixen C. 2010. Species-specific tree growth responses to 9 years of CO_2 enrichment at the alpine treeline. *Journal of Ecology* **99**: 382–394.

Dawes MA, Philipson CD, Fonti P, Bebi P, Hättenschwiler S, Hagedorn F, Rixen C. 2015. Soil warming and CO_2 enrichment induce biomass shifts in alpine tree line vegetation. *Global Change Biology* **21**: 2005–2021.

Dawes MA, Zweifel R, Dawes N, Rixen C, Hagedorn F. 2014. CO_2 enrichment alters diurnal stem radius fluctuations of 36-yr-old *Larix decidua* growing at the alpine tree line. *New Phytologist* **202**: 1237–1248.

Denne MP. 1988. Definition of latewood according to Mork (1928). *IAWA Journal* **10**: 59–62.

DeSmidt WJ. 1922. Studies of the distribution and volume of the wood rays in slippery elm (*Ulmus Fulva* Michx.). *Journal of Forestry* **20**: 352–362.

Domec JC, Pruyn ML, Gartner BL. 2005. Axial and radial profiles in conductivities, water storage and native embolism in trunks of young and old-growth ponderosa pine trees. *Plant, Cell and Environment* **28**: 1103–1113.

Eckstein D. 2013. 'A new star' - but why just parenchyma for dendroclimatology? *New Phytologist* **198**: 328–330.

Esteban LG, Martín JA, de Palacios P, Fernández FG. 2012. Influence of region of provenance and climate factors on wood anatomical traits of *Pinus nigra* Arn. subsp. *salzmannii*. *European Journal of Forest Research* **131**: 633–645.

Fatichi S, Leuzinger S, Körner C. 2014. Moving beyond photosynthesis: from carbon source to sink-driven vegetation modeling. *New Phytologist* **201**: 1086–1095.

Fatichi S, Rimkus S, Burlando P, Bordoy R, Molnar P. 2013. Elevational dependence of climate change impacts on water resources in an Alpine catchment. *Hydrology and Earth System Sciences Discussions* **10**: 3743–3794.

Fonti P, von Arx G, García-González I, Eilmann B, Sass-Klaassen U, Gärtner H, Eckstein D. 2010. Studying global change through investigation of the plastic responses of xylem anatomy in tree rings. *New Phytologist* **185**: 42–53.

Fonti P, Tabakova MA, Kirdyanov AV, Bryukhanova MV, von Arx G. 2015. Variability of ray anatomy of *Larix gmelinii* along a forest productivity gradient in Siberia. *Trees* **29**: 1165–1175.

Gartner BL, Baker DC, Spicer R. 2000. Distribution and vitality of xylem rays in relation to tree leaf area in Douglas-fir. *IAWA Journal* **21**: 389–401.

Gärtner H, Schweingruber FH, Dikau R. 2001. Determination of erosion rates by analyzing structural changes in the growth pattern of exposed roots. *Dendrochronologia* **19**: 81–91.

Gleason SM, Westoby M, Jansen S, Choat B, Hacke UG, Pratt RB, Bhaskar R, Brodribb TJ, Bucci SJ, Cao K, *et al.* 2016. Weak tradeoff between xylem safety and xylem-specific hydraulic efficiency across the world's woody plant species. *New Phytologist* **209**: 123–136.

Hacke UG, Sperry JS, Pockman WT, Davis SD, Mcculloh KA. 2001. Trends in wood density and structure are linked to prevention of xylem implosion by negative pressure. *Oecologia* **126**: 457–461.

Hagedorn F, Martin MA, Rixen C, Rusch S, Bebi P, Zürcher A, Siegwolf RTW, Wipf S, Escape C, Roy J, *et al.* 2010. Short-term responses of ecosystem carbon fluxes to experimental soil warming at the Swiss alpine treeline. *Biogeochemistry* **97**: 7–19.

Handa IT, Körner C, Hättenschwiler S. 2005. A test of the treeline carbon limitation hypothesis by in situ CO_2 enrichment and defoliation. *Ecology, Functional* **86**: 1288–1300.

Handa IT, Körner C, Hättenschwiler S. 2006. Conifer stem growth at the altitudinal treeline in response to four years of CO_2 enrichment. *Global Change Biology* **12**: 2417–2430.

Harsch M a, Hulme PE, McGlone MS, Duncan RP. 2009. Are treelines advancing? A global meta-analysis of treeline response to climate warming. *Ecology Letters* **12**: 1040–1049.

Hättenschwiler S, Handa IT, Egli L, Asshoff R, Ammann W, Körner C. 2002. Atmospheric CO_2 enrichment of alpine treeline conifers. *New Phytologist* **156**: 363–375.

Hoch G, Körner C. 2012. Global patterns of mobile carbon stores in trees at the high-elevation tree line. *Global Ecology and Biogeography* **21**: 861–871.

Hölttä T, Vesala T, Sevanto S, Perämäki M, Nikinmaa E. 2006. Modeling xylem and phloem water flows in trees according to cohesion theory and Münch hypothesis. *Trees* **20**: 67–78.

King DA. 2011. *Size-related changes in tree proportions and their potential influence on the course of height growth.* In: Meinzer FC,, In: Lachenbruch B,, In: Dawson TE, eds. Tree Physiology. Tree Physiology. Dordrecht: Springer Netherlands, 165–191.

Kolb KJ, Sperry JS. 1999. Transport constraints on water use by the Great Basin shrub, *Artemisia tridentata*. *Plant, Cell and Environment* **22**: 925–935.

Körner C. 2012. *Alpine Treelines*. Basel: Springer Basel.

Koubaa A, Zhang SYT, Makni S. 2002. Defining the transition from earlywood to latewood in black spruce based on intra-ring wood density profiles from X-ray densitometry. *Annals of Forest Science* **59**: 511–518.

Larcher W. 2003. *Physiological plant ecology: ecophysiology and stress physiology of functional groups* (Springer Science & Business Media, Ed.).

Larson PR. 1963. Stem form development of forest trees. *Forest science* **9**: a0001–a0001.

Lazzarin M, Crivellaro A, Williams CB, Dawson TE, Mozzi G, Anfodillo T. 2016. Tracheid and pit anatomy vary in tandem in a tall *Sequoiadendron giganteum* tree. *IAWA Journal* **37**: 172–185.

Legendre P. 2014. lmodel2: Model II Regression. R package version 1.7-2. Available at: http://CRAN.R-project.org/package=lmodel2.

Lintunen A, Paljakka T, Jyske T, Peltoniemi M, Sterck F, von Arx G, Cochard H, Copini P, Caldeira MC, Delzon S, *et al.* 2016. Osmolality and non-structural carbohydrate composition in the secondary phloem of trees across a latitudinal gradient in Europe. *Frontiers in Plant Science* **7**: 726.

Martin MA, Gavazov K, Körner C, Hättenschwiler S, Rixen C. 2010. Reduced early growing season freezing resistance in alpine treeline plants under elevated atmospheric CO_2. *Global Change Biology* **16**: 1057–1070.

Martorell S, Medrano H, Tomàs M, Escalona JM, Flexas J, Diaz-Espejo A. 2015. Plasticity of vulnerability to leaf hydraulic dysfunction during acclimation to drought in grapevines: An osmotic-mediated process. *Physiologia Plantarum* **153**: 381–391.

Mayr S, Cochard H, Ameglio T, Kikuta SB. 2006a. Embolism formation during freezing in the wood of *Picea abies*. *Plant physiology* **143**: 60–67.

Mayr S, Wieser G, Bauer H. 2006b. Xylem temperatures during winter in conifers at the alpine timberline. *Agricultural and Forest Meteorology* **137**: 81–88.

McElrone AJ, Pockman WT, Martinez-Vilalta J, Jackson RB. 2004. Variation in xylem structure and function in stems and roots of trees to 20 m depth. *New Phytologist* **163**: 507–517.

Meinzer FC, Lachenbruch B, Dawson TE. 2011. *Size- and Age-Related Changes in Tree Structure and Function* (FC Meinzer, B Lachenbruch, and TE Dawson, Eds.). Dordrecht: Springer Netherlands.

Mitchell MD, Denne MP. 1997. Variation in density of *Picea sitchensis* in relation to within-tree trends in tracheid diameter and wall thickness. *Forestry* **70**: 47–60.

Myburg AA, Lev-Yadun S, Sederoff RR. 2013. Xylem Structure and Function. ELS. Chichester, UK: John Wiley & Sons, Ltd, 1–9.

Nardini A, Lo Gullo MA, Salleo S. 2011. Refilling embolized xylem conduits: is it a matter of phloem unloading? *Plant Science* **180**: 604–611.

Olano JM, Arzac A, García-Cervigón AI, von Arx G, Rozas V. 2013. New star on the stage: amount of ray parenchyma in tree rings shows a link to climate. *New phytologist* **198**: 486–95.

Olson ME, Anfodillo T, Rosell JA, Petit G, Crivellaro A, Isnard S, León-Gómez C, Alvarado-Cárdenas LO, Castorena M. 2014. Universal hydraulics of the flowering plants: vessel diameter scales with stem length across angiosperm lineages, habits and climates (B Enquist, Ed.). *Ecology Letters* **17**: 988–997.

Petit G, Anfodillo T. 2009. Plant physiology in theory and practice: an analysis of the WBE model for vascular plants. *Journal of Theoretical Biology* **259**: 1–4.

Petit G, Anfodillo T, Carraro V, Grani F, Carrer M. 2011. Hydraulic constraints limit height growth in trees at high altitude. *New phytologist* **189**: 241–52.

Petit G, Anfodillo T, De Zan C. 2009. Degree of tapering of xylem conduits in stems and roots of small *Pinus cembra* and *Larix decidua* trees. *Botany* **87**: 501–508.

Petit G, Pfautsch S, Anfodillo T, Adams MA. 2010. The challenge of tree height in *Eucalyptus regnans*: when xylem tapering overcomes hydraulic resistance. *New Phytologist* **187**: 1146–1153.

Pinheiro J, Bates D. 2000. *Mixed-effects models in S and S-Plus*. New York, NY, USA: Springer-Verlag.

R Development Core Team. 2014. R: A language and environment for statistical computing.

Rixen C, Dawes MA, Wipf S, Hagedorn F. 2012. Evidence of enhanced freezing damage in treeline plants during six years of CO_2 enrichment and soil warming. *Oikos* **121**: 1532–1543.

Salleo S, Trifilò P, Esposito S, Nardini A, Lo Gullo MA. 2009. Starch-to-sugar conversion in wood parenchyma of field-growing Laurus nobilis plants: a component of the signal pathway for embolism repair? *Functional Plant Biology* **36**: 815.

Savage VM, Bentley LP, Enquist BJ, Sperry JS, Smith DD, Reich PB, von Allmen EI. 2010. Hydraulic trade-offs and space filling enable better predictions of vascular structure and function in plants. *Proceedings of the National Academy of Sciences* **107**: 22722–22727.

Smith WK, Germino MJ, Hancock TE, Johnson DM. 2003. Another perspective on altitudinal limits of alpine timberlines. *Tree Physiology* **23**: 1101–1112.

Sperry JS, Meinzer FC, McCulloh KA. 2008. Safety and efficiency conflicts in hydraulic architecture: scaling from tissues to trees. *Plant, Cell and Environment* **31**: 632–645.

Spicer R. 2014. Symplasmic networks in secondary vascular tissues: parenchyma distribution and activity supporting long-distance transport. *Journal of Experimental Botany* **65**: 1829–1848.

Streit K, Siegwolf RTW, Hagedorn F, Schaub M, Buchmann N. 2014. Lack of photosynthetic or stomatal regulation after 9 years of elevated CO_2 and 4 years of soil warming in two conifer species at the alpine treeline. *Plant, Cell & Environment* **37**: 315–26.

Tyree MT, Zimmermann MH. 2002. *Xylem structure and the ascent of sap.* Spring series in wood sciences, 2nd edn (ed. Timell, T.E.). Springer-Verlag, Berlin, pp. 283.

West GB, Brown JH, Enquist BJ. 1999. A general model for the structure and allometry of plant vascular systems. *Nature* **400**: 664–667.

Wimmer R. 2002. Wood anatomical features in tree rings as indicators of environmental change. *Dendrochronologia* **20**: 21–36.

Zuur AF, Ieno EN, Walker N, Saveliev AA, Smith GM. 2009. *Mixed effects models and extensions in ecology with R*. New York, NY: Springer New York.

5 Ontogenetically stable axial widening and the imprinting of height growth information on the radial variation of conduit lumen diameter. A case study on the effects of climate change on tree growth at high altitude in Alpine conifers

Angela Luisa Prendin[1]*, Valentina Buttò[1], Daniele Castagneri[1], Georg von Arx[2], Patrick Fonti[2], Marco Carrer[1], Giai Petit[1]

[1] Dept. Territorio e Sistemi Agro-Forestali, Università degli Studi di Padova, Legnaro (PD), Italy

[2] Swiss Federal Institute for Forest, Snow and Landscape Research WSL, Birmensdorf, Switzerland

*** Corresponding author**

Keywords: axial allometry, cell wall thickness, conifers, elevated CO_2, elevated temperature, primary and secondary growth relationships, tracheid lumen size, tree-ring anatomy

5.1 Abstract

The lumen diameter of xylem conduits is reported to increase from the stem apex to base according to a supposedly universal scaling pattern (axial widening). While empirical data seemed to support this hypothesis, yet a thorough analysis to test whether the pattern is maintained throughout ontogeny is still missing. However, it had been argued that, if the axial widening is stable during ontogeny, then conduit diameter at the stem base in the last annual ring should depend primarily on the tree height achieved in that given year. We tested whether the comparison of the radial pattern of the hydraulic conduit diameter (*Dh)* could be used to test for differences in height growth between trees.

We measured the (*Dh*) from pith to bark (i) on 17 discs along the stem of a mature spruce tree to reconstruct the variation of axial widening during ontogeny, and (ii) on several tree cores from *Larix decidua (Mill.)*, *Picea abies (L.) Karst.* and *Pinus cembra* (L.) trees differing in age from three high altitude sites in the Alps.

We found that axial widening did not significantly vary during the ontogeny of our 220 year old spruce (P=0.09).

We found that the radial *Dh* profiles of young living trees of each species are in most cases steeper than those of older ones, thus suggesting a faster height growth.

We conclude that axial conduit widening is substantially stable during ontogeny. This allows us to state that, in our high altitude sites, those younger trees showing a steeper *Dh* radial profile are increasing in height at faster rates than older trees did at the same age, likely a consequence of the effects of global warming in stimulating the physiological processes in trees from cold environments.

5.2 Introduction

Trees are long-living organisms that continuously increase in size during ontogeny by accumulating xylem biomass in stem, branches and roots. Being sessile organisms, evolution favoured different mechanisms of adaptation and acclimation to survive a certain degree of climate variability. Woody plants, and trees in particular, need to continuously adjust the xylem structure to overcome the mechanical and hydraulic limitations while growing taller (Domec & Gartner, 2002; Fonti *et al.*, 2010; von Arx *et al.*, 2012; Aloni, 2013; Carrer *et al.*, 2015; Petit *et al.*, 2016). Indeed, xylem is a functional adaptive structure designed to safely and efficiently conduct water from roots to leaves to sustain transpiration by keeping stomata open and thus enable carbon uptake (Zimmermann, 1983; Sperry, 2003; Franks, P. J. & Brodribb, 2005).

For a tree, plastic adjustments of wood-anatomical features represent a key strategy to optimally balance the competing needs of support, storage and transport, which may vary during ontogeny and under changing environmental conditions (Chave *et al.*, 2009). Wider conduits contribute to enhance the hydraulic conductance (Brodribb & Feild, 2000), thus stimulating leaf-level photosynthesis and faster growth (Meinzer *et al.*, 2011; Petit *et al.*, 2011). However, wider conduits are also reported to increase the risk of embolism formation, with negative consequences on the total xylem conductance, thus limiting water transport and carbon assimilation (Tyree & Sperry, 1989). Throughout the life of a tree, different plastic adjustments in the xylem structures can respond to different requirements in terms of hydraulic efficiency or safety occurring at different temporal scales (Meinzer *et al.*, 2011). These adjustments in the xylem structure remain permanently fixed and chronologically archived in the different anatomical traits. Therefore, dendro-anatomy, i.e. the study of anatomical features of tree rings, is emerging as an important field of plant science to retrospectively analyze the functional responses of trees to climate variability (Fonti *et al.*, 2010). Anyway, there is still a lack of studies at the intraspecific level (Martin *et al.*, 2010) investigating on the long term xylem modifications occurring over the full life-span of a tree, and how these changes are imprinted along the axial and radial profiles of a tree (Sala *et al.*, 2012; Streit *et al.*, 2014). As a tree gets taller, the distance between leaves and roots becomes longer and the tensile strength of 'pulling' water to the transpiring leaves increases accordingly (Koch *et al.*, 2004). Plant species have evolved anatomical adjustments to compensate for the

hydraulic limitation imposed by the increased tree height. According to the Hagen-Poiseuille law, the hydraulic resistance of a cylindrical tube is directly proportional to its length and inversely proportional to the fourth power of its diameter (Tyree & Ewers, 1991). This implies that taller trees have to lower the leaf water potential to maintain leaf transpiration (Koch *et al.*, 2004), thus making the xylem system more vulnerable to cavitation through air seeding, occurring when air bubbles are aspirated into the water-filled conduits (Zimmermann, 1983; Tyree & Sperry, 1989). To overcome these ontogenetic-related hydraulic constraints of maintaining xylem safety and efficiency, the xylem system is constituted of small conduits close to the stem apex, where they can provide a higher safety (Hacke *et al.*, 2016) in a portion of the hydraulic pathway where the tension is highest. Below, xylem conduits increase in lumen area with increasing distance from the apex, following a power trajectory with the exponent generally converging to the value of around 0.18-0.20 (Anfodillo *et al.*, 2013; Olson *et al.*, 2014). With this axial configuration, most of the resistance is confined at the apex (Yang & Tyree, 1993; Becker *et al.*, 2000; Petit *et al.*, 2009, 2011), with conduit widening effectively minimize the effect of the increased height on the total hydraulic resistance. Empirical studies suggested that xylem widening is a universal feature in trees, independent of environmental conditions. Given the consistency of the pattern, it was reasonable to deduct that widening is also stable during ontogeny, although in this respect confirmatory studies are rare (Weitz *et al.*, 2006; Riondato, 2009).

Consequently, the tree hydraulic architecture is build up according to a strong mechanistic link between conduit lumen size and height growth, making the patterns of conduit dimension within a tree dependent to the stem elongation occurred during the different ontogenetic phases (Carrer *et al.*, 2015). Since the axial widening of xylem conduits seemed to be actually stable during ontogeny (Weitz *et al.*, 2006; Riondato, 2009), it follows that conduit lumen diameter increases radially with cambial age (i.e from pith to bark) at rates dependent on the rates of stem elongation occurred during ontogeny (Carrer *et al.*, 2015). Carrer *et al*. hypothesised that for a constant annual height growth from seedling to maturity, the pattern of conduit-diameter vs cambial age would reflect the stable power scaling of conduit widening, implying that any actual deviation from this radial pattern would reflect a positive or negative pulse of height growth during different periods (Carrer *et al.*, 2015). Therefore, the information imprinted in the radial patterns

of xylem anatomical features represent a strong link between the tree structures and the physiological responses to environmental variability and size-related constraints faced by trees during their ontogenetic development. For instance, comparing the steepness of the radial pattern of xylem conduit dimension of trees differing in age should provide information on the mean rate of height growth during different periods. In this respect, it would be ideal to test such a hypothesis in cold environments, where current climate changes, such as the increase in temperature and CO_2 concentration are more or less quickly releasing the local growth constraints.

Primary and secondary growth at the treeline is determined by co-occurring environmental constraints preventing a positive carbon balance in trees burdened with large proportions of non productive tissues (Hättenschwiler *et al.*, 2002), with atmospheric CO_2 concentration and temperatures playing a major role in influencing the rate of carbon availability for structural growth (Dawes *et al.*, 2010).

During the recent decades, a trend of shifting treeline position towards higher altitudes and latitudes has been observed at global scale (Körner, 1998; Harsch *et al.*, 2009), and attributed to the effects of increasing anthropogenic greenhouse gas emissions on global temperatures, atmospheric CO_2 concentration (Cannone *et al.*, 2007; Körner, 2012) and nitrogen deposition (Schlesinger, 2009). Global warming was supposed to reduce the temperature constraints of different metabolic activities, in particular the enzymatic fixation of non structural carbon compounds (NSCs) into xylem biomass (sink limitation hypothesis – SLH) (Li *et al.*, 2002; Körner, 2003a; Danby & Hik, 2007; Dawes *et al.*, 2015). The increase in CO_2 concentration would promote tree growth, especially at high altitude treelines of low-mid latitudes (Smith *et al.*, 2009), by reducing the negative effect of reduced CO_2 partial pressure with altitude (La Marche *et al.*, 1984; Körner, 2003a,b). Additionally, the recent levels of nitrogen deposition are altering the nitrogen cycle and soil nitrogen availability, thus stimulating the tree physiological responses and the overall forest carbon cycle (Magnani *et al.*, 2007; Leonardi *et al.*, 2012).

In this study, we present a comprehensive framework aimed to explore whether it is possible to extract information of ontogenetic growth from the radial patterns on xylem conduit dimension of tree rings.

First, we thoroughly tested the fundamental hypothesis of the ontogenetic stability of the axial xylem conduit widening. We used a dendro-anatomical approach to analyse the

radial profiles of xylem conduit diameter of tree rings at every 1 m along the stem of a single mature tree, and thus reconstruct at annual resolution the variation of the stem apex to base pattern of conduit widening during ontogeny (from seedling to maturity).
Additionally, we analysed the radial pattern of xylem conduit diameter in trees of different coniferous species and widely differing at different alpine treeline locations, to test whether younger trees, taking advantage from the current climate changes are growing faster than older trees did during their juvenile stage.

5.3 Material and methods

5.3.1 Study sites and plant material

For the test for the ontogenetic stability of conduit widening we used plant material already available in our lab. In 2007, a dominant 26 m tall Norway spruce (*Picea abies* Karst.) tree of around 220 years and a 20 m tall Stone pine (*Pinus cembra L.*) of around 175 years were felled from a mixed montane forest at 1400 m in the Dolimites, Italian Alps (Obereggen, Bolzano). Additionally, two European larch (*Larix decidua Mill.)* trees (4 m tall and about 40 years) collected in Stillberg reseach area, Davos (Switzerland). Stem disks were cut every 1 m (*P. abies* and *P. cembra*) or 15 cm (*L. decidua*) from the stem base to the treetop and then transported and stored in our lab.
For each disc, we extracted a radial segment from pith to bark, smoothly sanded the cross sectional surface, and measured the ring with (see below). We then reconstructed the total tree height achieved in the different years according to the different ring number between two successive discs. Consequently, we could attribute the corresponding distance from the apex (*L*) to each dated ring, calculated as the difference between the reconstructed tree height and the distance from the ground.
The comparative analysis of growth response assessed by radial patterns of xylem conduit dimension, we selected three different treeline locations across the Alps.
The three study sites are located in the Lötschental (46°23′N, 7°45′E, Central Swiss Alps), in Croda da Lago (46°27'N; 12°08'E, Eastern Italian Alps), and in valle Ventina (45°26'N, 28°33'E, Central Italian Alps).

Lötschental is a South-West-to-North-East oriented inner Alpine valley. The selected site was established at around 2200 m a.s.l., in an forested area with prevalence of Norway spruce and European larch.
Lötschental valley has a cold, dry climate with a mean annual temperature of 6° C, ranging from -3 (January) to 15° (July) and a mean annual precipitation exceeding 1000 (Schmidt *et al.*, 2009).
Croda da Lago site has a North-East aspect and is located at 2100 m a.s.l., in a *L. decidua*, *P. abies* and *P. cembra* subalpine forest. The air temperature, measured by the nearest meteorological station in Cortina d'Ampezzo, spans from -25 °C (January) to 30 °C (July) with an annual mean of 6.7 °C (Rossi *et al.*, 2006a,b), while the total annual precipitation is on average 1100 mm (Urbinati *et al.*, 1997).
Valle Ventina is oriented North-South and is an inner valley characterized by a continental climate. The sampling site was located at 2200 m a.s.l., where *L. decidua* is the dominant tree species with *P. abies*, *P. cembra* and mountain pine (*Pinus mugo* subsp. *Uncinata* Ramond ex DC) as co-dominant species throughout. Annual precipitation from 1921 to 1990 varied from 668 mm to 1551 mm, averaging 974.9 mm (Lanzada, 1000 m a.s.l.) (Garbarino *et al.*, 2010) and mean annual temperature of 3.4°C, varying between -4.5 °C (January) to 11.5 °C (July) (Harris *et al.*, 2014).
From each site, we extracted cores from breast height of trees widely differing in age. For Lötschental and Croda da Lago we sampled old (>150 years) vs. young (<50 years) trees. Sampled species were *Larix decidua* in all sites, *Picea abies* and *P. cembra* only in Croda da Lago. Selected trees did not show any damage of terminal leading shoot or signs of serious herbivory and/or diseases.

5.3.2 Measurements

Standard dendrochronological techniques were used to collect and prepare samples for tree-ring width (TRW) measurement (Schweingruber, 1996). All the 57 cores were prepared by sanding with a belt sander or by cutting with a the core-microtome (Gärtner & Nievergelt, 2010). Ring-widths (RW) were measured to the nearest 0.001 mm with a LINTAB tree-ring measuring system or with WinDENDRO (Regent Instruments Canada Inc. 2004) after scanning at 1900 dpi (Epson Expression 10000XL). Time series were then cross-dated with TSAP (RINNTECH Inc. Heidelberg, Germany). A minimum of two radii

per tree were measured in all but a few cases. Cross-dating accuracy was verified with COFECHA (Holmes, 1983).

In those cores not reaching the pith in their innermost part, the number of missing rings was estimated with standard techniques (i.e., by comparing the ring curvature against concentric circles to estimate the distance to the pith, divided by the average ring width of the youngest ten rings) (Sperry, 2010).

Cross sections of 57 tree cores (Tab. 1) and of radial segments of 44 discs were cut at 10-15 μm using a rotary microtome (RM2245, Leica, Heidelberg, Germany). The micro sections were stained with a solution of safranin (1% in distilled water) and Astrablue (0.5% in distilled water) and permanently fixed with Eukitt (BiOptica, Milan) following standard a standard protocol (von Arx *et al.*, 2016). Slides were photographed at 40X magnifications using a digital camera mounted on a light microscope (Nikon Eclipse 80i, Nikon, Tokyo, Japan) to get height resolution images (0.833 pixel/ μm) of the entire/or partial thin section. Multiple digital images (overlapping ca. 25%) were stitched together using PTGui v8.3 (New House Internet Service B.V., The Netherlands).

Stitched images of cross sections were automatically analysed using ROXAS v2.1 (von Arx & Dietz, 2005; von Arx & Carrer, 2014) for the measurement of several parameters performed at the cell level, such as ring width (RW) and single xylem conduit area (CA). Definitive analysis output required a previous manual editing to draw ring borders and cancel/draw wrong/missing tracheids (Carrer *et al.*, 2015).

Overall, more than 13000 rings and 20 millions of cells (with a mean of 1844 cells per ring) were processed.

For each ring of each core, ROXAS calculated the hydraulically weighted diameter (*Dh*) as (Kolb & Sperry, 1999):

$$Dh = \frac{\sum d_n 5}{\sum d_n 4} \qquad \text{eq. 1}$$

where d_n is the diameter of the *n*-conduit, assumed to be circular and estimated as:

$$d_n = 2 \cdot \left(\frac{A_n}{\pi}\right)^{1/2} \qquad \text{eq.2}$$

with A_n being the lumen area of the *n*-conduit.

5.3.3 Statistical analysis

Data were $\log_{10}$-transformed to comply with assumptions of normality and homoscedasticity (Zar, 1999). The ontogenetic effects on the relationship of *Dh* vs *L* and cambial age (C_{AGE}) were tested the linear regression model on $\log_{10}$-transformed variables.

Age and site effects on the axial patterns were tested using linear mixed-effects models fitted with restricted maximum likelihood. We established a models for *Dh* where C_{AGE}, growth period (GP), site (see Table 2) and their interactions were included as fixed effects, and tree identity as random factor in all initial models, reflecting the sample collection. Linear models were run using lme4 (Bates *et al.*, 2015) and MUMIN packages (Barton & Barton, 2015) with R v3.1.1. (R Development Core Team, 2014).

5.4 Results

5.4.1 Variation of axial conduit widening during ontogeny

We analyzed the variation of the hydraulic mean diameter (*Dh*) with the distance from the apex (*L*) for 220, 170 and 30 reconstructed annual apex-to-base profiles along the stem respectively for the *P. abies*, *P. cembra* and *L. decidua* trees. The patterns were remarkably univocal, with a steep increase in *Dh* until around 4-10 m from the apex, and further below *Dh* leveled off until the stem base. Although the patterns were not clearly following a pure power function (see the $\log_{10}$-transformed date not aligned on a straight line Fig.1c), yet the power fitting was best fitting the data (R^2=0.78) (Fig. 1c). We then tested whether this axial pattern remained stable during ontogeny, and found that the scaling exponents *b* averaged the value of 0.13 and did not significantly vary with age (*P*=0.20,*P*=0.27 and *P*=0.13, respectively for *P. abies*, *P. cembra* and *L. decidua*) (Fig. 2). In parallel, we found that the radial variation of *Dh* with cambial age (C_{AGE}) was similar for all the stem disc (Fig. 1b). In particular we found that the scaling exponent of the power equation fitting the data relative to the second basal discs (at 2 m from the ground, to avoid compression wood) and the first 60 years of growth was respectively *b*=0.28 (R^2=0.87) (Fig. 1d).

5.4.2 Comparative analysis of radial widening

Similarly to the radial profiles of *Dh* reported for the different stem collected at different height along the stem of our Norway spruce tree, in all the tree cores or discs sampled at the different high altitude sites across the Alps, we found that *Dh* increased from the pith to the bark. A more pronounced variation was found during the first phases of ontogenetic growth (50-100 years) (fig. 3). Our tests performed with linear mixed effects models on the influence of GP, species and site on the radial scaling of the *Dh* with the C_{AGE} (restricted to the first 60 years) showed several significant effects (Tab. 2 and Tab. 3).

L. decidua young (age < 100 years) living trees from Lötschental and Ventina showed a steeper increase in *Dh* with cambial age (C_{AGE}) compared to the other older trees. On the contrary, the radial trend of *Dh* vs. C_{AGE} showed a significant flattening in young trees at Croda da Lago (Tab. 2).

In Croda da Lago, P. abies and *P. cembra* young trees showed a steeper increase in *Dh* with C_{AGE} compared to older individuals (Tab. 2).

We then tested potential site differences in the radial *Dh* profiles (restricted to the first 60 years) of trees growing in different GP. In *L. decidua*, the radial Dh pattern was significantly steeper in Lötschental and Ventina compared to Croda da Lago, whereas the opposite trend was found for the older trees (Tab. 3).

5.5 Discussion

Our analyses confirmed that the whole xylem hydraulic architecture is build-up during the ontogenetic development according to a strong mechanistic link between conduit lumen size and height growth (Carrer *et al.*, 2015). We found that the hydraulic diameter of xylem conduits (*Dh*) increased from the stem apex downwards along the stem axis until the base following a pattern that was substantially maintained during all the 220 years of ontogenetic development of the analyzed tree. *Dh* steeply increased until 5-10 m from the apex, whereas further below it leveled off, i.e., not increasing much further until the stem base (Fig. 1a). This result strongly supported the hypothesis that the axial conduit widening is an ontogenetically stable feature of the whole xylem transport system (Weitz *et al.*, 2006; Riondato, 2009). As expected, the power function was the best fitting for the

measured values, and the obtained scaling exponent (b=0.13) was very similar to those reported in literature (e.g., Anfodillo *et al.*, 2013; Olson *et al.*, 2014), thus supporting also the remarkable universality of the axial conduit widening in vascular plants (West *et al.*, 1999; Anfodillo *et al.*, 2006; Olson *et al.*, 2014). This strict axial configuration of basal conduit widening represents a biophysical optimization to buffer the negative effect of path length on the total hydraulic resistance (West *et al.*, 1999; Petit *et al.*, 2009, 2010). In this way, most of the total resistance is confined close to the stem apex, thus allowing the adjustments of the whole transport system required during ontogeny to meet the changing functional and structural needs as the tree size increases. We demonstrated that the stability of the axial conduit widening configuration implies that, while growing taller, a tree compensate for the negative effect of the increased hydraulic path length simply by enlarging the xylem conduits at the stem base (Anfodillo *et al.*, 2006).

As consequence of the ontogenetic stability of the axial widening, we found that the conduit lumen diameter (Dh) increases radially with cambial age (C_{AGE}) (i.e from pith to bark) and thus supported the hypothesis that this patter is dependent on the rate of stem elongation occurred during ontogeny (Carrer *et al.*, 2015). This finding provided a solid theoretical basis for our following case study of comparing the height growth development of trees of different age, species and sites, based on the analysis of radial pattern of xylem conduit dimension at the stem base. However, it must be highlighted that this approach has some limitations due to the fact that the increase in conduit dimension strongly levels off after a certain distance from the apex, as also previously found (Mencuccini *et al.*, 2007; Petit *et al.*, 2010). However, the comparative analysis of height growth patterns by means of anatomical measurements of conduit dimension can be considered effective during the juvenile ontogenetic phase, as in our case.

The analysis of the radial scaling of the hydraulic conduit diameter (Dh) with cambial age (C_{AGE}), restricted to the first 60 years of tree development, overall showed that currently living young trees had a significantly steeper radial trend of Dh with C_{AGE}, thus suggesting that they are growing in height at faster rates compared to the past. This result is in agreement with other observations that recent climate changes, and in particular the increase in air temperatures, are stimulated tree growth in cold environments in the last decade (Körner & Paulsen, 2004; Körner, 2012), leading to a latitudinal and longitudinal shift of natural treeline positions (Körner, 1998; Harsch *et al.*, 2009). In addition, recent

studies reported that stem elongation is dependent from the "apical hydraulic bottleneck", i.e. by the effect of the narrow apical conduits on the total hydraulic resistance (Petit *et al.*, 2011). Increasing temperatures, together with an additional effect of increasing CO_2 concenntration can stimulate small modifications at the apical level that can have a much greater impact on the total xylem conductance, thus favoring gas exchange and ultimately primary and secondary (Petit *et al.*, 2011; Prendin et al., 2016 under review) growth.

In our case studies we found some species and site specific differences the radial pattern of young living trees and older trees. Most likely, these differences reflected the species specific response to the environmental conditions of the different sites. For instance, the historical forest management at the different sites might have favored one species over the others. At Croda da Lago, the forest is left to natural evolution since approximately 200 years, whereas in former times the site was managed to favor pasture, with *L. decidua* trees being advantaged over the other species for its lighter crown allowing the development of herbaceous species (Garbarino *et al.*, 2009, 2011, 2013). Indeed, tree growth of *L. decidua* profited of this type of management. In recent times the forest cover is progressively closing, thus determining a higher competitive pressure for the use of resources on this species. On the other hand, at Lötschental is likely that tree growth can be more strongly affected by physical disturbances such as winter snow cover and avalanches. *L. decidua* is certainly more adapted to supporting heavy snow loads because of its deciduousness and more elastic wood. In addition, the warming trend occurred over the last couple of decades has coincided with the reduction of the Larch budmoth [LBM; *Zeiraphera diniana* Gn. (Lepidoptera: Torticidae)] outbreaks across the European Alps (Johnson *et al.*, 2010, Peters et al., 2016 in prep), with positive effects on the competitiveness of *L. decidua*, especially in the Central and Western Alps.

At the Ventina site, we compared the radial trend of *Dh* in *L. decidua* trees divided in three different epochs according to their estimated year of birth. The three epochs referred to well known time windows characterized by particular climate conditions: the Little Ice Age (LIA: 1450-1850) and the Current Warm Period (CWP: 1900-present) (Buntgen et al., 2005). We found that the living young trees (CWP) are growing faster than in the past, and notably even if compared to trees from the MWP, when temperatures were supposedly higher than nowadays (Buntgen et al., 2005). This suggested that the forest

dynamics at that specific site, which is not heavily affected by human activities, is proceeding at an unprecedented speed over the last centuries.

Conclusions

With this study we presented a novel approach based on xylem anatomy to study at different time and spatial scales the tree growth during the juvenile phase under different climatic conditions. We provided empirical evidence that the assumption of this methodology, i.e. that the axial pattern of conduit widening is stable during ontogeny, holds true, thus allowing the possibility to provide the third dimensional component to the dendro-ecological analyses. However, further study are certainly needed to better understand the limitations and strengths of this novel approach to better interpret the tree responses to climate change.

Acknowledgements

This work was supported by the University of Padua (60A08-7773/14 and 60A08-2852/15). We warmly thank , Margherita Banalotti, Alessandro Farinati, Natasa Kiorapostolou, Francesca Marcon, Francesco Natalini, Richard Peters and Lucrezia Unterholzner for their help in carrying out part of the laboratory work.

Tables

Table 1: Height (H), diameter at breast height (DBH) and Age (mean ± SE) of the sampled trees growing in different epochs (Growth Period).

Specie	Growth Period	Croda da Lago				Lötschental				Ventina			
		cores	**Height**	**DBH**	**Age**	**cores**	**Height**	**DBH**	**Age**	**cores**	**Height**	**DBH**	**Age**
Larix decidua	1900-2015	5	11.42±0.15	17.89±0.16	43.1±1.25	5	8.88±0.12	18.32±0.27	27.64±1.38	4	-	-	31.14±1.68
	1500-2015	6	22.08±0.08	63.76±0.20	203.34±2.64	5	17.71±0.13	62.62±0.55	161.07±2.99	5	-	-	257.5±3.73
Picea abies	1900-2015	11	8.56±0.14	16.19±0.24	27.03±0.63	-	-	-	-	-	-	-	-
	1500-2015	6	20.24±0.09	53.62±0.30	145.20±2.25	-	-	-	-	-	-	-	-
Pinus cembra	1900-2015	5	8.72±0.09	18.86±0.13	25.61±0.99	-	-	-	-	-	-	-	-
	1500-2015	5	14±0.00	52.00±0.00	236.91±3.74	-	-	-	-	-	-	-	-

Table 2: Results of the optimal linear mixed-effect model predicting the period effects on the relationship between $Log_{10}Dh$ and $Log_{10}C_{AGE}$ (on *y*-intercept and slope, i.e., the interaction between period and $Log_{10}\ C_{AGE}$) for the different species, sites and growth period (see methods for details). Numbers indicate the estimates ± SE. Levels of significance are: * $P< 0.05$, ** $P< 0.01$ and *** $P< 0.001$.

	Croda da Lago			***Lötschental***		**Ventina**
Fixed effect	*Larix decidua*	*Picea abies*	*Pinus cembra*	*Larix decidua*	*Picea abies*	*Larix decidua*
			$Log_{10}\ Dh$			
Intercept (1500-2015)	1.01±0.02***	1.22±0.02***	1.13±0.02***	1.19±0.03***	0.74±0.05***	1.16±0.05***
$Log_{10}C_{AGE}$(1500-2015)	0.31±9.52x10^{-3}***	0.12±0.01***	0.19±9.67x10^{-3}***	0.17±0.01***	0.41±0.02***	0.21±0.01***
1900-2015	0.11±0.03***	-0.23±0.03***	0.02±0.03	-0.21±0.05***	0.10±0.07	-0.30±0.06**
$Log_{10}\ C_{AGE}$:1900-2015	-0.07±0.01***	0.20±0.01***	0.03±0.01.	0.19±0.02***	-0.06±0.03*	0.15±0.02***

Table 3: Results of the optimal linear mixed-effect models predicting the site effects on the relationship between $Log_{10}Dh$ and $Log_{10}C_{AGE}$ (on *y*-intercept and slope, i.e., the interaction between period and $Log_{10}C_{AGE}$) for the different species and sites (see methods for details). Numbers indicate the estimates ± SE. Levels of significance are: * $P< 0.05$, ** $P< 0.01$ and *** $P< 0.001$.

	Larix decidua		*Picea abies*	
Fixed effect	1900-2015	1500-2015	1900-2015	1500-2015
	Log₁₀ Dh			
Intercept (Croda da Lago)	1.13±0.03***	1.02±0.03***	0.99±0.02***	1.22±0.03***
Log_{10} C_{AGE} : Croda da Lago	0.24±0.01***	0.31±0.01***	0.31±9.25x10^{-3}***	0.12±0.01***
Lötschental	-0.15±0.04**	0.17±0.04**		
Log_{10} C_{AGE} : Lötschental	0.12±0.02***	-0.14±0.02***		
Ventina	-0.27±0.04***	0.14±0.04**		
Log_{10} C_{AGE} : Ventina	0.11±0.02***	-0.11±0.02***		

Figure captions

Figure 1: Variation of the xylem hydraulic diameter (*Dh*) with (a) the distance from the apex (*L*) and (b) cambial age (C_{AGE}). Log_{10}-transformed data, describe the axial scaling (*Dh* ~ *L)* (c) and radial scaling (*Dh* ~ C_{AGE}, restricted to the first 60 years) (d), solid lines represent the fitted linear regressions. The different colors refer to the data belonging to the *P. abies*, *P. cembra* and *L. decidua* trees analyzed.

Figure 2: Ontogenetic variation of the scaling exponent (*b*) of the power function fitting the axial profile of the xylem hydraulic diameter (*Dh*) vs. the distance from the apex (*L*) calculated for each year of growth of *P. abies*, *P. cembra* and *L. decidua* trees.

Figure 3: Radial variation of the xylem hydraulic diameter (*Dh*) with cambial age (C_{AGE}) for the different species, sites and reference growth period (*GP*). Colors represent the different growth periods: 1900-2015 (red) and 1500-2015 (light blue). In the insets, data are Log_{10}-transformed and solid lines represent the fitted linear regressions limited to the juvenile phase (i.e., $C_{AGE} \leq 60$ years).

Figures

Figure 1:

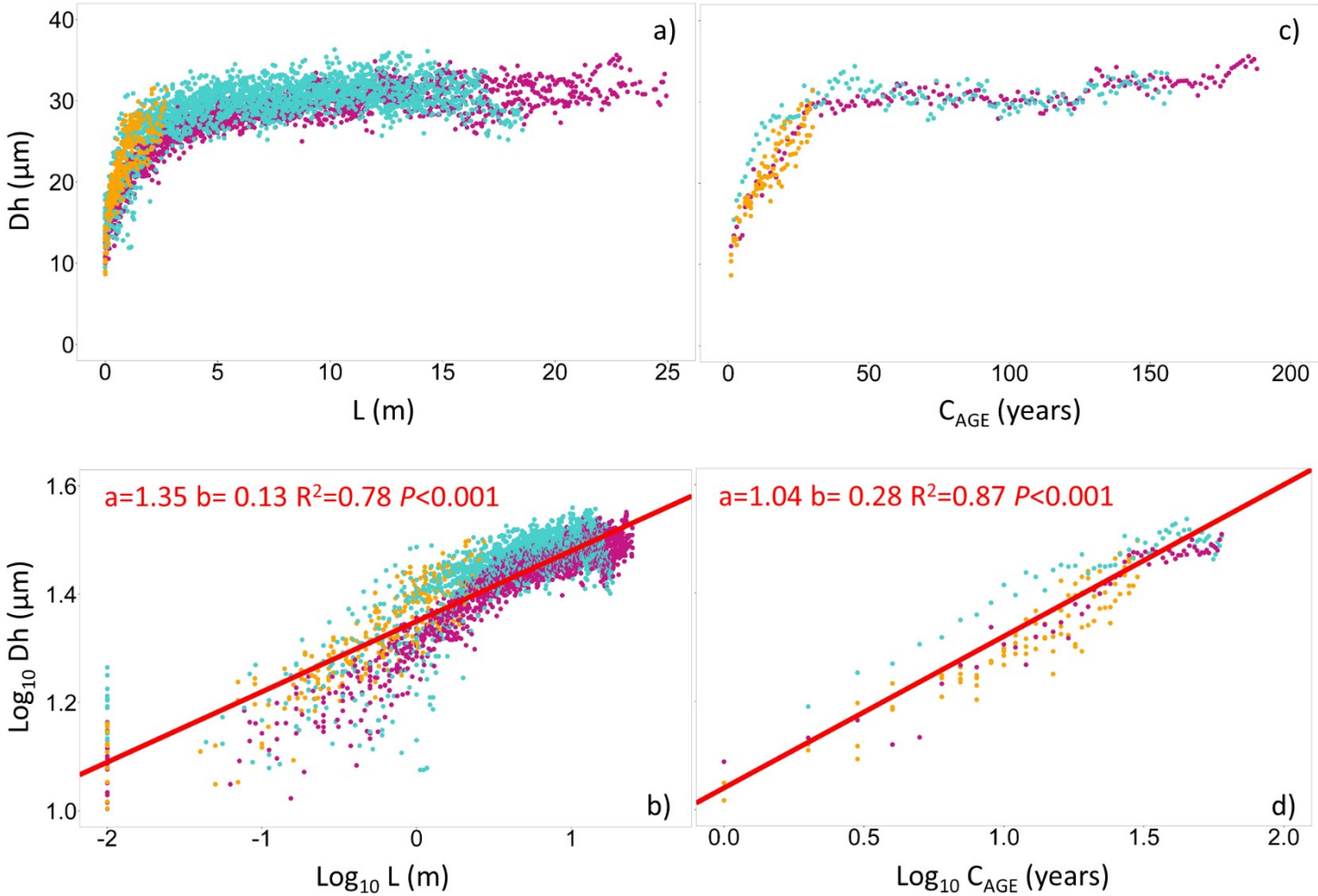

Figure 2:

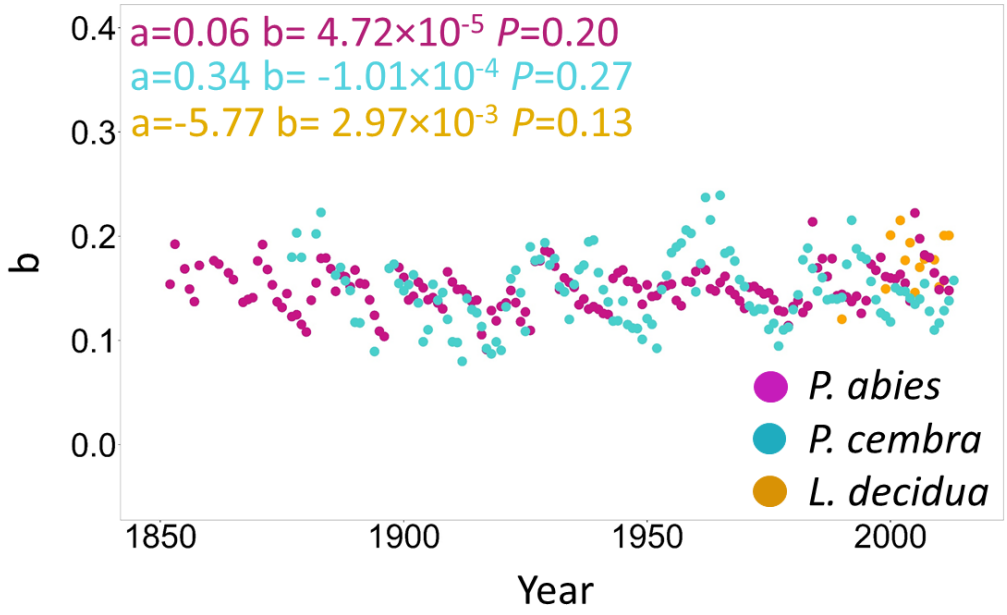
a=0.06 b= 4.72×10-5 P=0.20
a=0.34 b= -1.01×10-4 P=0.27
a=-5.77 b= 2.97×10-3 P=0.13
0.4
0.3
0.2
0.1
0.0
b
1850
1900
1950
2000
Year
P. abies
P. cembra
L. decidua

Figure 3:

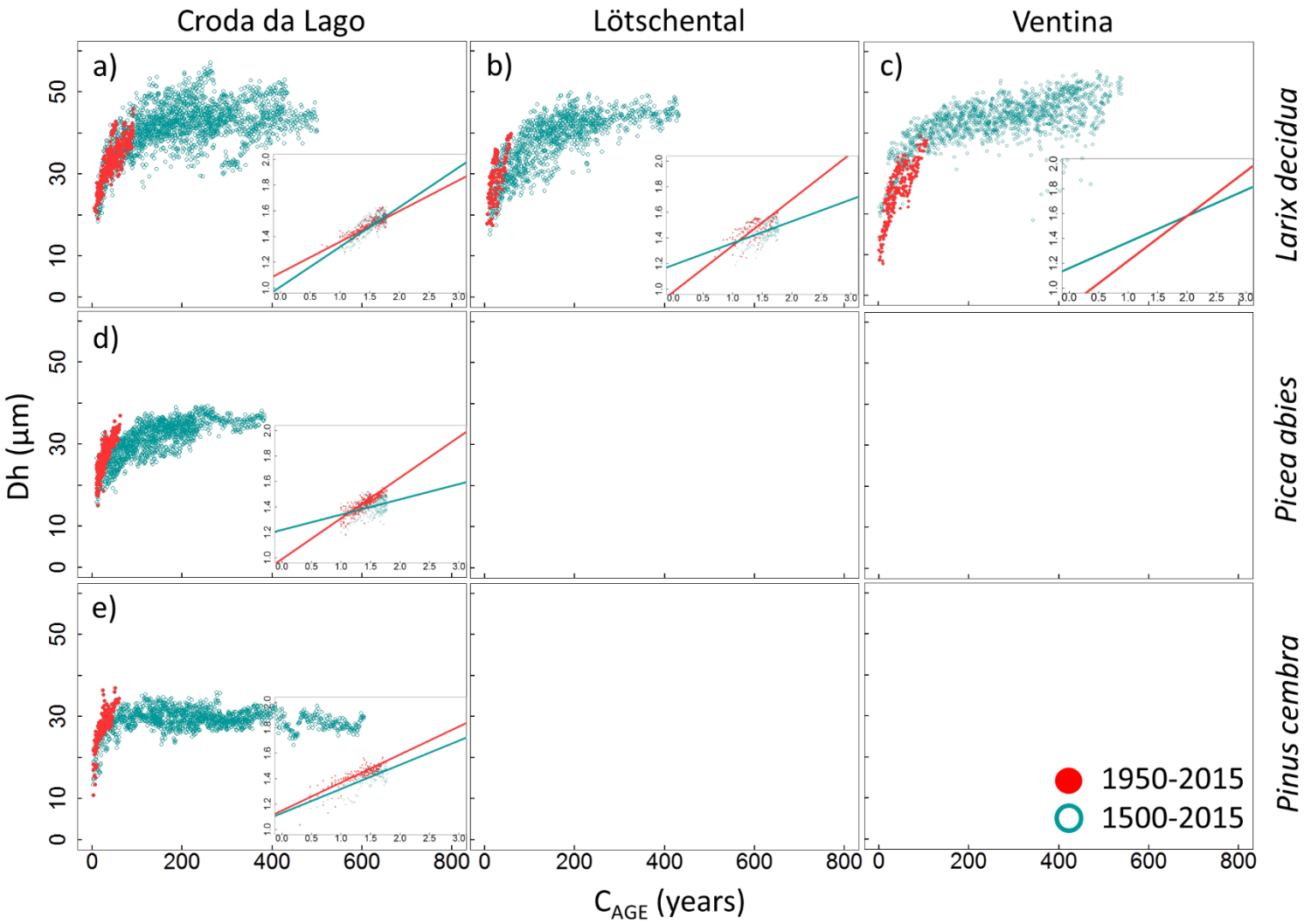
Croda da Lago
Lötschental
Ventina
a)
b)
c)
d)
e)
Dh (µm)
0
10
30
50
0
200
400
600
800
C_{AGE} (years)
1.0
1.2
1.4
1.6
1.8
2.0
0.0
0.5
1.0
1.5
2.0
2.5
3.0
Larix decidua
Picea abies
Pinus cembra
1950-2015
1500-2015

5.6 References

Aloni R. **2013**. *Cellular Aspects of Wood Formation* (J Fromm, Ed.). Berlin, Heidelberg: Springer Berlin Heidelberg.

Anfodillo T, Carraro V, Carrer M, Fior C, Rossi S. **2006**. Convergent tapering of xylem conduits in different woody species.

Anfodillo T, Petit G, Crivellaro A. **2013**. Axial conduit widening in woody species: a still neglected anatomical pattern. *IAWA Journal* **34**: 352–364.

von Arx G, Archer SR, Hughes MK. **2012**. Long-term functional plasticity in plant hydraulic architecture in response to supplemental moisture. *Annals of botany* **109**: 1091–100.

von Arx G, Carrer M. **2014**. ROXAS – A new tool to build centuries-long tracheid-lumen chronologies in conifers. *Dendrochronologia* **32**: 290–293.

von Arx G, Crivellaro A, Prendin AL, Čufar K, Carrer M. **2016**. Quantitative wood anatomy—practical guidelines. *Frontiers in Plant Science* **7**: 781.

von Arx G, Dietz H. **2005**. Automated image analysis of annual rings in the roots of perennial forbs. *International Journal of Plant Sciences* **166**: 723–732.

Barton K, Barton MK. **2015**. Package ' MuMIn '.

Bates D, Mächler M, Bolker B, Walker S. **2015**. Fitting Linear Mixed-Effects Models Using lme4. *Journal of Statistical Software* **67**: arXiv:1406.5823.

Becker P, Gribben RJ, Lim CM. **2000**. Tapered conduits can buffer hydraulic conductance from path-length effects. *Tree Physiology* **20**: 965–967.

Brodribb TJ, Feild TS. **2000**. Stem hydraulic supply is linked to leaf photosynthetic capacity: Evidence from New Caledonian and Tasmanian rainforests. *Plant, Cell and Environment* **23**: 1381–1388.

Buntgen et al. 2005. A 1052 year tree ring proxy for Alpine summer temperatures. Climate dynamics. *Climate Dynamics* **25(2-3)**: 141–153.

Cannone N, Sgorbati S, Guglielmin M. **2007**. Unexpected impacts of climate change on alpine vegetation. *Frontiers in Ecology and the Environment* **5**: 360–364.

Carrer M, von Arx G, Castagneri D, Petit G. **2015**. Distilling allometric and environmental information from time series of conduit size: the standardization issue and its relationship to tree hydraulic architecture. *Tree Physiology* **35**: 27–33.

Chave J, Coomes D, Jansen S, Lewis SL, Swenson NG, Zanne AE. **2009**. Towards a worldwide wood economics spectrum. *Ecology Letters* **12**: 351–366.

Danby RK, Hik DS. **2007**. Responses of white spruce (Picea glauca) to experimental warming at a subarctic alpine treeline. *Global Change Biology* **13**: 437–451.

Dawes MA, Hättenschwiler S, Bebi P, Hagedorn F, Handa IT, Körner C, Rixen C. **2010**. Species-specific tree growth responses to 9 years of CO2 enrichment at the alpine treeline. *Journal of Ecology*: no–no.

Dawes MA, Philipson CD, Fonti P, Bebi P, Hättenschwiler S, Hagedorn F, Rixen C. **2015**. Soil warming and CO 2 enrichment induce biomass shifts in alpine tree line vegetation. *Global Change Biology* **21**: 2005–2021.

Domec JC, Gartner BL. **2002**. Age- and position-related changes in hydraulic versus mechanical dysfunction of xylem: inferring the design criteria for Douglas-fir wood structure. *Tree physiology* **22**: 91–104.

Fonti P, Von Arx G, García-González I, Eilmann B, Sass-Klaassen U, Gärtner H, Eckstein D. **2010**. Studying global change through investigation of the plastic responses of xylem anatomy in tree rings. *New Phytologist* **185**: 42–53.

Franks, P. J., Brodribb TJ. **2005**. *Stomatal control and water transport in the xylem* (VT in Plants, Ed.).

Garbarino M, Lingua E, Nagel TA, Godone D, Motta R. **2010**. Patterns of larch establishment following deglaciation of Ventina glacier, central Italian Alps. *Forest Ecology and Management* **259**: 583–590.

Garbarino M, Lingua E, Subirà MM, Motta R. **2011**. The larch wood pasture: Structure and dynamics of a cultural landscape. *European Journal of Forest Research* **130**: 491–502.

Garbarino M, Lingua E, Weisberg PJ, Bottero A, Meloni F, Motta R. **2013**. Land-use history and topographic gradients as driving factors of subalpine Larix decidua forests. *Landscape Ecology* **28**: 805–817.

Garbarino M, Weisberg PJ, Motta R. **2009**. Interacting effects of physical environment and anthropogenic disturbances on the structure of European larch (Larix decidua Mill.) forests. *Forest Ecology and Management* **257**: 1794–1802.

Gartner & Schweingruber. **2013**. Microscopic preparation techniques for plant stem analysis. *Kessel* **95**: 132–150.

Gärtner H, Nievergelt D. **2010**. The core-microtome: A new tool for surface preparation on cores and time series analysis of varying cell parameters. *Dendrochronologia* **28**: 85–92.

Hacke UG, Spicer R, Schreiber SG, Plavcová L. **2016**. An ecophysiological and developmental perspective on variation in vessel diameter. *Plant, Cell & Environment*.

Harris I, Jones PD, Osborn TJ, Lister DH. **2014**. Updated high-resolution grids of monthly climatic observations - the CRU TS3.10 Dataset. *International Journal of Climatology* **34**: 623–642.

Harsch M a, Hulme PE, McGlone MS, Duncan RP. **2009**. Are treelines advancing? A global meta-analysis of treeline response to climate warming. *Ecology Letters* **12**: 1040–1049.

Hättenschwiler S, Handa IT, Egli L, Asshoff R, Ammann W, Körner C. **2002**. Atmospheric CO2 enrichment of alpine treeline conifers. *New Phytologist* **156**: 363–375.

Holmes RL. **1983**. Computer-assisted quality control in tree- ring dating and measurement. *Tree-ring Bulletin* **43**: 69–78.

Johnson DM, Büntgen U, Frank DC, Kausrud K, Haynes KJ, Liebhold AM, Esper J, Stenseth NC. **2010**. Climatic warming disrupts recurrent Alpine insect outbreaks. *Proceedings of the National Academy of Sciences of the United States of America* **107**: 20576–20581.

Koch GW, Sillett SC, Jennings GM, Davis SD. **2004**. The limits to tree height. *Nature* **428**: 851–854.

Kolb KJ, Sperry JS. **1999**. Transport constraints on water use by the Great Basin shrub, Artemisia tridentata. *Plant, Cell and Environment* **22**: 925–935.

Körner C. **1998**. A re-assessment of high elevation treeline positions and their explanation. *Oecologia* **115**: 445–459.

Körner C. **2003a**. *Alpine Plant Life* (U Seeliger and B Kjerfve, Eds.). Berlin, Heidelberg: Springer Berlin Heidelberg.

Körner C. **2003b**. Carbon limitation in trees. *Journal of Ecology* **91**: 4–17.

Körner C. **2012**. *Alpine Treelines*. Basel: Springer Basel.

Körner C, Paulsen J. **2004**. A world-wide study of high altitude treeline temperatures. *Journal of Biogeography* **31**: 713–732.

Leonardi S, Gentilesca T, Guerrieri R, Ripullone F, Magnani F, Mencuccini M, Noije T V., Borghetti M. **2012**. Assessing the effects of nitrogen deposition and climate on carbon isotope discrimination and intrinsic water use efficiency of angiosperm and conifer trees under rising CO2 conditions. *Global Change Biology* **18**: 2925–2944.

Li H, Hoch G, Körner C. **2002**. Source/sink removal affects mobile carbohydrates in Pinus cembra at the Swiss treeline. *Trees* **16**: 331–337.

Magnani F, Mencuccini M, Borghetti M, Berbigier P, Berninger F, Delzon S, Grelle A, Hari P, Jarvis PG, Kolari P, *et al.* 2007. The human footprint in the carbon cycle of temperate and boreal forests. *Nature* **447**: 849–851.

La Marche VC, Graybill DA, Fritts HC, Rose MR. **1984**. Increasing Atmospheric Carbon Dioxide: Tree Ring Evidence for Growth Enhancement in Natural Vegetation. *Science* **225**: 1019–1021.

Martin M, Gavazov K, Körner C, Hättenschwiler S, Rixen C. **2010**. Reduced early growing season freezing resistance in alpine treeline plants under elevated atmospheric CO 2. *Global Change Biology* **16**: 1057–1070.

Meinzer FC, Lachenbruch B, Dawson TE. **2011**. *Size- and Age-Related Changes in Tree Structure and Function* (FC Meinzer, B Lachenbruch, and TE Dawson, Eds.). Dordrecht: Springer Netherlands.

Mencuccini M, Hölttä T, Petit G, Magnani F. **2007**. Sanio's laws revisited. Size-dependent changes in the xylem architecture of trees. *Ecology Letters* **10**: 1084–1093.

Olson ME, Anfodillo T, Rosell JA, Petit G, Crivellaro A, Isnard S, León-Gómez C, Alvarado-Cárdenas LO, Castorena M. **2014**. Universal hydraulics of the flowering plants: vessel diameter scales with stem length across angiosperm lineages, habits and climates (B Enquist, Ed.). *Ecology Letters* **17**: 988–997.

Petit G, Anfodillo T, Carraro V, Grani F. **2011**. Hydraulic constraints limit height growth in trees at high altitude. *New Phytologist* **241-252**: 241–252.

Petit G, Anfodillo T, De Zan C. **2009**. Degree of tapering of xylem conduits in stems and roots of small Pinus cembra and Larix decidua trees. *Botany* **87**: 501–508.

Petit G, Pfautsch S, Anfodillo T, Adams MA. **2010**. The challenge of tree height in Eucalyptus regnans: when xylem tapering overcomes hydraulic resistance. *New Phytologist* **187**: 1146–1153.

Petit G, Savi T, Consolini M, Anfodillo T, Nardini A. **2016**. Interplay of growth rate and xylem plasticity for optimal coordination of carbon and hydraulic economies in *Fraxinus ornus* trees. *Tree Physiology*: 1–10.

R Development Core Team. **2014**. R: A language and environment for statistical computing. **5**.

Riondato R. **2009**. ' Xilogenesi ed accrescimento longitudinale al limite superiore del bosco : determinanti ambientali e fisiologici '.

Rossi S, Anfodillo T, Deslauriers A. **2006a**. Assessment of Cambial Activity and Xylogenesis by Microsampling Tree Species: An Example at the Alpine Timberline. *IAWA Journal* **27**: 383–394.

Rossi S, Deslauriers A, Anfodillo T, Carraro V. **2006b**. Evidence of threshold temperatures for xylogenesis in conifers at high altitudes. *Oecologia* **152**: 1–12.

Sala A, Woodruff DR, Meinzer FC. **2012**. Carbon dynamics in trees: feast or famine? *Tree physiology* **32**: 764–75.

Schlesinger WH. **2009**. On the fate of anthropogenic nitrogen. *Proceedings of the National Academy of Sciences* **106**: 203–208.

Schmidt S, Weber B, Winiger M. **2009**. Analyses of seasonal snow disappearance in an alpine valley from micro- to meso-scale (Loetschental, Switzerland). *Hydrological Processes* **23**: 1041–1051.

Schweingruber FH. **1996**. *Tree rings and environment: dendroecology* (PHA Bern, Ed.).

Smith WK, Germino MJ, Johnson DM, Reinhardt K. **2009**. The Altitude of Alpine Treeline: A Bellwether of Climate Change Effects. *The Botanical Review* **75**: 163–190.

Sperry JS. **2003**. Evolution of Water Transport and Xylem Structure. *International Journal of Plant Sciences* **164**: S115–S127.

Sperry JS. **2010**. *Fundamentals of tree-ring research* (U of A Press, Ed.).

Streit K, Siegwolf RTW, Hagedorn F, Schaub M, Buchmann N. **2014**. Lack of photosynthetic or stomatal regulation after 9 years of elevated [CO2] and 4 years of soil warming in two conifer species at the alpine treeline. *Plant, cell & environment* **37**: 315–26.

Tyree M, Ewers F. **1991**. The hydraulic architecture of trees and other woody plants. *New Phytologist* **119**: 345–360.

Tyree MT, Sperry JS. **1989**. Vulnerability of xylem to cavitation and embolism. *Annual Review of Plant Physiology and Plant Molecular Biology* **40**: 19–36.

Urbinati C, Carrer M, Sudiro S. **1997**. Dendroclimatic response variability of Pinus cembra L. in upper timberline forests of Italian Eastern Alps. *Dendrochronologia* **15**: 101–117.

Weitz JS, Ogle K, Horn HS. **2006**. Ontogenetically stable hydraulic design in woody plants. *Functional Ecology* **20**: 191–199.

West GB, Brown JH, Enquist BJ. **1999**. A general model for the structure and allometry of plant vascular systems. *Nature* **400**: 664–667.

Yang S, Tyree MT. **1993**. Hydraulic resistance in Acer saccharum shoots and its influence on leaf water potential and transpiration. *Tree physiology* **12**: 231–42.

Zar J. **1999**. Biostatistical analysis, New Jersey. *USA: Prentice Hall*: 4159–4165.

Zimmermann MH. **1983**. Xylem structure and the ascent of sap. *Springer Verlag*.

6. Xylem anatomical adjustments maintain hydraulic efficiency but cause reduced safety in tall Norway spruce trees

A.L. Prendin[1*], S. Mayr[2], B. Beikircher[2], G. Petit[1]

[1] Dept. Territorio e Sistemi Agro-Forestali, Università degli Studi di Padova, Legnaro (PD), Italy

[2] Institut für Botanik, Universität Innsbruck, Innsbruck, Austria

*** Corresponding author**

Keywords: hydraulic conductivity, hydraulic diameter, number of cell, *P50,* safety-efficiency trade off, tracheid lumen size, vulnerability curves

6.1 Abstract

In trees, water transport from roots to leaves can be limited by size related safety and efficiency constraints due to the combined negative effects of tree height i) on leaf and xylem water potential due to gravity, and ii) on the total xylem resistance due to increased frictional forces. However, how these conflicting requirements of hydraulic safety and efficiency are managed in taller trees is still unknown.

We assessed the vulnerability curves (VCs) and performed detailed xylem cell anatomical quantification of the leader shoots of *Picea abies* trees of different height (from 2 to 37 m) from two different sites. We found significant trends of hydraulic and anatomical traits with tree height. The xylem water potential triggering 50% of loss of conductivity ranged from -5.86 MPa in small to -3.40 MPa in tall trees (P=0.007), the hydraulic conductivity from $3.34 \cdot 10^{-13}$ to $9.10 \cdot 10^{-12}$ ($(kg \cdot m \cdot MPa^{-1} \cdot s^{-1})10^{-15}/m$) ($P$<0.001), the hydraulic diameter from 10.92 to 14.88 µm (P=0.007) and the total number of xylem conduits from $7.65 \cdot 10^{3}$ to $1.02 \cdot 10^{5}$ (P=0.005). We found a strong trade off between efficiency vs. safety, with conduit number being the best anatomical predictor of *the* 50% of loss of conductivity (R^2=0.63, P<0.001).

In conclusion, taller trees are then more vulnerable to drought induced cavitation, and thus are more exposed to the risk of hydraulic failure under extreme drought events, which are predicted to more frequently occur with climate change.

6.2 Introduction

One of the major current challenges in plant sciences is to gain a better understanding tree species acclimation to current and forecasted climate changes (Sala, Piper & Hoch 2010). In recent years, widespread natural tree mortality followed extreme episodes of drought (Allen *et al.* 2010). Moreover, it has been observed that these events more strongly attempt to the survival of big sized trees, often leading to more or less pronounced top dieback or even complete plant death (Nepstad *et al.* 2007; McDowell *et al.* 2008; Lewis *et al.* 2011; Rowland *et al.* 2015). While several studies already shed light on the biophysical limitations imposed by tree height on the plant physiology and growth, yet a comprehensive understanding of the actual chain of physiologic events leading to tree top dieback or even death of big trees after drought events still requires some solid bricks of knowledge (Hartmann *et al.* 2015).

Trees are long-living organisms that continuously increase in size during ontogeny, with some tree species growing up to more than 100 m in height (Koch *et al.* 2004). Increased size *per se* ultimately reduces vigor in big trees (Mencuccini *et al.* 2005; Martínez-Vilalta, Vanderklein & Mencuccini 2007) because it triggers a number of constraints to physiological processes. On one hand, the whole carbon balance is affected by the increased maintenance cost of having a larger body biomass (Meinzer, Lachenbruch & Dawson 2011). On the other, the increased stature imposes stronger limitations to water flow (Ryan & Yoder 1997). The gravitational pressure gradient of 0.01 $MPa \cdot m^{-1}$ determines higher xylem tensions with increasing tree height. in addition, the water flow through xylem conduits over a longer roots-to-leaves path is negatively affected by the increased frictional forces imposed by the cell wall surfaces, in agreement with Hagen-Poiseuille law predicting the hydraulic resistance of a capillary tube to be linearly proportional to its length and inversely proportional to the fourth power of its diameter (Tyree & Ewers 1991). In the xylem, if conduit number did not change axially (Shinozaki *et al.* 1964), the total hydraulic resistance of a xylem pipe from roots to leaves would increase with tree height unless the diameter of chained conduits varies axially (Petit & Anfodillo 2009). Indeed, empirical studies demonstrated that the xylem architecture of vascular plants shares a common design (known as widening), according to which the conduit diameter increases from the apex downwards along the stem axis following a power-like trajectory (Anfodillo, Petit & Crivellaro 2013; Olson *et al.* 2014) that is

maintained throughout ontogeny (Prendin et al. 2017). In such a way, the negative effect of path length gets substantially buffered by conduit widening, and the total hydraulic resistance becomes nearly independent of tree height (Mäkelä & Valentine 2006; Petit & Anfodillo 2009; Petit *et al.* 2010). It follows that resistances increase towards the terminal twigs (Yang & Tyree 1993; Petit, Anfodillo & Mencuccini 2008), where the xylem tension is highest because of gravity and accumulated flow resistances. This results in conflicts between xylem efficiency and safety (Hacke & Sperry 2001) and has important consequences for the whole tree hydraulics and physiology.

In addition, it is also linked to the carbon balance as, the carbon costs of building up a renewed xylem architecture in tall trees must account for the higher osmotic potential required for cell expansion under the effect of gravity (Woodruff *et al.* 2007), and for the higher biomass required to extend conduits over a longer path length.

According to a recent report, under limited soil water resources *Fraxinus ornus* trees reduce the carbon investment into xylem by decreasing the number of vessels and slightly increasing their size in order not to compromize much the total conductance (Petit *et al.* 2016). Under this perspective, it can be hypothesized that the optimal coordination between carbon balance and xylem hydraulics can be conditioned by the effect of tree height on xylem safety and efficiency. How carbon allocation into new xylem biomass can resolve these conflicts bewteen hydraulic safety and efficiency? Is there any modification to xylem anatomy that play a key role in this respect? In partucular, we hypotized that xylem adjustments are developed to maintain the efficiency of water transport, and thus allowing the vital processes of leaf transpiration and photosynthesis also in taller trees, but at the cost of increasing their vulnerability to drought induced cavitation.

In this study we present a comparative analysis of the xylem anatomical adjustments of the leader shoots of *Picea abies* trees differing in tree height in relation to their vulnerability to drought induced xylem cavitation, and discussed the results in the context of sensitivity of big sized trees to the predicted climate change scenarios.

6.3 Material and methods

6.3.1 Study site and selected trees

We selected two study sites in the Dolomites, Eastern Italian Alps at approximately 1650 m a.s.l.. At Cinque Torri (Cortina d'Ampezzo, BL: 46°27'N, 12° 08' E) the forest is characterized by a mixed and open clumps of *Larix decidua* Miller and *Picea abies* Karst. trees, on a south-facing and shallow calcareous soil. At Pian de Sire (Lorenzago di Cadore, BL: 46° 50' N, 12°59' E) the forest is a dense monospecific Norway spruce stand on a south-east facing and deep calcareous soil. The climate in both areas is the typical of the South-Eastern Alpine region. According to the nearest meteorological station of Cortina d'Ampezzo, mean annual temperature is 6.3°C and total annual precipitations around 1200 mm, mostly occurring during summer and early autumn.

At the end of September 2014, we collected the apical shoots (40 cm) of 36 *P. abies* individuals of different height (from 2 to 37 m) and measured the height (H) and the diameter at the breast height (DBH) (Fig. 1).Immediately after felling, apical shoots were cut under water, wrapped with a moist tissue and stored in a plastic bag in a cold box. Shoots were then transported to the laboratory and frozen.

For each apical shoot, we used a segment of 10 cm starting from the apex for the anatomical analyses, and the consecutive segment between 10 and of 40 cm for hydraulic measurements.

6.3.2 Vulnerability curves

Frozen samples were left overnight in a cooling room at 4 °C to slowly melt xylem water. Samples were then immersed in cold water and cut for 1 cm at both ends. Stem twigs were fixed in a custom-built rotor designed by JS Sperry for a Sorvall RC-5 centrifuge (Thermo Fisher Scientific, Waltham, MA, USA; see Li et al., 2008, for details) and the method described in (Beikircher *et al.* 2010) was followed.

Vulnerability curves (VCs) were elaborated using the Cavitron technique (Cochard 2002; Jacobsen & Pratt 2012; Cochard *et al.* 2013) with a 28cm rotor. VCs were assessed after repeated measurements of the sample's hydraulic conductance (K) while exposed in their middle part to progressively more negative pressures produced by accelerated centrifugation.

The percentage loss of conductance (*PLC*) was calculated from the ratio of the actual (*K*) to the maximum conductance of the stem (K_{MAX})(Cochard 2002):

$$PLC = 100 * (1 - \frac{K}{(K\max)}) \quad \text{eq. 1}$$

6.3.3 Anatomical analysis

We carried out the anatomical analyses of the base of the 10-cm-long apical segments by following standard protocols (von Arx *et al.* 2016). Cross sections of the whole segment base were cut at 10-12 µm with a rotary microtome (RM2245, Leica, Heidelberg, Germany). Sections were stained with safranin and Astrablue (1% and 0.5% in distilled water, respectively), permanently fixed with Eukitt (BiOptica, Milan), and then photographed using a digital automated microscope (D-sight, Menarini Diagnostic, Italy). Images were analyzed using ROXAS v 3.0.31 (von Arx & Dietz 2005; von Arx & Carrer 2014) for the measurement of xylem anatomical features. We focused our analyses on the total xylem area (*XA*), the number of tracheids (*Cn*) and their hydraulically weighted conduit diameter (*Dh*), assessed as (Kolb & Sperry 1999):

$$Dh = \frac{\sum d_n 5}{\sum d_n 4} \quad \text{eq. 2}$$

where d_n is the diameter of the *n*-conduit.

We calculated the theoretical hydraulic conductivity (Kh_{theor}) for the entire xylem area according to the Hagen-Poiseuille law (Tyree & Zimmermann 2002), and the index of bending resistance of earlywood tracheids (identified based on Mork's index) (Denne 1988) against implosion (BI_{EW}), as (Hacke et. al 2001):

$$BI_{EW} = \left(\frac{DCWT}{d_n}\right)^2 \quad \text{eq.3}$$

where D*CWT* is the double-cell wall thickness and d_n is the lumen diameter of the *n*-conduit measured perpendicularly to the double-cell wall.

In total, we analyzed a total of more than 1.5 millions of tracheids.

6.3.4 Statistical analysis

Vulnerability curves (VCs) were obtained by plotting the data of percent loss of hydraulic conductivity (*PLC*) against the applied negative xylem water potential (Ψ) and by using a sigmoidal fitting function (Pammenter & Van der Willigen 1998). Curves were fitted for each sample and Ψ corresponding to *PLC*=12 (*P12*), *PLC*=50 (*P50*) and *PLC*=88% (*P88*) extracted, accordingly to Domec & Gartner (2001) definition.

Additionally, mean curves were fitted for the five tallest and five smallest *P. abies* of each side and the mean *P12*, *P50* and *P88* calculated.

The relationships between tree height, P50 and several anatomical traits were assessed on $\log_{10}$-transformed data to comply with assumptions of normality and homoscedasticity (Zar 1999), and fitted with a linear regression model where the site was included as random factor. All the analysis were performed with R (v 3.1.1;R Development Core Team 2014).

6.4 Results

6.4.1 Vulnerability to xylem embolism

The vulnerability curves of leader shoots slightly differed, depending on the height of trees (Fig. 2). *P50* (i.e., the xylem water potential (Ψ) at which *PLC*=50 %) slightly but significantly increased (i.e., became less negative) with increasing tree height (approximately 0.07 MPa/m: Fig. 3a), ranging from a minimum of -5.86 MPa (H=1m) to a maximum of -3.40 MPa (H=36m). Significant differences were not found between sites (Tab. S1, supplementary material).

6.4.2 Xylem anatomy

The anatomical analyses revealed a rather narrow range of conduit size variation between samples. The mean hydraulic diameter (*Dh*) of the leader shoot (at 10 cm from the stem apex) varied between 10.92 and 14.88 µm. Overall, we found that both *Dh* and the conduit number (*Cn*) significantly increased with tree height, approximately 0.11 µm/m and 2610 cells/m (Fig. 4).

The theoretical hydraulic conductivity (Kh_{theor}) well correlated to the hydraulic conductivity at full saturation (K_{MAX}) measured with the cavitron (Fig. S1), and significantly increased (approximately $1.36 \cdot 10^{-13}$ (kg·m·MPa^{-1}·s^{-1})10^{-15}/m) with tree height (Fig. 3b).We found no significant relationships between the bending index of earlywood tracheids (BI_{EW}) and tree height (H), between BI_{EW} and *P50* (Fig. S2) and between the ratio of conduit number and xylem area (*Cn/XA) and* tree height (H) (Fig. S3).

6.4.3 Trade-off of safety vs. efficiency

We investigated the tradeoff between hydraulic safety and efficiency by analyzing the theoretical hydraulic conductivity (Kh_{theor}) and its two related anatomical traits, i.e. tracheid hydraulic diameter (*Dh*) and number (*Cn*) against *P50* (Fig. 5). Kh_{theor} significantly increased with *P50* (P<0.001). Of the two traits correlated with Kh_{theor}, *Dh* was not significantly correlated with *P50* (P=0.32), whereas 63% of the total variance of *P50* could be explained by the variation in conduit number (P<0.001).

6.5 Discussion

Our hydraulic and anatomical analyses of the leader shoots of Norway spruce trees revealed a progressive modulation of conflicting requirements of hydraulic safety vs. efficiency with increasing individual height. The obtained results supported the hypothesis that taller trees prioritize the xylem efficiency (Fig. 3b) at the cost of being more vulnerable to drought induced cavitation (Fig. 3a).

The problem of maintaining an efficient physiological performance under the constraining effects of the increased tree height had already been addressed by other plant ecologists. Size imposes strong biophysical constraints to leaf gas exchanges (Mencuccini *et al.* 2005). Leaf osmoregulation was reported to increase with tree height accordingly to the gravitational pressure drop of 0.01 MPa·m^{-1} (Koch *et al.* 2004; Burgess & Dawson 2007). Nevertheless, this strategy seemed not sufficient for maintaining homeostasis of leaf gas exchanges, as carbon assimilation was contextually reported to decrease with tree height, because of the supposedly stronger effect of the increasing path length resistance (Koch *et al.* 2004). According to the analyses of Domec *et al.* (2008), the requirements for taller trees of having higher xylem safety to resist their operational

lower xylem water potentials would determine substantial modifications in pit anatomy with the side effect of strongly reducing the total xylem conductance, and ultimately set the limit to tree height. Even though in our study we did not measure the world's tallest trees as in Koch et al. (2004) and Domec et al. (2008), we could demonstrate height related changes in vulnerability to cavitation (Cochard, Cruiziat & Tyree 1992; Meinzer *et al.* 2009) and in anatomical characteristics of leader shoots by a comparison of trees between 2 and 37 m. In contrast to previous reports (Domec *et al.* 2008), we found a rather different indication on the strategical prioritization between the conflicting requirements of safety vs. efficiency occurring during the ontogenetic development of a tree. In fact, safety against drought induced cavitation was significantly lower in our tallest trees, with *P50* varying more than 1 MPa across our size range from 2 to 37 m of height (Fig. 2). In agreement with Rosner (2013), small trees having shallow root system and less access to soil moisture, need to produce safer xylem. In parallel, xylem anatomical features, such as conduit size and number increased (Fig. 4), strongly suggesting that taller trees invested more to ensure sufficient xylem conductance, even if at cost of reduced hydraulic safety. Beside the slight increase in conduit lumen area, the anatomical adjustment that much affected both efficiency and safety was the increase in tracheid number (Fig. 5c). In terms of carbon costs, it is more expensive to increase the conductance by an increase in conduit number than by an increase in lumen area. So why not increasing conduit size rather than their number? Even though *Dh* significantly increased with height, the absolute variation is rather small. A likely explanation is that cell size can be strongly constrained by safety requirements under the high xylem tension close to the apex (Hacke & Sperry 2001) and because cell wall distension is more difficult (Woodruff et al. 2007). In conifers, vulnerability to cavitation is known to be related to the torus overlap in the pit chamber (Delzon et al. 2010), and a higher number of conduits corresponds to a higher number of pits and a thus a higher probability of occurrence of leaky pits (Christman, Sperry & Adler 2009). The increased conduit number, as expected, caused an increase in *P50* and thus in hydraulic vulnerability (Fig. 5).

Since leaf and xylem water potential become more negative with increasing tree height (Koch *et al.* 2004; Burgess & Dawson 2007), our results would suggest that taller trees operate at a reduced margin of hydraulic safety (Fig. 6), defined as the water potential interval separating the stomatal closure, occurring approximately at seasonal minimum

leaf water potential (Ψ_{MIN}), from embolism formation (by convention *P50,* or more realistically *P12* in conifers) (hydraulic safety margin: $HSM=\Psi_{MIN}-P50$) (Choat *et al.* 2012). According to our empirical evidence that taller trees are not only more vulnerable to drought induced cavitation, but also likely operate with a reduced margin of hydraulic safety, we provided a mechanistic explanation of why taller trees are more exposed to the negative consequences of drought events, such as top dieback or even complete death (Nepstad *et al.* 2007; McDowell *et al.* 2008; Lewis *et al.* 2011; Hentschel *et al.* 2014; Rowland *et al.* 2015; Rosner *et al.* 2016).

Viewed in the context of climate change, the predicted increase in extreme drought events (IPCC 2014) will likely expose big sized trees to higher risks of survival.

Acknowledgements

We thank Birgit Dämon, Universitt Innsbruck, Institut für Botanik, for valuable assistance during vulnerability measurements and Georg Von Arx, Swiss Federal Institute for Forest, Snow and Landscape Research WSL, Birmensdorf, Switzerland, for the support with ROXAS. Parts of the study were supported by a Sparkling Science Project funded by the Federal Ministry of Science, Research and Economy (Bundesministerium für Wissenschaft, Forschung und Wirtschaft) Austria.

Figure captions

Figure 1: Variation of diameter at the breast height (DBH) and height (H) ofthe sampled *Picea abies* trees from both Cinque Torri (open circles) and Pian de Sire (filled circles). Point size refers to the estimated elongation rate (ΔH, in cm·year^{-1}) estimated according to the number of rings (*Cn*) at the base of the apical segment of 10 cm.

Figure 2: Mean vulnerability curves (percent loss of conductivity (PLC) vs. xylem water potential (Ψ)) of the leader shoots of the 5 smaller (open red dots) and 5 taller (filled blue dots) *Picea abies* trees from both Cinque Torri (a) and Pian de Sire (b). Fitting curves were estimated according to a logistic function (Pammenter and Vander Willingen, 1998), where 50% of loss of conductivity (*P50*) is indicated by thick solid vertical lines (solid for tall and dashed for small trees), 12 (*P12*) and 88 percent of conductivity loss (*P88*) are represented thin solid lines (solid for tall and dashed for small trees).

Figure 3: Relationships of (a) *P50* and (b) hydraulic conductivity of the entire xylem area (Kh_{theor}) with tree height (*H*). Data are $\log_{10}$-transformed. Filled and open circles represent Pian de Sire and Cinque Torri data, respectively. Solid lines represent the fitted linear regressions for Pian de Sire and Cinque Torri together.

Figure 4: Relationships of (a) mean hydraulic diameter (*Dh*) and (b) conduit number (*Cn*), both relative to the entire xylem surface, with tree height (*H*). Data are $\log_{10}$ transformed. Filled and open circles represent Pian de Sire and Cinque Torri data, respectively. Solid lines represent the fitted linear regression for Pian de Sire and Cinque Torri together.

Figure 5: Trade-off of hydraulic efficiency vs. safety. Relationships of (a) hydraulic conductivity (Kh_{theor}) and (b) mean hydraulic diameter (*Dh*), and (c) conduit number (*Cn*) with *P50*. Filled and open circles represent Pian de Sire and Cinque Torri data, respectively. Solid lines represent the significant linear regression for Pian de Sire and Cinque Torri together.

Figure 6: Schematic representation of the estimated percent loss of conductivity (*PLC*) (blue) and idealized stomatal conductance (g_S) (red) vs. xylem water potential (Ψ) of tall (solid line) and small trees (dashed line). Horizontal solid line represents the hydraulic safety margin ($HSM=\Psi_{MIN}-P50$) of tall (solid line) and small trees (dashed line). Vertical lines represent *P50* values and Ψ_{MIN}, assumed equal to the point of stomatal closure, fixed at g_S=12 %.

Figures

Figure 1:

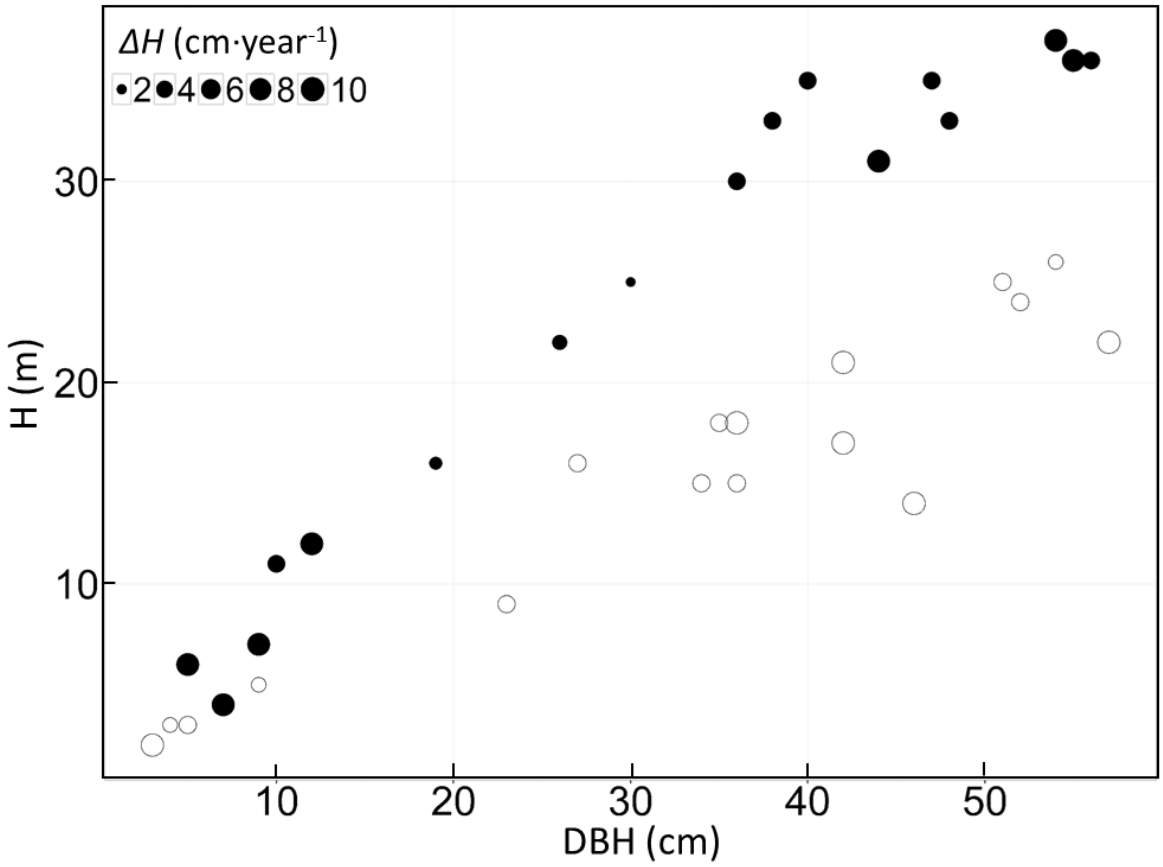

Figure 2:

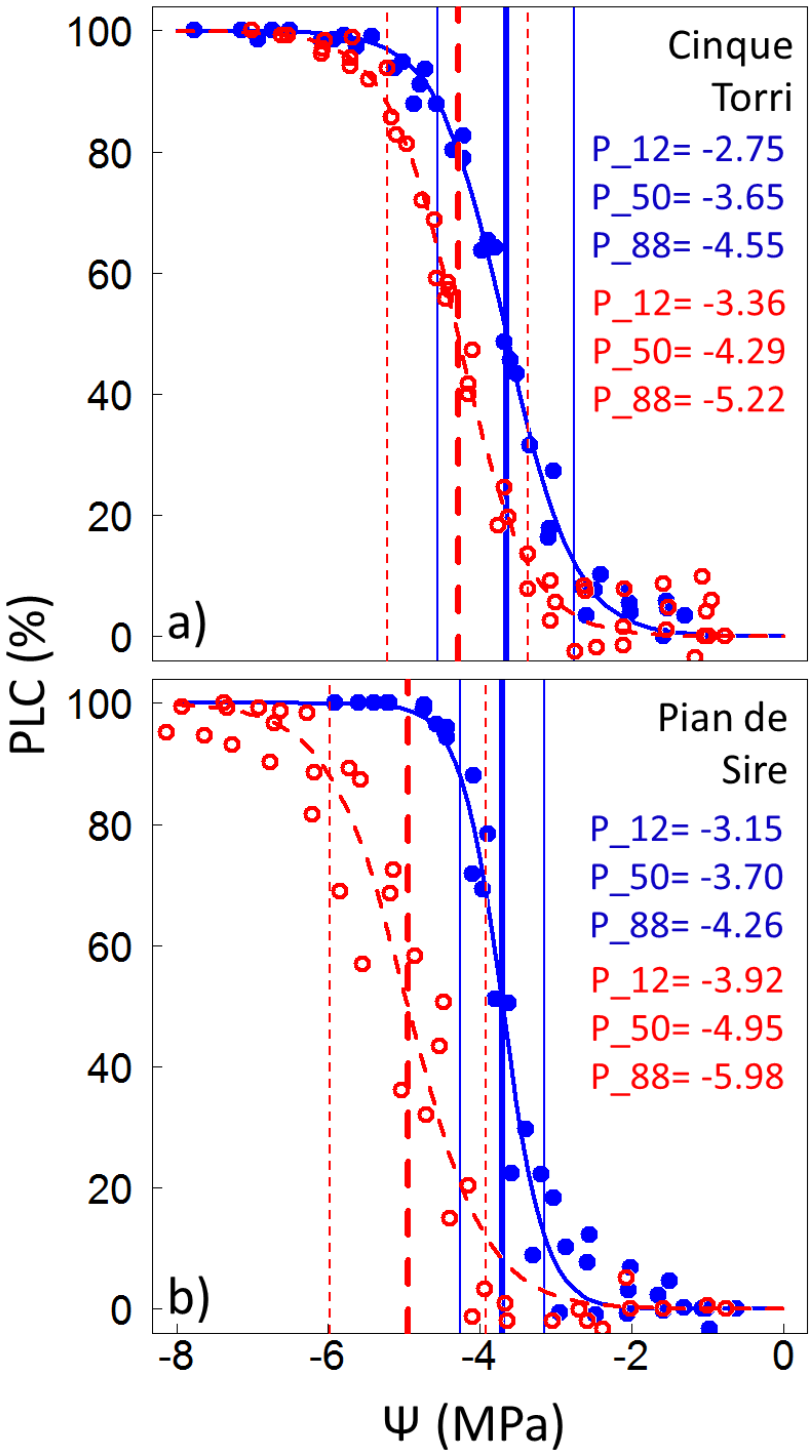
Cinque Torri
P_12= -2.75
P_50= -3.65
P_88= -4.55
P_12= -3.36
P_50= -4.29
P_88= -5.22
a)
Pian de Sire
P_12= -3.15
P_50= -3.70
P_88= -4.26
P_12= -3.92
P_50= -4.95
P_88= -5.98
b)
PLC (%)
Ψ (MPa)
100
80
60
40
20
0
-8
-6
-4
-2
0

Figure 3:

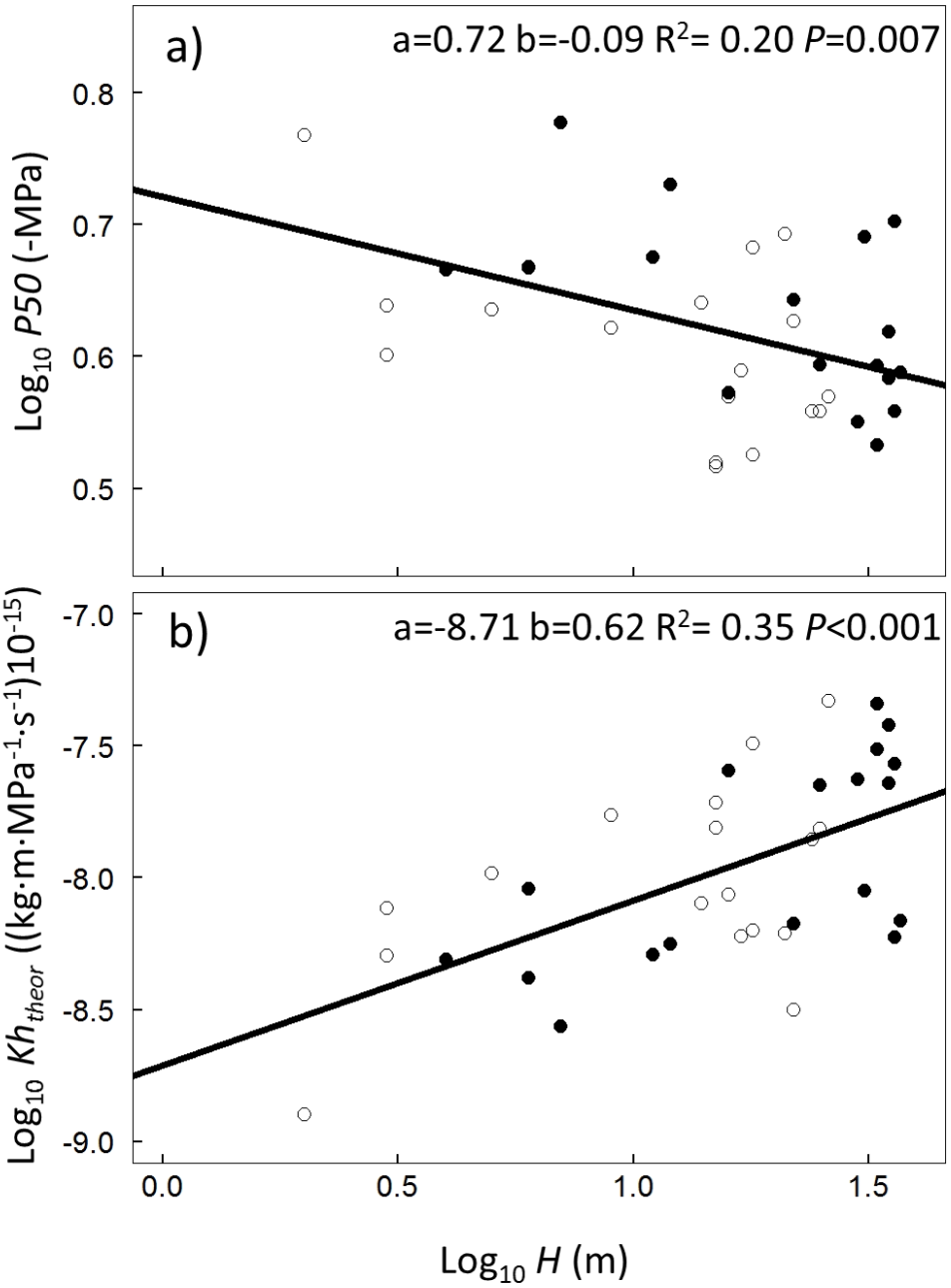
a)
a=0.72 b=-0.09 R²= 0.20 P=0.007
Log10 P50 (-MPa)
0.8
0.7
0.6
0.5
b)
a=-8.71 b=0.62 R²= 0.35 P<0.001
Log10 Kh_theor ((kg·m·MPa-1·s-1)10-15)
-7.0
-7.5
-8.0
-8.5
-9.0
0.0
0.5
1.0
1.5
Log10 H (m)

Figure 4:

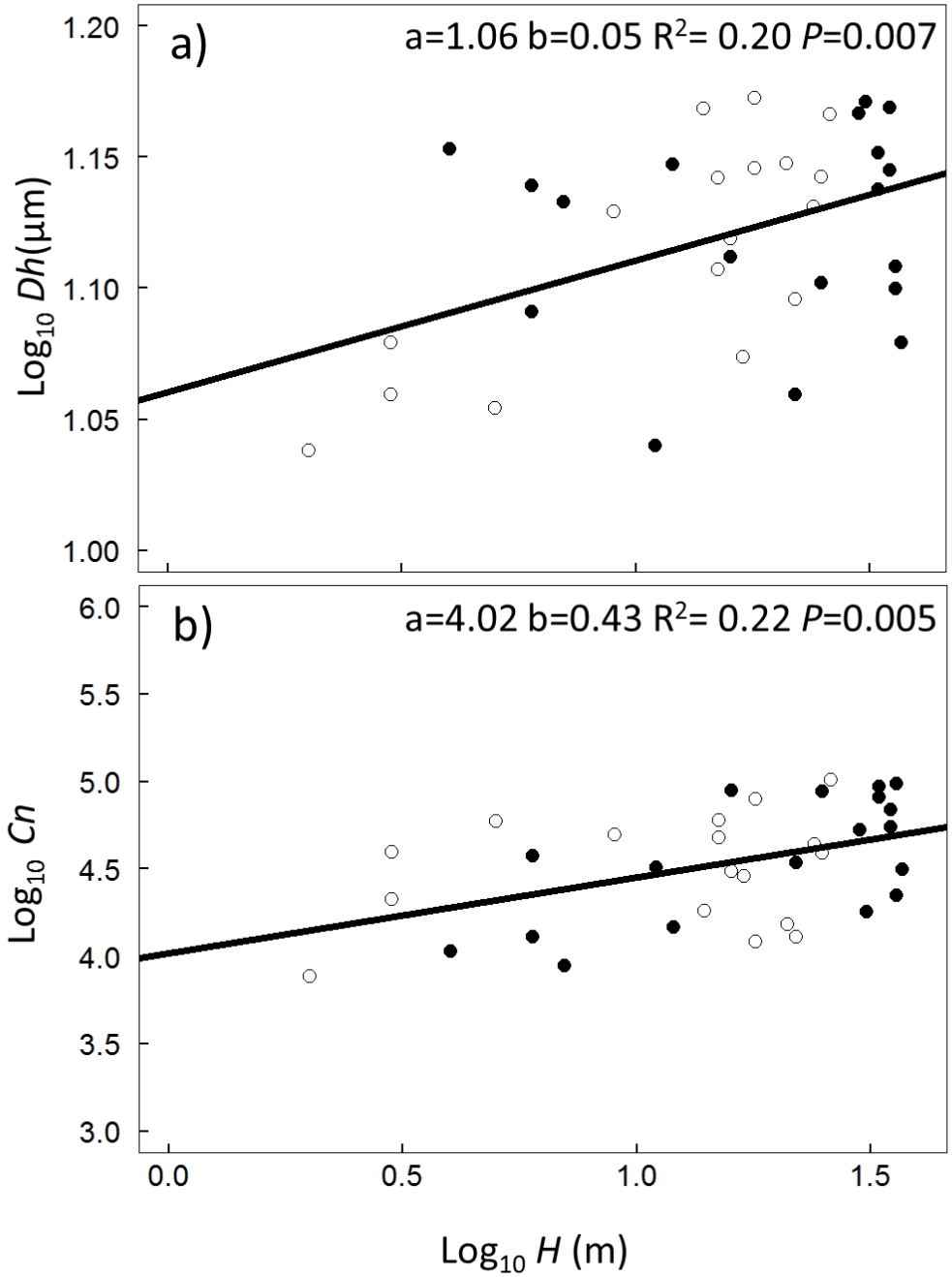
a)
a=1.06 b=0.05 R²= 0.20 P=0.007
Log10 Dh(µm)
1.20
1.15
1.10
1.05
1.00
b)
a=4.02 b=0.43 R²= 0.22 P=0.005
Log10 Cn
6.0
5.5
5.0
4.5
4.0
3.5
3.0
0.0
0.5
1.0
1.5
Log10 H (m)

Figure 5:

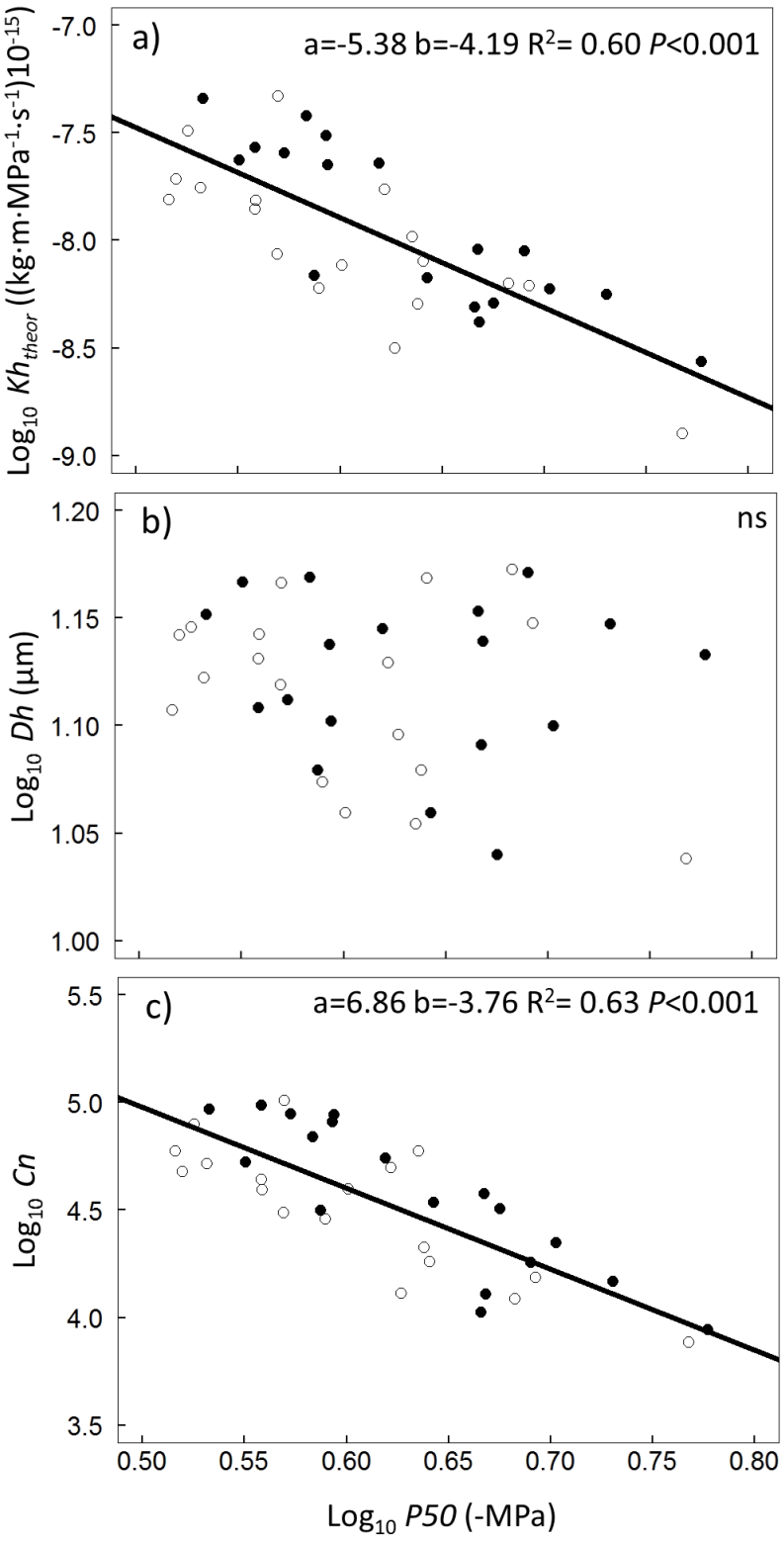
a)
a=-5.38 b=-4.19 R²= 0.60 P<0.001
Log10 Kh_theor ((kg·m·MPa-1.s-1)10-15)
-7.0
-7.5
-8.0
-8.5
-9.0
b)
ns
Log10 Dh (µm)
1.20
1.15
1.10
1.05
1.00
c)
a=6.86 b=-3.76 R²= 0.63 P<0.001
Log10 Cn
5.5
5.0
4.5
4.0
3.5
0.50
0.55
0.60
0.65
0.70
0.75
0.80
Log10 P50 (-MPa)

Figure 6:

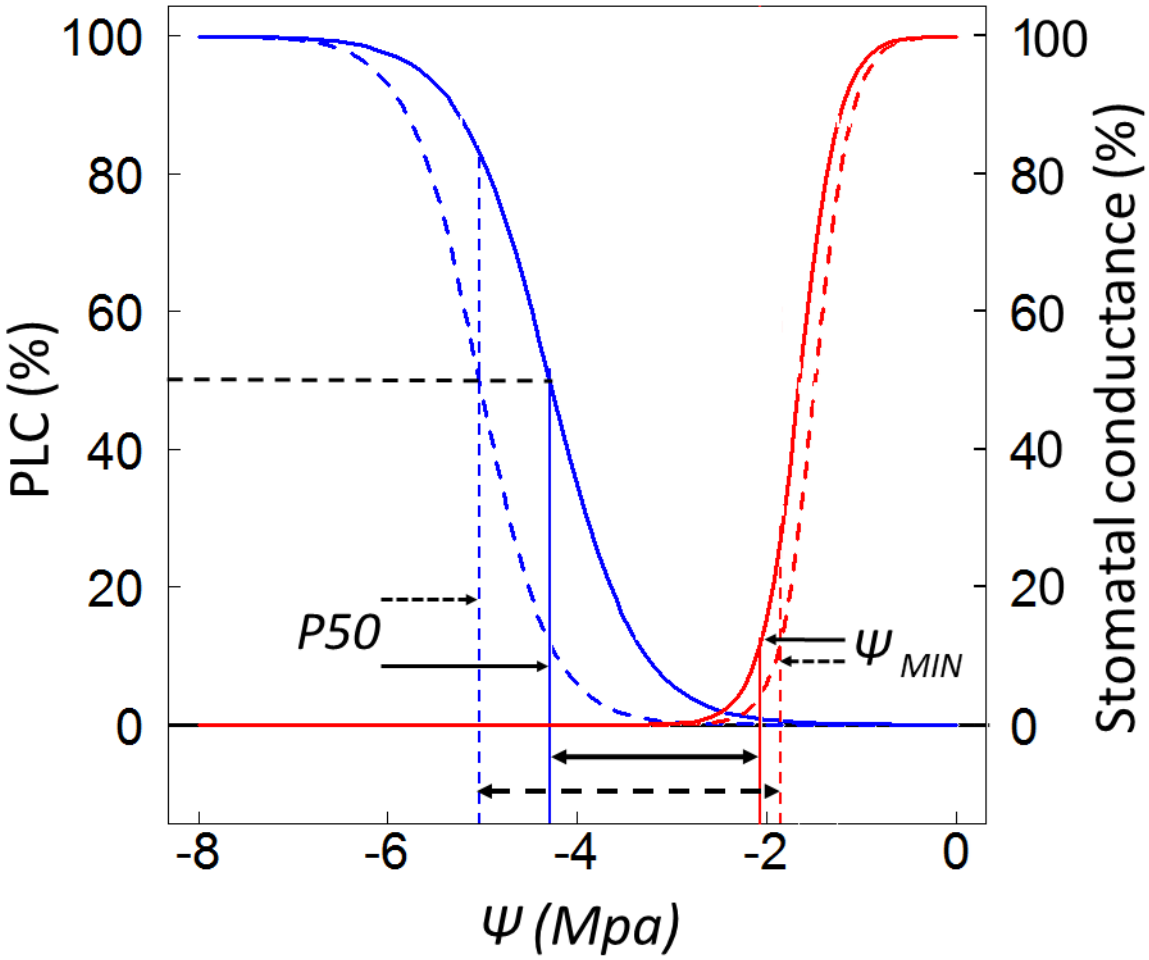
100
80
60
40
20
0
PLC (%)
100
80
60
40
20
0
Stomatal conductance (%)
P50
Ψ MIN
-8
-6
-4
-2
0
Ψ (Mpa)

6.6 Supplementary material

Method

Site effect on the axial patterns were tested using linear mixed-effects models fitted with restricted maximum likelihood. We established a models for *P50*, Kh_{theor}, *Dh* and *Cn* where height, site and their interactions were included as fixed effects, and site identity was included as random factors in all initial models, reflecting the sample collection. Data were $\log_{10}$-transformed to comply with assumptions of normality and homoscedasticity (Zar 1999). Analyses were performed using lme4 package (Bates *et al.* 2015) with R version 3.1.1. (R Development Core Team 2014)

Table S1: Results of the optimal linear mixed-effect models predicting the site effects on the Log_{10} *P50,* Kh_{theor}*, Dh* and *Cn* variation with Log_{10} H (see method above).
Numbers indicate the estimates ± 1 SE. * $P< 0.05$, ** $P< 0.01$ and *** $P< 0.001$.

Fixed effect	**Log_{10} (*P50*)**	**Log_{10} (Kh_{theor})**	**Log_{10} (*Dh*)**	**Log_{10} (*Cn*)**
Intercept (Cinque Torri)	0.71±0.05	-8.60±0.25	1.02±0.03	4.25±0.23***
Log_{10} H (Cinque Torri)	-0.09±0.04*	0.53±0.22*	0.09±0.02***	0.23±0.21
(Pian de Sire)	0.08±0.07	-2.29±0.40	0.09±0.04	-0.56±0.37
Log_{10} H: Pian de Sire	-0.02±0.06	0.22±0.32	-0.08±0.03*	0.45±0.30

Figure S1: Relationship of Kh_{theor} with K_{MAX}. Data are reported for Pian de Sire only, as measurements of KMAX (i.e., at full saturation) for Cinque Torri samples were likely affected by the higher amount of resin inside the wooden tissue.

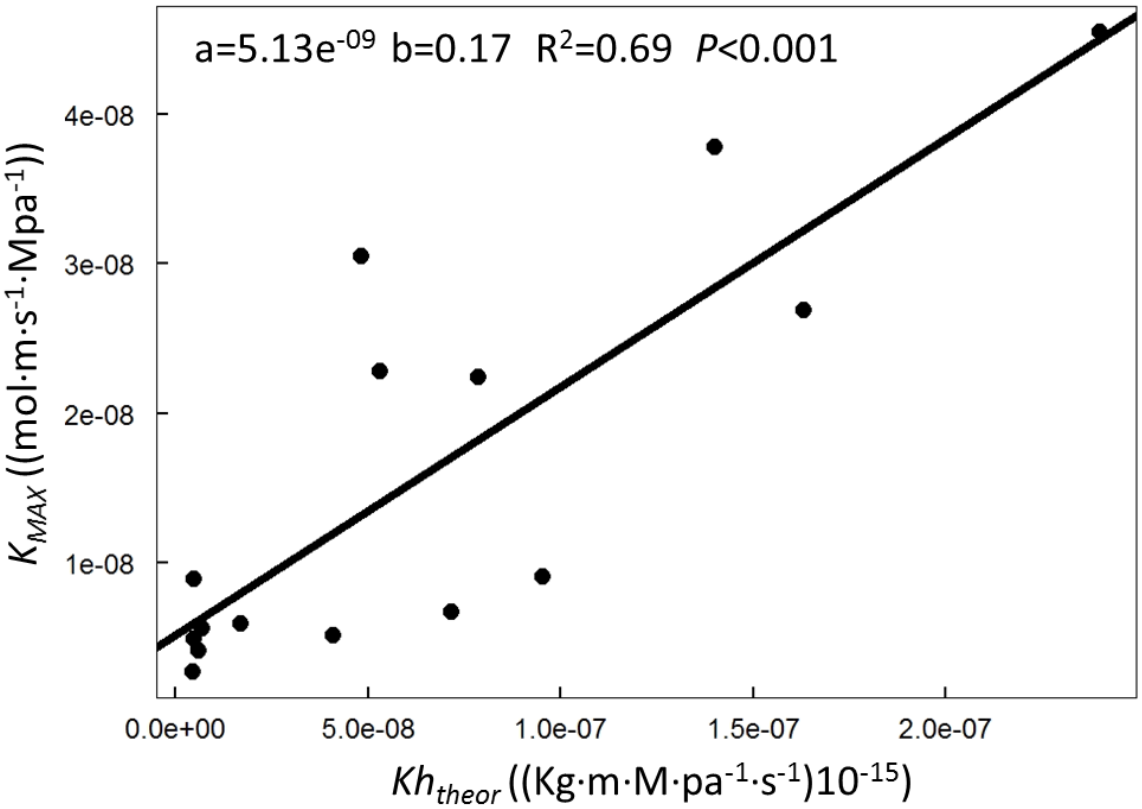

Figure S2: Variation of BI_{EW} with (a) tree height (H) and *P50* (b). Data are log_{10}-transformed. Filled and open circles represent Pian de Sire and Cinque Torri data, respectively.

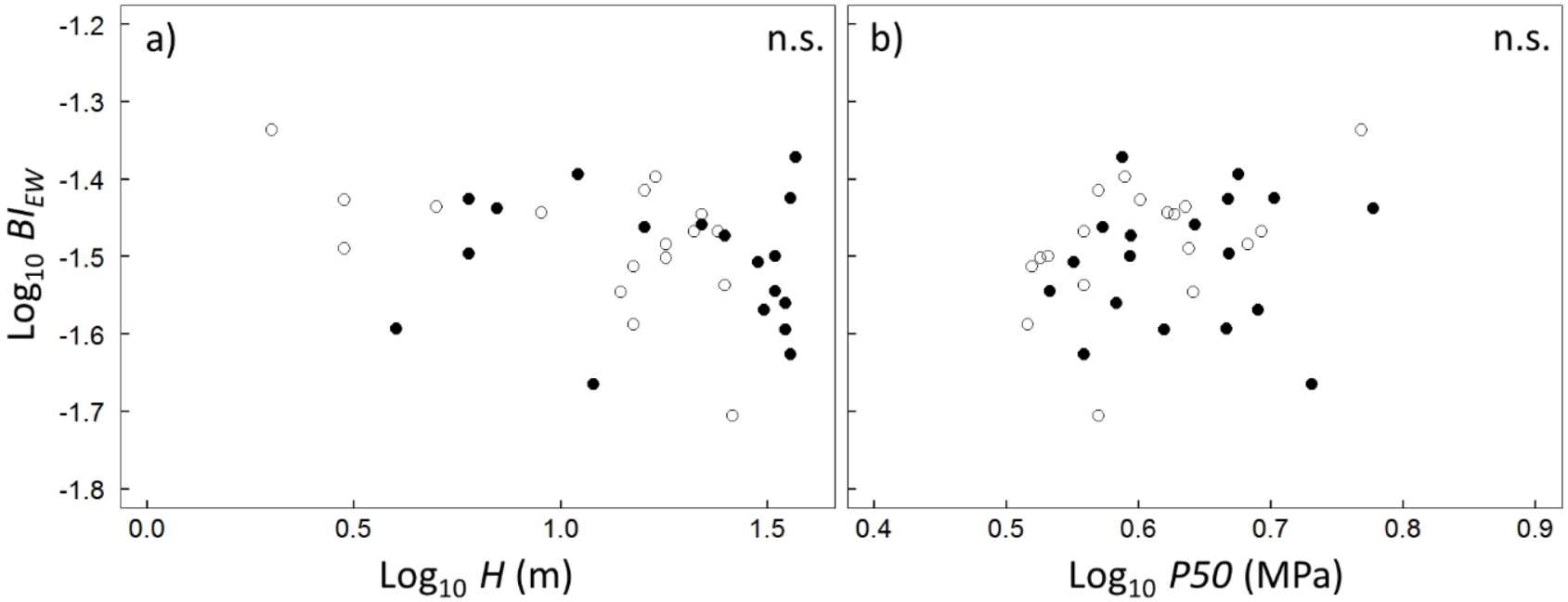

Fig S3: Variation of the tradeoff between cell number and xylem area (Cn/XA) with tree height (H). Data are log_{10}-transformed. Filled and open circles represent Pian de Sire and Cinque Torri data, respectively.

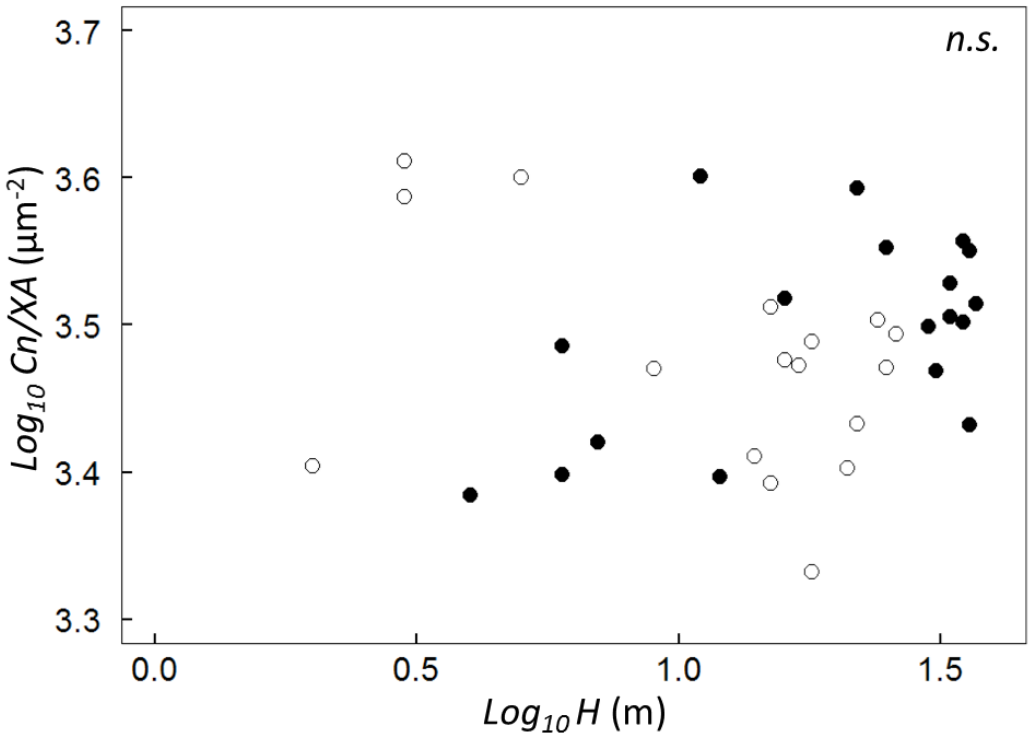

6.7 References

Allen CD, Macalady AK, Chenchouni H, Bachelet D, McDowell N, Vennetier M, Kitzberger T, Rigling A, Breshears DD, Hogg EH (Ted), *et al.* 2010. A global overview of drought and heat-induced tree mortality reveals emerging climate change risks for forests. *Forest Ecology and Management* **259**: 660–684.

Anfodillo T, Petit G, Crivellaro A. 2013. Axial conduit widening in woody species: a still neglected anatomical pattern. *IAWA Journal* **34**: 352–364.

von Arx G, Carrer M. 2014. ROXAS – A new tool to build centuries-long tracheid-lumen chronologies in conifers. *Dendrochronologia* **32**: 290–293.

von Arx G, Crivellaro A, Prendin AL, Čufar K, Carrer M. 2016. Quantitative wood anatomy—practical guidelines. *Frontiers in Plant Science* **7**: 781.

von Arx G, Dietz H. 2005. Automated image analysis of annual rings in the roots of perennial forbs. *International Journal of Plant Sciences* **166**: 723–732.

Bates D, Mächler M, Bolker B, Walker S. 2015. Fitting Linear Mixed-Effects Models Using lme4. *Journal of Statistical Software* **67**: arXiv:1406.5823.

Beikircher B, Ameglio T, Cochard H, Mayr S. 2010. Limitation of the Cavitron technique by conifer pit aspiration. *Journal of Experimental Botany* **61**: 3385–3393.

Burgess SSO, Dawson TE. 2007. Predicting the limits to tree height using statistical regressions of leaf traits. *New Phytologist* **174**: 626–636.

Choat B, Jansen S, Brodibb TJ, Cochard H, Delzon S, Bhaskar R, Bucci SJ, Feild taylor s, Gleason SM, Al E. 2012. Global convergence in the vulnerability of forest to drought. *Nature* **491**: 752–755.

Christman MA, Sperry JS, Adler FR. 2009. Testing the 'rare pit' hypothesis for xylem cavitation resistance in three species of Acer. *New Phytologist* **182**: 664–674.

Cochard H. 2002. A technique for measuring xylem hydraulic conductance under high negative pressures. *Plant, Cell and Environment* **25**: 815–819.

Cochard H, Badel E, Herbette S, Delzon S, Choat B, Jansen S. 2013. Methods for measuring plant vulnerability to cavitation: a critical review. *Journal of Experimental Botany* **64**: 4779–4791.

Cochard H, Cruiziat P, Tyree MT. 1992. Use of Positive Pressures to Establish Vulnerability Curves: Further Support for the Air-Seeding Hypothesis and Implications for Pressure-Volume Analysis. *Plant Physiology* **100**: 205–209.

Denne MP. 1988. Definition of Latewood According to Mork (1928). *IAWA Journal* **10**: 59–62.

Domec J-C, Gartner BL. 2001. Cavitation and water storage capacity in bole xylem segments of mature and young Douglas-fir trees. *Trees* **15**: 204–214.

Domec J-C, Lachenbruch B, Meinzer FC, Woodruff DR, Warren JM, McCulloh K a. 2008. Maximum height in a conifer is associated with conflicting requirements for xylem design. *Proceedings of the National Academy of Sciences of the United States of America* **105**: 12069–12074.

Hacke et. al. 2001. Trends in wood density and structure are linked to prevention of xylem implosion by negative pressure. *Oecologia* **126**: 457–461.

Hacke UG, Sperry JS. 2001. Functional and ecological xylem anatomy (U Hacke, Ed.). *Perspectives in Plant Ecology, Evolution and Systematics* **4**: 97–115.

Hartmann H, Adams HD, Anderegg WRL, Jansen S, Zeppel MJB. 2015. Research frontiers in drought-induced tree mortality: crossing scales and disciplines. *New Phytologist* **205**: 965–

969.

Hentschel R, Rosner S, Kayler ZE, Andreassen K, Børja I, Solberg S, Tveito OE, Priesack E, Gessler A. **2014**. Norway spruce physiological and anatomical predisposition to dieback. *Forest Ecology and Management* **322**: 27–36.

IPCC. **2014**. *Climate change 2014: Fifth Assessment Report of the Intergovernmental Panel on Climate Change.* (C Cambridge University Press, Ed.).

Jacobsen AL, Pratt RB. **2012**. No evidence for an open vessel effect in centrifuge-based vulnerability curves of a long-vesselled liana (Vitis vinifera). *The New phytologist* **194**: 982–90.

Koch GW, Sillett SC, Jennings GM, Davis SD. **2004**. The limits to tree height. *Nature* **428**: 851–854.

Kolb KJ, Sperry JS. **1999**. Transport constraints on water use by the Great Basin shrub, Artemisia tridentata. *Plant, Cell and Environment* **22**: 925–935.

Lewis SL, Brando PM, Phillips OL, van der Heijden GMF, Nepstad D. **2011**. The 2010 Amazon drought. *Science (New York, N.Y.)* **331**: 554.

Mäkelä A, Valentine HT. **2006**. Crown ratio influences allometric scaling in trees. *Ecology* **87**: 2967–2972.

Martínez-Vilalta J, Vanderklein D, Mencuccini M. **2007**. Tree height and age-related decline in growth in Scots pine (Pinus sylvestris L.). *Oecologia* **150**: 529–544.

McDowell N, Pockman WT, Allen CD, Breshears DD, Cobb N, Kolb T, Plaut J, Sperry J, West A, Williams DG, *et al.* 2008. Mechanisms of plant survival and mortality during drought: why do some plants survive while others succumb to drought? *New Phytologist* **178**: 719–739.

Meinzer FC, Domec J-C, Lachenbruch B, Warren JM. **2009**. Safety Factors for Xylem Failure by Implosion and Air-Seeding Within Roots, Trunks and Branches of Young and Old Conifer Trees. *IAWA Journal* **30**: 101–120.

Meinzer FC, Lachenbruch B, Dawson TE. **2011**. *Size- and Age-Related Changes in Tree Structure and Function* (FC Meinzer, B Lachenbruch, and TE Dawson, Eds.). Dordrecht: Springer Netherlands.

Mencuccini M, Martínez-Vilalta J, Vanderklein D, Hamid HA, Korakaki E, Lee S, Michiels B. **2005**. Size-mediated ageing reduces vigour in trees. *Ecology Letters* **8**: 1183–1190.

Nepstad DC, Tohver IM, David R, Moutinho P, Cardinot G. **2007**. Mortality of large trees and lianas following experimental drought in an amazon forest. *Ecology* **88**: 2259–2269.

Olson ME, Anfodillo T, Rosell JA, Petit G, Crivellaro A, Isnard S, León-Gómez C, Alvarado-Cárdenas LO, Castorena M. **2014**. Universal hydraulics of the flowering plants: vessel diameter scales with stem length across angiosperm lineages, habits and climates (B Enquist, Ed.). *Ecology Letters* **17**: 988–997.

Pammenter NW, Van der Willigen C. **1998**. A mathematical and statistical analysis of the curves illustrating vulnerability of xylem to cavitation. *Tree Physiology* **18**: 589–593.

Petit G, Anfodillo T. **2009**. Plant physiology in theory and practice: An analysis of the WBE model for vascular plants. *Journal of Theoretical Biology* **259**: 1–4.

Petit G, Anfodillo T, Mencuccini M. **2008**. Tapering of xylem conduits and hydraulic limitations in sycamore (Acer pseudoplatanus) trees. *New Phytologist* **177**: 653–664.

Petit G, Pfautsch S, Anfodillo T, Adams MA. **2010**. The challenge of tree height in Eucalyptus regnans: when xylem tapering overcomes hydraulic resistance. *New Phytologist* **187**: 1146–1153.

Petit G, Savi T, Consolini M, Anfodillo T, Nardini A. **2016**. Interplay of growth rate and xylem plasticity for optimal coordination of carbon and hydraulic economies in Fraxinus ornus trees

(M Mencuccini, Ed.). *Tree Physiology* **36**: 1–10.

R Development Core Team. **2014**. R: A language and environment for statistical computing. **5**.

Rosner S. **2013**. Hydraulic and biomechanical optimization in norway spruce trunkwood - A review. *IAWA Journal* **34**: 365–390.

Rosner S, Světlík J, Andreassen K, Børja I, Dalsgaard L, Evans R, Luss S, Tveito OE, Solberg S. **2016**. Novel Hydraulic Vulnerability Proxies for a Boreal Conifer Species Reveal That Opportunists May Have Lower Survival Prospects under Extreme Climatic Events. *Frontiers in Plant Science* **7**: 831.

Rowland L, da Costa ACL, Galbraith DR, Oliveira RS, Binks OJ, Oliveira AAR, Pullen AM, Doughty CE, Metcalfe DB, Vasconcelos SS, *et al.* 2015. Death from drought in tropical forests is triggered by hydraulics not carbon starvation. *Nature* **528**: 119–122.

Ryan MG, Yoder BJ. **1997**. Hydraulic Limits to Tree Height and Tree Growth. *BioScience* **47**: 235–242.

Sala A, Piper F, Hoch G. **2010**. Physiological mechanisms of drought-induced tree mortality are far from being resolved. *New Phytologist* **186**: 274–281.

Shinozaki K, Yoda K, Hozumi K, Kira T. **1964**. A quantitative analysis of plant form-the pipe model theory: I. Basic analyses. *Jap. J. Ecol. 日本生態学会誌* **14.3**: 97–105.

Tyree M, Ewers F. **1991**. The hydraulic architecture of trees and other woody plants. *New Phytologist* **119**: 345–360.

Tyree MT, Zimmermann MH. **2002**. *Xylem Structure and the Ascent of Sap* (E Sjöström and R Alén, Eds.). Berlin, Heidelberg: Springer Berlin Heidelberg.

Woodruff DR, Mcculloh KA, Warren JM, Meinzer FC, Lachenbruch B. **2007**. Impacts of tree height on leaf hydraulic architecture and stomatal control in Douglas-fir. *Plant, Cell & Environment* **30**: 559–569.

Yang S, Tyree MT. **1993**. Hydraulic resistance in Acer saccharum shoots and its influence on leaf water potential and transpiration. *Tree physiology* **12**: 231–42.

Zar JH. **1999**. Biostatistical analysis Fifth edition. *USA: Prentice Hall 4165* **4159-4165**.

7. General conclusion

With this study I presented a series of experiments on xylem anatomical and functional features that revealed how the developing fields of quantitative wood anatomy and dendro-anatomy can become very important tools to increase our understanding on the tree response to changing growing conditions.

First, I contributed to the development and improvement the procedures to analyze a huge amount of anatomical data by using a specific software (ROXAS), and to increase the flexibility of obtaining output customized to the specific aims of the study, providing some practical guidance and identifying several pitfalls to successfully use quantitative wood anatomy in research. As a result, the accuracy of the analysis allows now to create reliable anatomical data even for intra-ring analysis (such as latewood or earlywood), by increasing the number of measurable cells from hundreds to hundreds of thousands (i.e., three orders of magnitude). This is of particular relevance if the research goals are oriented towards, for example, intra-annual density profiles including maximum latewood density, or mechanical strength of cells. The increased power and versatility allows to efficiently create comprehensive datasets of cell anatomical features, including CWT, customized for a wide range of novel research applications, e.g. for investigating structure-function relationships, tree stress responses and carbon allocation patterns, and for reconstructing climate based on intra- and interannual variability of wood density.

I applied this new dendro-anatomical approach to investigate the environmental effect and biophysical constraints on xylem physiology and tree growth in high altitude conifers in the Alps. This high elevation environment is among the most sensitive to the effects of the ongoing climate change, as tree growth is primarily constrained by low temperatures. I found that the xylem transport system is subjected to strong biophysical constraints. The modifications of xylem anatomical parameters, such as conduit number, size and cell wall thickness, are primarily designed to guarantee the hydraulic efficiency of the xylem system over its safety against embolism formation during the entire ontogenetic development.

These adjustments in the xylem structure remain permanently fixed and chronologically archived in the wood, and, given the tight link between structures and functions, provide

a ‘time component’ to functional responses induced by xylem plasticity, thus allowing to reconstruct growth dynamics under different environmental conditions.

I showed that taller trees tend to prioritize efficiency against safety, enhancing the hydraulic conductivity (both conduits number and dimension), despite the higher cost of carbon investment and the increasing risk of becoming more vulnerable to cavitation. With this finding it is possible to better understand the mechanism behind the common phenomenon of decreasing tree vigor with tree height, and it is possible to explain the reason why the effects of extreme drought events are commonly more pronounced in dominant trees, leading to phenomena like top dieback or even tree mortality. This study provides a novel empirical evidence that the hydraulic efficiency prevail on safety in taller trees, at least in Norway spruce and likely in other conifer species, thus suggesting that the response to extreme drought events may differ with tree size.

I tested a novel anatomical approach permitted to retrospectively analyze the axial variability of different xylem functional traits in response to the ontogenetic development and environmental variability. This approach is based on the assumption that the axial pattern of increasing conduit lumen diameter (Dh) with the distance from the apex (L) is stable during ontogeny. I found that this assumption holds true, supporting the remarkable universality of the axial conduit widening in vascular plants. The axial conduit widening showed a high prioritization and biophysical determination of hydraulic efficiency to support transpiration and carbon assimilation necessary for tree growth, while the other functional traits (mechanical support and metabolic functions) responded more plastically to intrinsic and extrinsic factors.

The increase in hydraulic conductivity at the apex could have important consequences for the whole transport system with the final effect of promoting primary and even secondary growth. However, my results demonstrated that the cost of increasing the efficiency of the stem apex is the consequent reduction in the hydraulic safety margin, thus a narrower physiological limit to potential xylem dysfunction by air seeding.

Finally, as a consequence of the ontogenetic stability of the axial widening, the conduit lumen diameter (Dh) increases radially with cambial age (C_{AGE}) (i.e from pith to bark), supporting the hypothesis that this pattern is dependent on the rate of stem elongation occurred during ontogeny.

This provided a solid theoretical, almost practical, basis for comparing the height growth development of trees of different age, species and sites, based on the analysis of radial pattern of xylem conduit dimension at the stem base. The presented case studies confirmed the validity of this new approach that might provide the third dimensional component to the dendro-ecological analyses. This represents a completely new approach for retrospective tree growth and climate analyses, where radial patterns of conduit diameter can be used to assess the species-specific growth response to the environmental conditions in a given site at different epochs.

In conclusion, this study represents an important contribution to increase the general understanding on the trade-off mechanisms determining the tree growth patterns and on the current and future vegetation dynamics occurring in ecosystems particularly sensitive to climate change, like the high altitude forests.

References

Anfodillo T, Carraro V, Carrer M, Fior C, Rossi S. **2006**. Convergent tapering of xylem conduits in different woody species.

Baig & Tranquillini. **1980**. The effect of wind and temperature on cuticular transpiration of Picea abies and Pinus cembra and their significance in desiccation damage at alpine treeline. *Oecologia* **47**: 252–256.

Brodersen CR, McElrone AJ. **2013**. Maintenance of xylem Network Transport Capacity: A Review of Embolism Repair in Vascular Plants. *Frontiers in Plant Science* **4**: 1–11.

Brodribb TJ, Holbrook NM, Edwards EJ, Gutiérrez M V. 2003. Relations between stomatal closure, leaf turgor and xylem vulnerability in eight tropical dry forest trees. *Plant, Cell and Environment* **26**: 443–450.

Carrer M, von Arx G, Castagneri D, Petit G. **2015**. Distilling allometric and environmental information from time series of conduit size: the standardization issue and its relationship to tree hydraulic architecture. *Tree Physiology* **35**: 27–33.

Dawes MA, Hagedorn F, Zumbrunn T, Handa IT, Hättenschwiler S, Wipf S, Rixen C. **2011**. Growth and community responses of alpine dwarf shrubs to in situ CO2 enrichment and soil warming. *New Phytologist* **191**: 806–818.

Dawes MA, Philipson CD, Fonti P, Bebi P, Hättenschwiler S, Hagedorn F, Rixen C. **2015**. Soil warming and CO 2 enrichment induce biomass shifts in alpine tree line vegetation. *Global Change Biology* **21**: 2005–2021.

Delzon S, Douthe C, Sala A, Cochard H. **2010**. Mechanism of water-stress induced cavitation in conifers: bordered pit structure and function support the hypothesis of seal capillary-seeding. *Plant, Cell & Environment* **33**: 2101–2111.

Dorrepaal E, Toet S, van Logtestijn RSP, Swart E, van de Weg MJ, Callaghan T V., Aerts R. **2009**. Carbon respiration from subsurface peat accelerated by climate warming in the subarctic. *Nature* **460**: 616–619.

Fatichi S, Rimkus S, Burlando P, Bordoy R, Molnar P. **2013**. Elevational dependence of climate change impacts on water resources in an Alpine catchment. *Hydrology and Earth System Sciences Discussions* **10**: 3743–3794.

Fonti P, Von Arx G, García-González I, Eilmann B, Sass-Klaassen U, Gärtner H, Eckstein D. **2010**. Studying global change through investigation of the plastic responses of xylem anatomy in tree rings. *New Phytologist* **185**: 42–53.

Gleason SM, Westoby M, Jansen S, Choat B, Hacke UG, Pratt RB, Bhaskar R, Brodribb TJ, Bucci SJ, Cao K, *et al.* 2016. Weak tradeoff between xylem safety and xylem- specific hydraulic efficiency across the world ' s woody plant species . *New Phytologist* **209**: 123–136.

Hacke UG, Sperry JS. **2001**. Functional and ecological xylem anatomy (U Hacke, Ed.). *Perspectives in Plant Ecology, Evolution and Systematics* **4**: 97–115.

Hacke UG, Spicer R, Schreiber SG, Plavcová L. **2016**. An ecophysiological and developmental perspective on variation in vessel diameter. *Plant, Cell & Environment*.

Hättenschwiler S, Handa IT, Egli L, Asshoff R, Ammann W, Körner C. **2002**. Atmospheric CO2 enrichment of alpine treeline conifers. *New Phytologist* **156**: 363–375.

Hoch G, Körner C. **2005**. Growth, demography and carbon relations of Polylepis trees at the world's highest treeline. *Functional Ecology* **19**: 941–951.

Koch GW, Sillett SC, Jennings GM, Davis SD. **2004**. The limits to tree height. *Nature* **428**: 851–

854.
Körner C. **1998**. A re-assessment of high elevation treeline positions and their explanation. *Oecologia* **115**: 445–459.
Körner C. **2003**. *Alpine Plant Life* (U Seeliger and B Kjerfve, Eds.). Berlin, Heidelberg: Springer Berlin Heidelberg.
Körner C. **2006**. Plant CO 2 responses: an issue of definition, time and resource supply. *New Phytologist* **172**: 393–411.
Körner C. **2012**. *Alpine Treelines*. Basel: Springer Basel.
Körner C, Paulsen J. **2004**. A world-wide study of high altitude treeline temperatures. *Journal of Biogeography* **31**: 713–732.
Larcher W. **2003**. *Physiological plant ecology: ecophysiology and stress physiology of functional groups* (Springer Science & Business Media, Ed.).
La Marche VC, Graybill DA, Fritts HC, Rose MR. **1984**. Increasing Atmospheric Carbon Dioxide: Tree Ring Evidence for Growth Enhancement in Natural Vegetation. *Science* **225**: 1019–1021.
Mayr S, Cochard H, Ameglio T, Kikuta SB. **2007**. Embolism Formation during Freezing in the Wood of Picea abies. *Plant physiology* **143**: 60–67.
Meinzer FC, Lachenbruch B, Dawson TE. **2011**. *Size- and Age-Related Changes in Tree Structure and Function* (FC Meinzer, B Lachenbruch, and TE Dawson, Eds.). Dordrecht: Springer Netherlands.
Miyajima Y, Takahashi K. **2007**. Changes with altitude of the stand structure of temperate forests on Mount Norikura, central Japan. *Journal of Forest Research* **12**: 187–192.
Nardini A, Lo Gullo MA, Salleo S. **2011**. Refilling embolized xylem conduits: Is it a matter of phloem unloading? *Plant Science* **180**: 604–611.
Niklaus PA, Körner C. **2004**. Syntesis of a six-year study of calcareous grassland responses to in situ CO2 enrichment. *Ecological Monographs* **74**: 491–511.
Olano JM, Arzac A, García-Cervigón AI, von Arx G, Rozas V. **2013**. New star on the stage: amount of ray parenchyma in tree rings shows a link to climate. *The New phytologist* **198**: 486–95.
Olson ME, Anfodillo T, Rosell JA, Petit G, Crivellaro A, Isnard S, León-Gómez C, Alvarado-Cárdenas LO, Castorena M. **2014**. Universal hydraulics of the flowering plants: vessel diameter scales with stem length across angiosperm lineages, habits and climates (B Enquist, Ed.). *Ecology Letters* **17**: 988–997.
Petit G, Anfodillo T, Carraro V, Grani F. **2011**. Hydraulic constraints limit height growth in trees at high altitude. *New Phytologist* **241-252**: 241–252.
Petit G, Anfodillo T, Mencuccini M. **2008**. Tapering of xylem conduits and hydraulic limitations in sycamore (Acer pseudoplatanus) trees. *New Phytologist* **177**: 653–664.
Petit G, Anfodillo T, De Zan C. **2009**. Degree of tapering of xylem conduits in stems and roots of small Pinus cembra and Larix decidua trees. *Botany* **87**: 501–508.
Rossi S, Deslauriers A, Griçar J, Seo J-W, Rathgeber CB, Anfodillo T, Morin H, Levanic T, Oven P, Jalkanen R. **2008**. Critical temperatures for xylogenesis in conifers of cold climates. *Global Ecology and Biogeography* **17**: 696–707.
Rustad LE, Campbell JL, Marion GM, Norby RJ, Mitchell MJ, Hartley AE, Cornelissen JHC, Gurevitch J, Alward R, Beier C, *et al.* 2001. A meta-analysis of the response of soil respiration, net nitrogen mineralization, and aboveground plant growth to experimental ecosystem warming. *Oecologia* **126**: 543–562.
Salleo S, Trifilò P, Esposito S, Nardini A, Lo Gullo MA. **2009**. Starch-to-sugar conversion in

wood parenchyma of field-growing Laurus nobilis plants: a component of the signal pathway for embolism repair? *Functional Plant Biology* **36**: 815.

Smith WK, Germino MJ, Hancock TE, Johnson DM. **2003**. Another perspective on altitudinal limits of alpine timberlines. *Tree Physiology* **23**: 1101–1112.

Smith WK, Germino MJ, Johnson DM, Reinhardt K. **2009**. The Altitude of Alpine Treeline: A Bellwether of Climate Change Effects. *The Botanical Review* **75**: 163–190.

Streit K, Siegwolf RTW, Hagedorn F, Schaub M, Buchmann N. **2014**. Lack of photosynthetic or stomatal regulation after 9 years of elevated [CO2] and 4 years of soil warming in two conifer species at the alpine treeline. *Plant, cell & environment* **37**: 315–26.

Tranquillini. **1979**. Physiological ecology of alpine timberline. *Ecological Studies 31. Berlin, Germany: Springer-Verlag*.

Walker M, Wahren C. **2006**. Plant community responses to experimental warming across the tundra biome. *Proceedings of the …* **103**: 1342–6.

West GB, Brown JH, Enquist BJ. **1999**. A general model for the structure and allometry of plant vascular systems. *Nature* **400**: 664–667.

Acknowledgements

The tree-ring world was almost new to me when I started my PhD. During these years a lot of people helped me to run down this course… even if sometimes it seemed a class V+ river.

A special thanks to Giai that showed me the right lines to follow. He also let me explore my own lines down the rapids, but a safety rope was always there for me. We have not only worked together but also shared some other amazing experiences too. It was great!

I am grateful to Georg not only for the "Angi's button" but for his enthusiasm and for all the support I received even if little by little I have become his ROXAS nightmare.

I would like to thank to all the co-authors of the papers forming this thesis for their useful comments, suggestions and support. I also thank Sabine Rosner and Jordi Martinez Vitalta for reading and evaluating the previous version of this thesis. I really appreciated their comments and suggestions.

Thanks to Marco, Tommaso, Alan & Daniele for their advices, and for creating a nice working atmosphere with the help of Raffaella, Enrico, Arturo (the best travel-mate ever!), Elena, Silvia & Natasa.

I want to express my great gratitude to Patrick Fonti and Stefan Mayr for hosting me in their group during my internship abroad.

I spent several periods at the Swiss Federal Institute for Forest, Snow and Landscape Research in Switzerland, and a month at the Institut für Botanik in Innsbruck where I met several people that supported me in many ways (Christian Rixen, Melissa Dawes, Richard Peters, Barbara Beikircher and Birgit Damon).

Thanks to my PhD colleagues (Thomas, Massimo, Niccolò, Alma, Alessia, Adriano, Richard, Stefan, Nacho and Flor) for all the nice time spent together.

I also would like to thank Chiara, Irene and Filo that always tried to understand what I was doing during these three years! In particular, I thank Filo for refreshing my mind with some real white water!

I also thank Lorenzo for putting me in my white slalom suit again with all the related consequences.

Finally, a special thanks to Matti, Flay and Mami, they always encouraged and supported me, especially in the trickiest moments.